New Methods in Modeling and Control of Modern Electrohydraulic Systems

By

Sameh Nabil Alkam

B.Sc., San Jose State University, San Jose, CA, 2003

M.S. University of Illinois at Chicago, Chicago, IL, 2006

THESIS

Submitted in partial fulfillment of the requirements

for the degree of Doctor of Philosophy in Mechanical Engineering

in the Graduate College of the University of Illinois at Chicago, 2014

Chicago, Illinois

Defense Committee:

Dr. Sabri Cetinkunt, Chair and Advisor

Dr. Mohsen Issa, Civil engineering

Dr. Michael Brown, Mechanical Engineering

Dr. Saeed Manafzadeh, Mechanical Engineering

Dr. Matthew Bolton, Industrial Engineering

I would like to dedicate this work to those who made me who I am today, to those who inspired me, and to those whom I aspire; my family, my friends, and my people.

ACKNOLEDGEMENTS

First of all I would like to thank my advisor and mentor Dr. Sabri Cetinkunt for giving me the chance to join the mechatronics lab at UIC, and for providing me with the interesting topic of IMVs. Deep appreciation and gratitude to you for being there for me both academically and personally.

Next , I want to thank my committee members who took the time and effort to review my work, and who gave me advice and guidance through this process; Dr. Mohsen Issa, Dr. Michael Brown, Dr. Saeed Manafzadeh, ad Dr. Matthew Bolton.

The technical and theoretical support, and the discussions of my work provided by my colleagues Riad Zghayer, Mohammad Zaher, Ahmad Ezaby, and by Dr. Joseph Pfaff from Husco international for the donation of the INCOVA, and for Dr. Amir Shenouda, all your inputs were very helpful and highly appreciated.

I am very thankful to the Department of Mechanical ad Mechatronics Engineering at Birzeit University in Palestine for granting me their trust, and for being flexible and supportive.

Last and least the center of my personal universe, my family and friends, my parents, siblings, grandmothers, to my lifelong friend Maher Abdellatif, and above all my better half Nisreen, you made this success, and you earned this degree only my name is on it.

Sameh Alkam 2014

Table of Contents

LIST OF FIGURES

LIST OF TABLES

SUMMARY

The concept of the independent metering valve (IMV) is compared to traditional valves, modeled, and analyzed, and its digital control is discussed. Valve control is studied in terms of sensitivity, physical limitations, work port pressure, and the cavitation condition.

The potential energy saving capabilities of the IMV system have been investigated by many researchers. IMV performance in each one of its modes is compared to the corresponding performance of the conventional load sensing pump control (LSPC).

This work introduced the sixth mode which is the High Side Regeneration Retraction that was not addressed by previous work, besides introducing a more systematic way of calculating the equivalent pressure and the pressure supply set point.

Mathematical models that represent the different components of the hydraulic system are studied. The most important is the electro hydraulic poppet valve (EHPV), a second order dynamic model of this valve is validated. The actuator dynamic model is then derived, and a state space representation of the system is introduced, experimental validations of the models were reviewed from other papers in literature.

Continuously variable modes, which is a more general approach, is then introduced and analyzed. The idea behind it is using three valves instead of two to control the system, and this will reduce the five distinct modes to three modes and solve many of the problems inherent by the discontinuity of flow when only two valves are used. The three modes are: powered high side regeneration extension (PHSRE), the powered low side regeneration retraction (PLSRR), and the powered low side regeneration extension (PLSRE). The contribution of this paper to this field was introducing a fourth CVM which is the powered high side regeneration retraction mode, and deriving all the equation related to it.

1 INTRODUCTION

1.1 Introduction

Hydraulic energy has been used since the beginning of civilization, but the industrial application started after the discovery of the Pascal Law in the 1650's. At the present time hydraulic power is used in most earth moving applications, mining, agricultural, naval vehicles among others. Hydraulic power's main advantage is its high power to weight ratio, in addition to its reliability, durability, and ease of control in many aspects [15, 29]. However, there are drawbacks to hydraulic power; the most important of all its inherent non-linear behavior, in addition to sensitivity to contamination [29].

The main components of the hydraulic system are the tank that holds the liquid which is often oil, the pump that is driven by an electric motor or internal combustion engine, the valves to control the flow rate, pressure and direction of liquid in the system, the actuator which is the rotary motor, or linear cylinder to convert the fluid energy to motion, and finally the piping system that transmits the energy between the components of the system [15].

Classical control of hydraulic system is achieved manually; this requires the positioning of the valve to be in the operator's cabinet with long piping connecting the valve to the actuator, adding more complexity to the non linear nature of hydraulic systems [31]. The electronic revolution of the 1970's and the emerging of the mechatronics field boosted the use of electronics in controlling hydraulic systems. The use of microcontrollers allowed for more complex control algorithms that took into consideration the complexity of hydraulic systems [7].

The hydraulic circuit starts by pressurizing the fluid by the pump, where it is transferred through the pipes to the actuator, which requires the power to achieve a certain task. The fluid is controlled by the valves that can meter the flow rate, the pressure, or guide the flow to the desired location. The traditional control valve is the spool valve that is machined to allow the flow in and out from the actuator and the tank by shifting the spool. This motion of the spool controls the openings of the valve ports [29].

The inherent problem of the spool valve is the coupling of the inlet and outlet openings allowing only one degree of freedom. In other words it can only control the speed of the actuator or the pressure in one of the chambers but not both at the same time [1,7,45].

The spool design then gives a good control of position, speed or force, but it tends to use more energy than required because of the dependence of the spool lands on one motion, and there is no way of achieving good control along with energy saving [25,26].

In hydraulic systems the pump is used to pressurize the fluid which is then used to power the actuator. The amount and direction of force is controlled using a traditional valve. The traditional valve consists of a spool inside a housing that has inports and outports. The spool is specially designed and fabricated for a certain task; the openings of the inports and outports are calculated and the shape of the spool is designed accordingly. The spool is usually controlled using two solenoids that move linearly in proportion to current commanded through its coils [29]. The principle behind the conventional valve is shown in the figure one below.

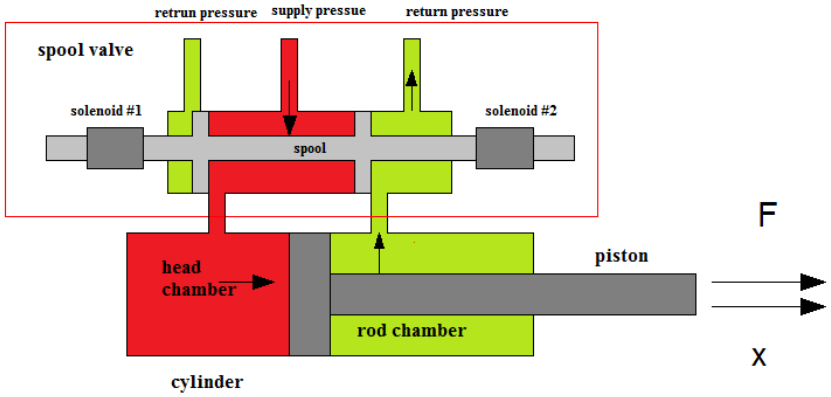

Figure 1. A hydraulic actuator controlled by a spool valve.

The most common valve used in industry is the four way three position spool valve. The design of the spool has the inherent characteristic of coupling the metering in and metering out of the flow, although this provides excellent controllability of the valve, it will allow for only one degree of freedom, so one can control the flow rate or the pressure in one chamber of the actuator and cannot control both chambers which in turn results in energy loss [26,27]. In some cases such as overrunning loads, the weight of the load can generate some pressure that can be cultivated, but the traditional valve cannot take advantage of the gravity assistance due to the inherent design that focuses on control and not energy saving [4,5].

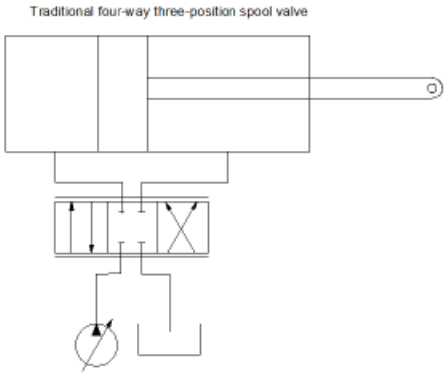

Figure 2. The four way three position traditional hydraulic valve.

Advantages of IMVs

1. It allows for more flexibility in control, so in addition to the speed of flow in one chamber of the actuator, the pressure in any chamber can be achieved.
2. More efficient energy potential, which is a direct result of the decoupling of the metering in and metering out of the inlets and outlets openings.
3. Lower cost since these valves can be used for any application and no specific design and manufacturing of the spool is required each time, rather functionality is defined in the real time control software.

1.2 Literature Review

The literature reviewed can be classified into three categories: the emergence and development of the Independent Metering Valves, energy saving using IMVs, and the control of the IMVs.

The first ideas of the IMVs started to develop as a result of the electronic revolution of the seventies and eighties. The hydraulic power is a mature science, so it is only natural to extend its branches, which means the marriage of electronics with hydro-mechanics to improve it [31].

The earliest attempt to save energy using IMV ideas was reported by Garnjost in 1989 [18] without addressing the issue directly. To save energy he came up with gravity assisted load to achieve regeneration, which is supplying fluid with high pressure from one chamber of the hydraulic actuator to the lower pressure chamber of the same actuator. He used two valves with a double acting actuator to do so without using the flow from the pump or dumping the whole flow back to the tank. The two valves were independently actuated to open and close the inlet and outlet of the actuator chambers as needed.

The first patent that realistically resembles IMV system was invented by Kramer [22]. It was called Electrohydraulic Valve System. Four pilot- operated proportional poppet valves were used to control the flow from and to a double acting hydraulic cylinder connected to a pump and a tank. The four valves were controlled by four solenoids, which in turn were controlled by the error signal feedback. The command signal sent by the operator was compared to the cylinder position and the error signal was feedback to control operations such as float, shutdown, deadband, and pressure compensation.

Crosser's patent in 1992 [13] was not too far from the previous ideas; he proposed a Hydraulic Circuit and Control System based on it. The inventions used only two valves instead of the many valves usually used. The control signal was a manual positions signal of a joystick that turned into current signal sent to a microprocessor. This signal then controls the valve openings to output the desired flow rate and direction. Each valve was responsible of the flow in and out of one side of the actuator.

Janson and Palmberg's research focused on increasing the flexibility of a hydraulic valve by separating the meter in and meter out flows using poppet valves instead of the traditional spool valve, which couples the input and output flows. Their work focused on achieving independence of flow between the inlet and outlet of the hydraulic actuator [21,22].

One of the most significant works on IMVs was done by Aardema[2]. It was the first patent for Caterpillar, and it was a hydraulic circuit having dual electro-hydraulic control valves where he used two electro-hydraulic valves. The first was used to control the flow from the pump to both sides of the actuator, while the second was used to control the flow from both ends of the actuator to the tank. The valves used were displacement proportional pilot operated valves, and the control scheme was based on coordinating the movement of both valves to establish the needed communication between both sides of the actuator.

Wilke in 1999 [51] came up with pilot solenoid control valve and hydraulic control system using same. His invention was a pilot operated control valve that has a housing covering an inlet and an outlet with a poppet moving according to input control flow. This control flow selectively moves the poppet to a desired location. The poppet has an opening that establishes a connection with the control chamber away from the valves seat. The movement of the poppet opens the inlet to control chamber or the outlet to control chamber according to the motion.

Aardema and Kohler patent [2] is the first complete IMV system as we know it. This patent proposed a method for controlling an IMV operating in a hydraulic circuit. A displacement command for a certain valve is send to the valve to provide the desired flow through it and pressure drop across it as needed. This command signal is based on the operation mode and the velocity of the actuator which is determined by the flow available to that valve. All four valves are independently controlled electronically.

Yang [53] developed the pilot solenoid control valve with pressure responsive diaphragm, which is the basis of Husco's work on IMVs. The patent is a pilot control valve which has a body with an inlet and an outlet, the fluid between the inlet and the outlet is controlled using a poppet that moves within the main valve, and it has a flexible diaphragm with a pilot passage. This pilot passage opens and closes by moving the poppet. The diaphragm flexes due to a pressure differential that acts on the pilot poppet, and this flexing compensates for adverse effects that the pressure differential has on the operation of the pilot poppet.

Another important invention in the field was Liberfarb's [24] "the Bidirectional Flow Control Valve". The valve includes two port housing with a hollow cage inside. The hollow cage has rows of cross sectional holes to communicate with various ports. A compensating spool slides in the cage between the cross section holes according to pressure difference among the holes. This motion causes reduction of opening of row and increases the opening of another. This opening and closing provides consistent flow control behavior for both directions.

The next phase of the IMVs was focusing more on the control and energy aspects of the new technology. Yao and Liu [25] investigated the energy saving control of hydraulic system with novel programmable valve. They studied the energy saving in a single rod hydraulic cylinder using programmable valves using the adaptive robust control on IMVs. IMVs decouple the meter in and meter

out flows and provide regeneration capabilities. The control algorithm required for IMVs is more complicated but provides potential for energy saving while preserving control accuracy.

Yao and Liu[26,27] published another paper the next year about coordinate control of energy saving programmable valves. They found that programmable valves save energy because they decouple the control of flow in and out of the valve and provide flow cross ports in addition to improved and precise control, but the IMVs require more complicated control algorithms due to the multi inputs.

Yoshino [58] had another idea about energy saving and control in his patent hydraulic control system with regeneration. He stipulated that a control system consisting of a pump, a tank, a cylinder with head end and rod end, IMV, and pressure sensors at the head chamber. In this system a controller communicates with the IMV and the pressure sensor, and based on the sensor signal and the mode of the operation, the controller activates one valve of the IMV's arrangement. The four valves connecting the rod end and the head end chambers of the cylinder to the pump and tank, with a fifth check valve is used as a load hold valve to control fluid communication between the pump and the cylinder. One pressure sensor measuring pressure at the head chamber is also used in addition to a controller connected to the valves and the sensor. The controller sends signals to actuate the desired valve based on sensor signal and mode of operation.

The next phase is the most important and resulted in the development of INCOVA, the most advanced IMV at the present time; it stands for Intelligent Control Valve by Husco International. Tabor [47] patented a “Velocity Based Method for Controlling a Hydraulic System,”. The load pressure signal and the speed of the actuator are used to calculate the flow coefficients that determines the flow of the circuit. The flow coefficient can be a conduction coefficient or a restriction coefficient. The flow coefficient is then used to activate each one of the electro -hydraulic poppet valves to achieve desired actuator velocity and to control the pressure from the pump and to the tank.

Pfaff patent [40] “Velocity Based Electronic Control System for Operating Hydraulic Equipment”, built on the previous patent. The control system operating a hydraulic system includes a user input device that generates an electric signal proportional to desired motion of the actuator. He came up with a mapping routine to convert the input signal to a desired velocity command to the actuator. Then a valve opening routine transforms the desired velocity into flow coefficients that determines the fluid flow to the various components of the system. From these flow coefficients, various signals of different currents are sent to the valve actuators. The pressure controller controls the pressure from the pump in

proportion to the velocity requirements, and in this multi-task system the control system distributes the available flow among all subsystems if no enough flow is available to all [39].

Yang, Pfaff and Paik [54] patented a “Pilot Operated Control Valve Having a Poppet with Integral Pressure Compensating Mechanism”. It provides a bidirectional fluid control using a poppet that moves in response to the pressure of a control chamber. It has a mechanism to provide proportional pressure compensation across the two sides of the orifice.

The problem of multi hydraulic actuators in a single hydraulic circuit was studied by Pfaff [40] who invented a method of sharing flow of fluid among multiple hydraulic functions in a velocity based control system. When the flow supplied is not enough for all tasks, a decision is needed to distribute the flow from the supply to the different actuators according to a flow sharing routine, where each actuator is given a fraction of the total supply available. Those fractions are used to map the desired velocity for the actuator into a velocity command indicating the actual velocity that can be achieved with the available flow supplied, this velocity command is used to control the flow to each hydraulic actuator.

Reiners [44] was working on something similar at the same time and he patented IMV assembly for multiple hydraulic load functions. He suggested that for each hydraulic load, there will be a load function, the IMV will have a set of independent electronically controlled valves, with an inlet connected to a pressure source with a first outlet coupled with a hydraulic load and a second outlet coupled with the second hydraulic load.

Opdenbosch [35] developed learning control applied to electro-hydraulic poppet valves. His goal was to find a controller to force the output to follow a desired input state with many details of the plant dynamics. Therefore he considered the tracking of the desired supply pressure, which is controlled by knowing the flow conductance coefficient Kv of the EHPV. This was done by knowing the inverse input state mapping of the valve while the state mapping is being used in the forward loop. The mapping learning was achieved using a simple neural network structure called the Nodal Link Perceptron Network (NLPN). The NLPN is trained online using a gradient descent method to minimize the error in the inverse input state mapping approximation.

1.3 Proposed Research

The IMV concept leads to the decoupling of metering in and metering out of the flow, which makes it more flexible in terms control, but the control algorithm becomes much more complicated and difficult to achieve. The methods used currently are way too complicated and have their own disadvantages. Previous works derived most of the equations for the IMV system, but a certain modes were not studied, in this thesis the derivation of the High Side regeneration Extension in the distinct modes, and the Powered High Side Regeneration Retraction in the Continuously Variable Mode are presented along with all the mathematical results.

The second contribution of this research is developing an experimental approach to modeling and control of electrohydraulic system, this is very useful if the data of the system is not available or not accurate, so the mathematical model is not reliable in this case. The system in the mechatronics lab is used to verify the method validity.

The third contribution of this research is proposing a controller to the IMV system using a simple PID controller on each valve of the IMV assembly, starting with a traditional valve dynamics and finding a the gains for the controller, then using the IMV system with some modifications on the gains to the previous ones. This way the two valves will be completely independent with independent control gains for each valve.

2 IMV CONCEPT AND MODELING

2.1 The IMV Concept

The traditional four way three position proportional spool valve is replaced by four proportional poppet valves; the first valve connects the head chamber side of the cylinder to the supply line, the second valve connects the rod chamber side of the cylinder to the supply line, the third valve connects the head chamber of the cylinder to the tank line, and the fourth valve connects the rod chamber of the cylinder to the tank line. In any task, only two of the 4 valves ideally will open, which will allow for flow regeneration and hence energy saving due to less demand on the pump [2,12,11]. Figure 3 below shows the principle of the IMV and the nomenclature associated with it. As the name implies the independence of control of all four valves allow for more degrees of freedom which leads to more controllability of the system. The pattern in which the valves are opened or closed is called mode. There are five distinct modes in which the valve can be operated [45].

The modes of operation of IMV were first described in [40,41,45,48,49,122]. A summary of their results is presented here for the sake of completeness.

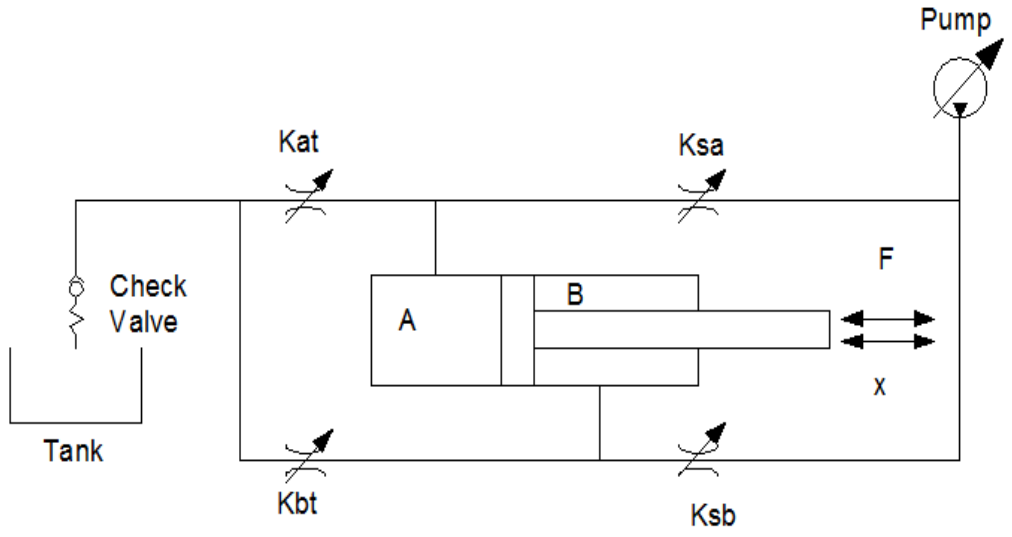

Figure 3. The concept of the four valves assembly constituting IMV.

2.1.1 Powered Extension Mode (PE):

The PE has the same principle of operation as the conventional valve to extend a piston of a cylinder (Fig. 4). Pressurized fluid is supplied from the pump line to the head chamber A of the cylinder through valve K_{sa}, this will cause the piston to extend, which forces the fluid in the rod chamber B to flow out to the tank through valve K_{bt}. The only difference is that the opening of valves K_{sa} and K_{bt} are independently controlled [45].

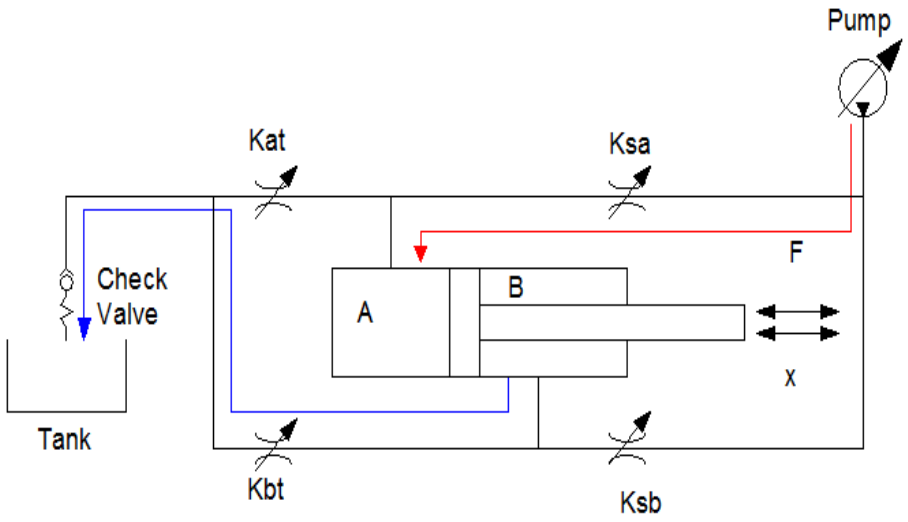

Figure 4. IMV mode one: powered extension.

2.1.2 Powered Retraction Mode (PR):

The PR has the same principle of operation as the conventional valve retraction (Fig 5). Pressurized fluid is supplied from the pump line to the rod chamber B of the cylinder through valve K_{sb} causing the piston to retract. This motion will force the fluid in the head chamber A to flow out to the tank through valve K_{at}. Again, both valves K_{sb} and K_{at} are independently controlled [45].

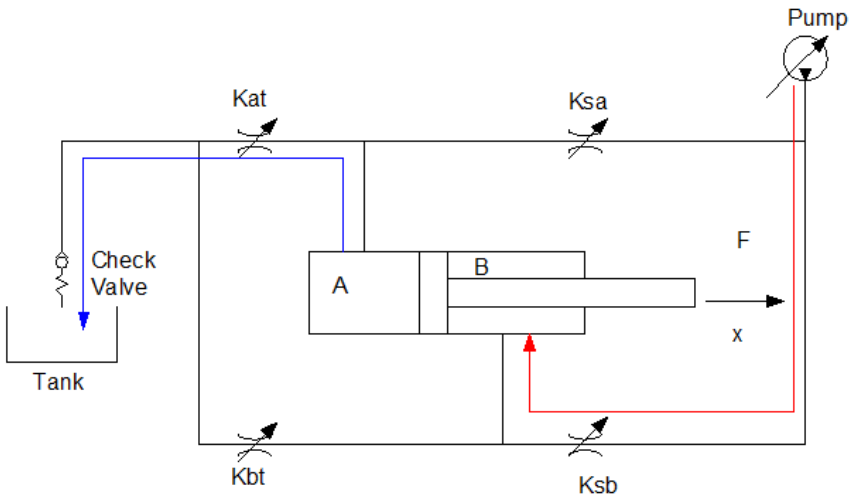

Figure 5. IMV mode two: powered retraction.

2.1.3 High Side Regeneration Extension Mode (HSRE):

HSRE is the first of the three regenerative modes that cannot be achieved using the conventional valve (Fig. 6). High pressure fluid coming out of rod chamber B is circulated through valve K_{sb} to the pump line and then to the head chamber A through valve K_{sa} instead of going to the tank causing the rod to extend. However the flow from chamber B is less than that is needed in chamber A due to the area difference $(A_a > A_b)$, and since $Q = A\,\dot{x}$ and the velocity is the same for both chambers then $(Q_A > Q_B)$. The difference in flow is supplied by the pump. The high side regeneration extension mode has the potential of energy saving proportional to the flow rate $Q = A\,\dot{x}$ This mode is called High Side Regeneration Extension because the flow goes through valves K_{sb} and K_{sa} which lie on the high side (pump side) of pressure lines. Figure 6 shows how this mode works [45].

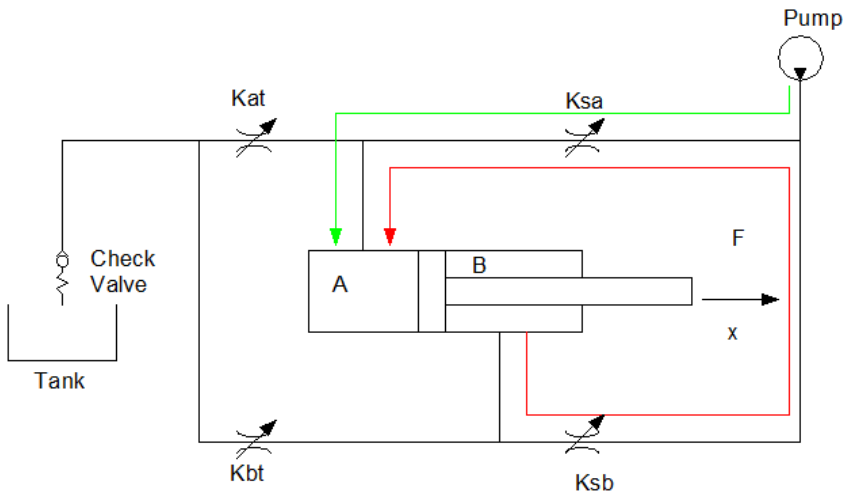

Figure 6. IMV mode 3: high side regeneration extension.

2.1.4 Low Side Regeneration Extension Mode (LSRE):

LSRE is best used for overrunning loads, which is when the load is in the same direction of motion of the rod as in the case of gravity assisted lowering of a load (Fig. 7).

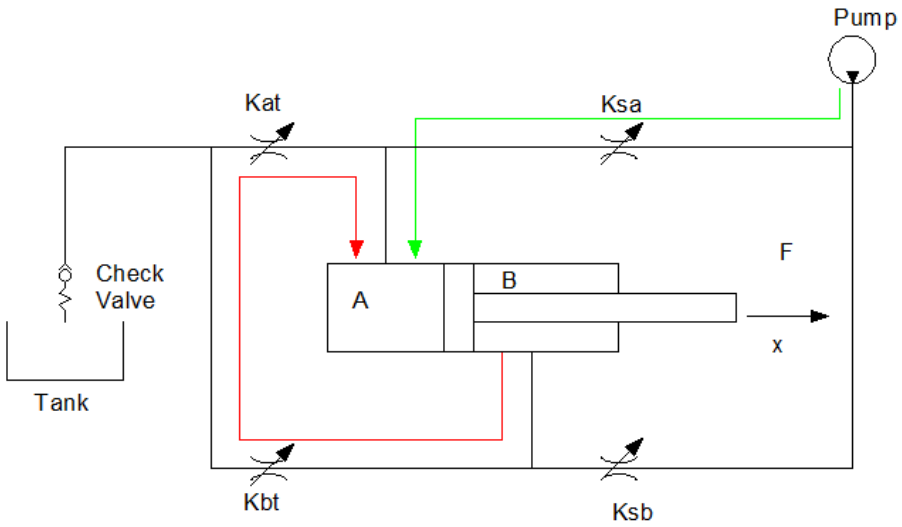

Figure 7. IMV mode 4: low side regeneration extension.

The flow coming out of rod chamber B is circulated through valves K_{bt} and K_{at} in the head chamber A instead of going to the tank. This will cause the piston to extend, but the flow from chamber B is not enough for chamber A, because both ends have the same speed and area A is bigger than area B, so $(Aa > Ab)$ since $(Q = A\dot{x})$. The difference between the two is supplied by the pump, or by other functions of the hydraulic circuits that have excess flow. The needed pressure is built using a check valve especially set for this operation. In conventional valves the spool is designed such that the outlet opening is set to control the flow so that the load is lowered at a controllable speed under the gravity effect. The problem is that when lifting a load this opening is too small and it is fixed so the pressure drops are huge and losses cannot be avoided. Therefore the control of the outlet opening through LSRE has the potential for energy saving. It is called LSRE because the fluid flows through the paths of K_{bt} and K_{at} which is on the low side (tank side) of the pressure line [45].

2.1.5 Low Side Regeneration Retraction Mode (LSRR):

LSRR mode is used with overrunning loads where the load is in the same direction of motion of the piston rod, as in the case of lowering a load with gravity assistance (Fig. 8).

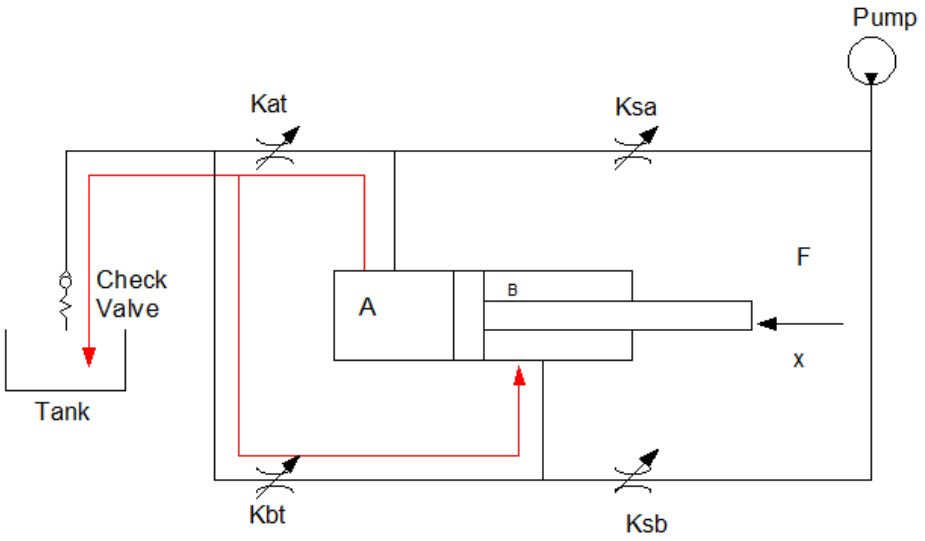

Figure 8. IMV mode 5: low side regeneration retraction.

The fluid coming out of head chamber A is circulated through valve K_{at} and K_{bt} into rod chamber B instead of going to the tank; this will cause the piston to retract. The fluid coming out of chamber A is more than needed in chamber B because both have the same speed, but area A is bigger than area B as explained before. The extra flow is directed through a check valve to the tank. In this case the pump flow is zero and energy saving potential is optimum. This is called LSRR because the fluid flows through K_{at} and K_{bt} which are on the low side (tank side) of pressure line [45].

2.2 System Modeling

The mathematical modeling of the five modes was first introduced by Merritt [29], Tabor [47-50], and Shenouda [45] from whom the schematics of the modes were recreated.

The system under study is assumed to have very slow dynamic changes, in addition to ignoring the capacitance of the chambers and lines, which makes the system “quasi-static system”. The other assumption is that we are looking on one actuator in the system, so flow distribution among multiple actuators is not considered.

The goal of this section is to determine equivalent pressure and equivalent conductance coefficient for the entire hydraulic circuit representing each of the five modes**.** The importance of these parameters is that they will be used to control the valves. The derivation of the first mode will be presented here in details while the rest of the results of the other modes will be just listed as presented by Tabor's work. Further details can be found in [45,47-50].

The equivalent pressure is defined as the combination of the pump pressure, the head chamber pressure, the tank pressure, and the rod chamber pressure, while the equivalent conductance coefficient is defined as the combination of the two valves used in the specific mode in addition to the area ratio between the head chamber area and the rod chamber area (R).

2.2.1 Powered Extension Mode (PE):

The figure below shows a simplified version of the equivalent circuit of the PE mode in IMVs. As mentioned before, the two valves used are K_{sa} and K_{bt}; we can replace all the pressures and conductance coefficients with P_{eq} and K_{eq} as shown in figure 9 [45].

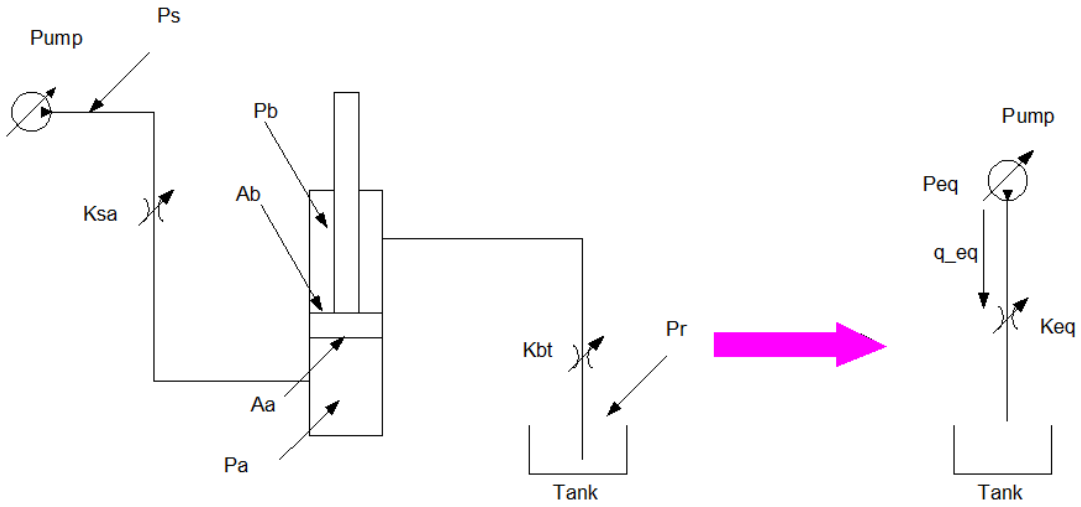

Figure 9. The equivalent reduced hydraulic circuit of powered extension mode

Merritt [29] defines the pressure across the first and the second valve as:

$$\Delta P_1 = P_s - P_a \tag{2.1}$$

$$\Delta P_2 = P_b - P_r \tag{2.2}$$

$$q_{in} = K_{sa}\sqrt{\Delta P_1} = K_{sa}\sqrt{P_s - P_a} = A_a\dot{x} \tag{2.3}$$

$$q_{out} = K_{bt}\sqrt{\Delta P_2} = K_{bt}\sqrt{P_b - P_r} = A_b\dot{x} \tag{2.4}$$

From Newton's second law $\sum F = ma$, the external forces can be expressed as:

$$P_s A_a - P_r A_b = \Delta P_1 A_a + (P_a A_a - P_b A_b) + \Delta P_2 A_b \tag{2.5}$$

Dividing by A_b and defining $A_a/A_b \equiv R$

$$RP_s - P_r = R\Delta P_1 + (RP_a - P_b) + \Delta P_2 \tag{2.6}$$

$$(RP_s - P_r) + (-RP_a + P_b) = R\Delta P_1 + \Delta P_2 \tag{2.7}$$

Define P_{eq} as:

$$P_s = (RP_s - P_r) + (-RP_a + P_b) = R\frac{{q_{in}}^2}{{K_{sa}}^2} + \frac{{q_{out}}^2}{{K_{bt}}^2} \tag{2.8}$$

But recall from 2.3 that $\Delta P1 = \frac{{q_{in}}^2}{{K_{sa}}^2}$ and $\Delta P2 = \frac{{q_{out}}^2}{{K_{bt}}^2}$

Substitute in the right hand side of equation 2.7, and recall that since the speed is the same and $q_{in} = A_a x'$ and $q_{out} = A_b x'$ Then:

$$\frac{q_{in}}{q_{out}} = \frac{A_a}{A_b} = R \tag{2.9}$$

$$P_{eq} = \frac{R^3 {q_{out}}^2}{{K_{sa}}^2} + \frac{{q_{out}}^2}{{K_{bt}}^2} = {q_{out}}^2 \left[\frac{R^3 {K_{bt}}^2 + {K_{sa}}^2}{{K_{sa}}^2 {K_{bt}}^2}\right] \tag{2.10}$$

Where:

$$q_{out} = \frac{K_{sa}K_{bt}}{\sqrt{R^3 {K_{bt}}^2 + {K_{sa}}^2}}\sqrt{P_{eq}} = K_{eq}\sqrt{P_{eq}} \tag{2.11}$$

$$K_{eq} = \frac{K_{sa}K_{bt}}{\sqrt{R^3 {K_{bt}}^2 + {K_{sa}}^2}} \tag{2.12}$$

$$P_{eq} = (RP_s - P_r) + (-RP_a + P_b) \tag{2.13}$$

This K_{eq} represents all the combinations of K_{sa} and K_{bt} that give the opening of the whole system required to achieve a specific flow and speed for a certain load condition. As expected, the flow will depend on both valves and not on only one [41]. This means that the speed of the piston will not only depend on the load applied but also on both openings K_{sa} and K_{bt}, in addition to the supply pressure (P_s) and the return pressure (P_r) [49,50]. Combining equations 2.4 and 2.11 we get:

$$K_{eq} = \frac{A_b x'}{\sqrt{P_{eq}}} = \frac{A_b x'}{\sqrt{(RP_s - P_r) + (-RP_a + P_b)}} \tag{2.14}$$

It is clear that when the piston is not moving x'= 0, then K_{eq}= 0, and hence at least one of the valves is completely closed .

2.2.2 Powered Retraction Mode (PR):

The same analysis of the PE mode is applied here, except that the two valves used here are K_{sb} and K_{at}, the equivalent values obtained are:

$$K_{eq} = \frac{K_{sb} K_{at}}{\sqrt{R^3 K_{sb}^2 + K_{at}^2}} \tag{2.15}$$

$$P_{eq} = (P_s - RP_r) + (-P_b + RP_a) \tag{2.16}$$

$$K_{eq} = \frac{-A_b x'}{\sqrt{P_{eq}}} = \frac{-A_b x'}{\sqrt{(P_s - RP_r) + (-P_b + RP_a)}} \tag{2.17}$$

The minus sign indicates restriction (opposite direction of motion) [41].

2.2.3 High Side Regeneration Extension Mode (HSRE):

The same analysis is applied here again using K_{sa} and K_{sb} valves. The results are presented here will be all the possible combinations of the openings of the two valves that will achieve the desired speed under a specific loading condition. Further details are available in [47-50,45].

$$K_{eq} = \frac{K_{sa} K_{sb}}{\sqrt{R^3 K_{sb}^2 + K_{sa}^2}} \tag{2.18}$$

$$P_{eq} = (R - 1)P_s + (-RP_a + P_b) \tag{2.19}$$

$$K_{eq} = \frac{A_b x'}{\sqrt{P_{eq}}} = \frac{A_b x'}{\sqrt{(R-1)P_s + (-RP_a + P_b)}} \tag{2.20}$$

2.2.4 Low Side Regeneration Extension Mode (LSRE):

The same analysis is applied here again using K_{at} and K_{bt} valves. The results presented here will be all the possible combinations of the openings of the two valves that will achieve the desired speed under a specific loading condition [47].

$$K_{eq} = \frac{K_{at} K_{bt}}{\sqrt{R^3 K_{bt}^2 + K_{at}^2}} \tag{2.21}$$

$$P_{eq} = (R - 1)P_r + (-RP_a + P_b) \tag{2.22}$$

$$K_{eq} = \frac{A_b x'}{\sqrt{P_{eq}}} = \frac{A_b x'}{\sqrt{(R-1)P_r + (-RP_a + P_b)}} \quad (2.23)$$

2.2.5 Low Side Regeneration Retraction Mode (LSRR):

The same analysis is applied here again using K_{at} and K_{bt} valves. The results presented here will be all the possible combinations of the openings of the two valves that will achieve the desired speed under a specific loading condition [47].

$$K_{eq} = \frac{K_{bt}\, K_{at}}{\sqrt{K_{at}^2 + R^3 K_{bt}^2}} \quad (2.24)$$

$$P_{eq} = -(R - 1)P_r + (-P_b + RP_a) \quad (2.25)$$

$$K_{eq} = \frac{-A_b\, \dot{x}}{\sqrt{P_{eq}}} = \frac{A_b\, \dot{x}}{\sqrt{-(R-1)P_r + (-P_b + RP_a)}} \quad (2.26)$$

Again the negative sign indicates retraction (motion in the opposite direction).

2.3 Valve Control

This is done by providing the correct flow rate in and out of the cylinder chambers A and B, which are controlled through the valve openings of each chamber K_a and K_b. It is assumed that the desired speed is known, and it will be the command speed $\dot{x}_{com}$. If the load, the supply pressure, and the return pressure are all known, then we can use equation 2.26 to calculate the equivalent conductance coefficient:

$$K_{eq} = \frac{A_b \dot{x}_{com}}{\sqrt{P_{eq}}} \quad (2.27)$$

we can generalize the expression of K_{eq} to all modes and it can be written as:

$$K_{eq} = \frac{K_a K_b}{\sqrt{K_a^2 + R^3 K_b^2}} \quad (2.28)$$

K_{eq} depends on which mode is being used, but we generalize the results here where K_a and K_b can be either the openings to the supply or to the tank. As mentioned before, there is an infinite number of combinations that can achieve K_{eq} for each cylinder with constant area ration R, so it is important to plot the variation of K_{eq} as a function of both of K_a and K_b which result in a three dimensional surface. An example is when R=1.3405[47] which gives the surface shown in figure 10 [45].

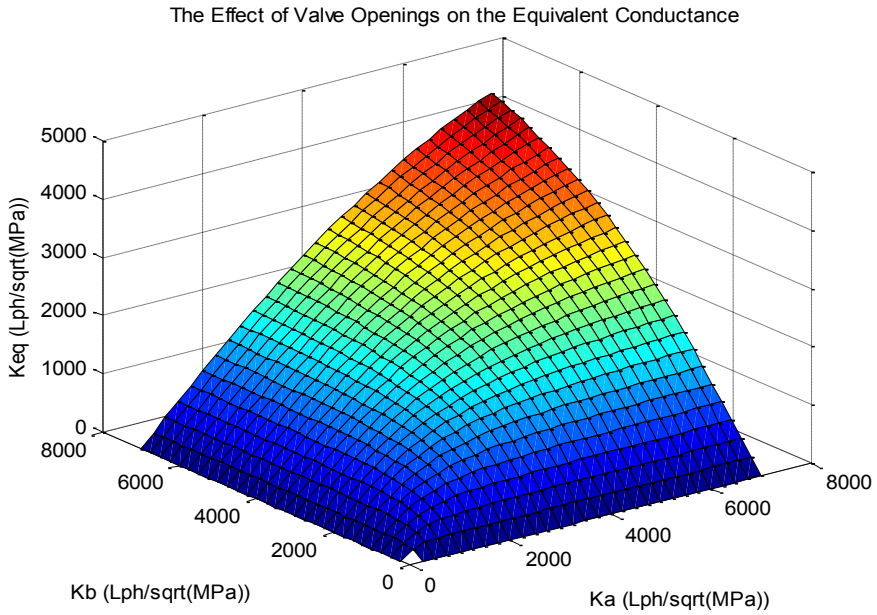

Figure 10. The equivalent conductance variation with the inlet and outlet valve openings

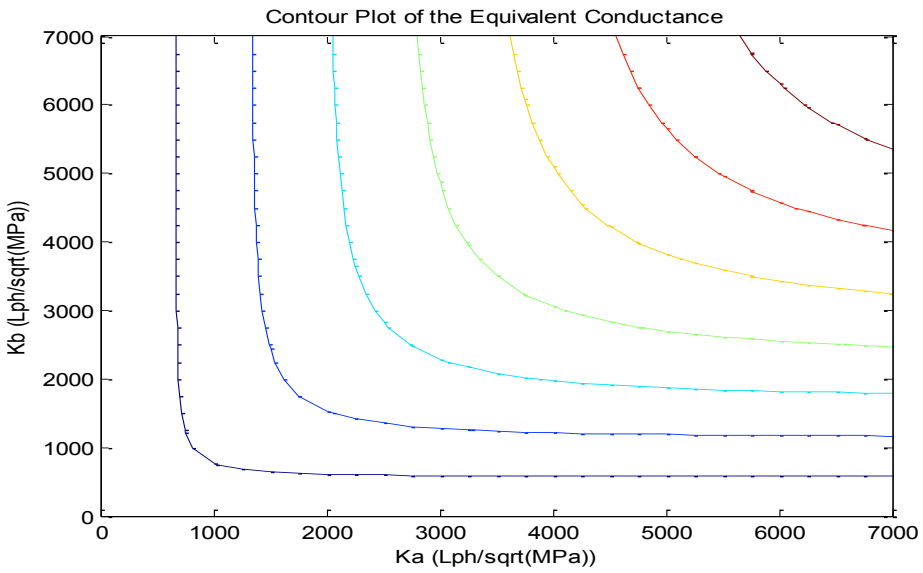

Figure 11. The equivalent conductance variation with the inlet and outlet valve openings(Keq=constant).

It is noticed that for every value of K_{eq}, there is one curve corresponding to the combination of two values of K_a and K_b [45]. The question then becomes which values of K_a and K_b should one choose among the infinite number of combinations?

2.3.1 Valve Sensitivity

The answer to the previous question is to choose the best combination of K_a and K_b, but again what constitutes the best combination? For a specific flow we need to achieve K_{eq} that will provide the needed opening for the flow. These openings are achieved by sending a commanded current to the solenoids that move in proportion to the commanded current and hence the speed of the motion of actuator. The problem is that this commanded current, which in theory corresponds to K_{eq}, may not achieve the desired opening at all pressures and temperatures. Then our choice of K_{eq} represented by figure 10 should be such that our controller is least affected by these variations. In other words, the controller should operate in the region of the curve that is least sensitive to valve errors in K_a and K_b, so K_{eq} should be least sensitive to errors in K_a and K_b. The method of magnitude of gradient was used by Tabor to measure the sensitivity of K_{eq} with respect to K_a and K_b [48,49].

$$|\nabla Keq| = \sqrt{\frac{K_a^6 + R^6 K_b^6}{(K_a^2 + R^3 K_b^2)^3}} \tag{2.29}$$

The graph of this equation yields the figure 12 [45]:

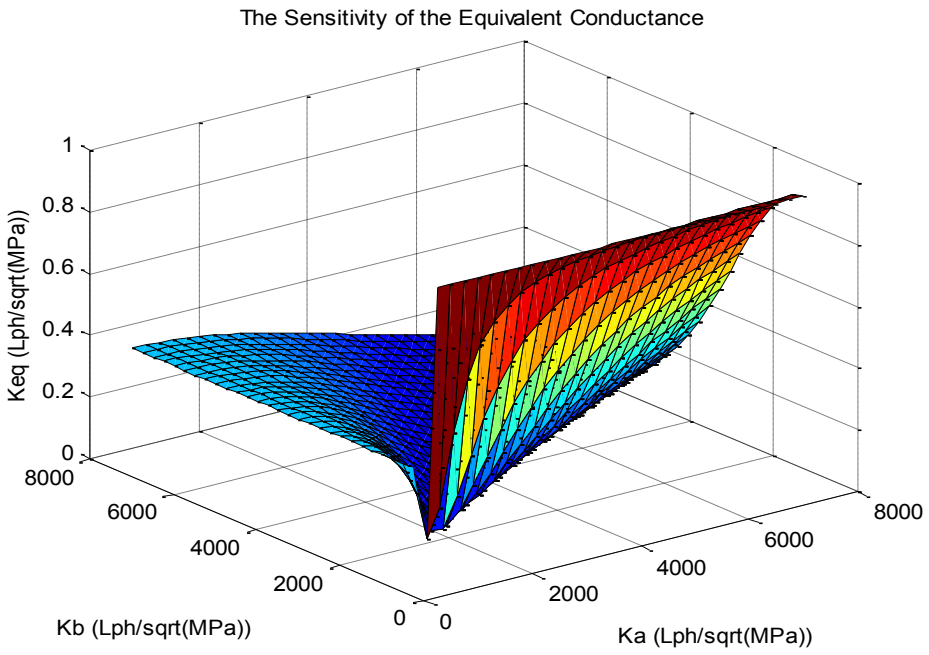

Figure 12.The sensitivity of K_{eq} to errors in K_a and K_b

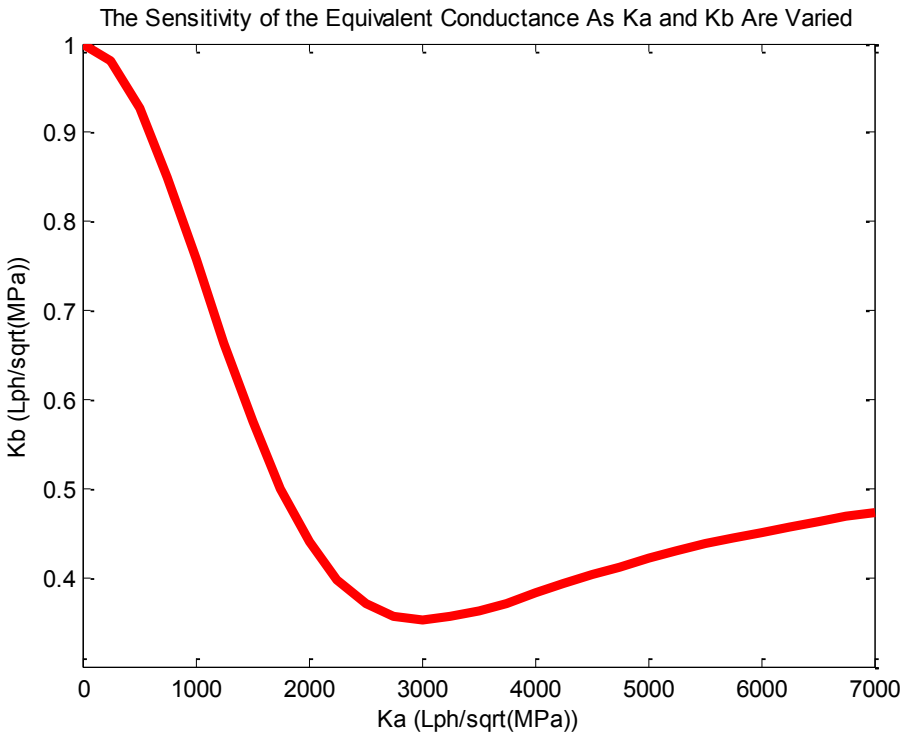

Figure 13. The gradient of the equivalent conductance at a specific inlet opening

Figures 12 and 13 represents the sensitivity of K_{eq} with respect to K_a and K_b as derived by the equation of magnitude of gradient. They show that there is a curve of minimum value, which means a curve that is least sensitive K_{eq}. Figure 13 shows this least sensitive curve in a two dimensional curve for a specific value of K_{eq} [45,58,49].

Figure 12 shows how K_{eq} varies with the variation of K_a and K_b. The bottom of the valley implies a linear relationship between K_a and K_b at which the gradient is minimum [50].

$$K_a = \alpha_{opt} K_b \tag{2.30}$$

This α_{opt} is found to be $R^{3/4}$, so the optimum combination of K_a and K_b which makes the controller least sensitive to error lies on a line where:

$$K_a = \alpha_{opt} K_b = R^{3/4} K_b \tag{2.31}$$

Figure 14 shows the contour plot of K_{eq} Vs K_a and K_b for $R = 1.5$ along with the optimum line.

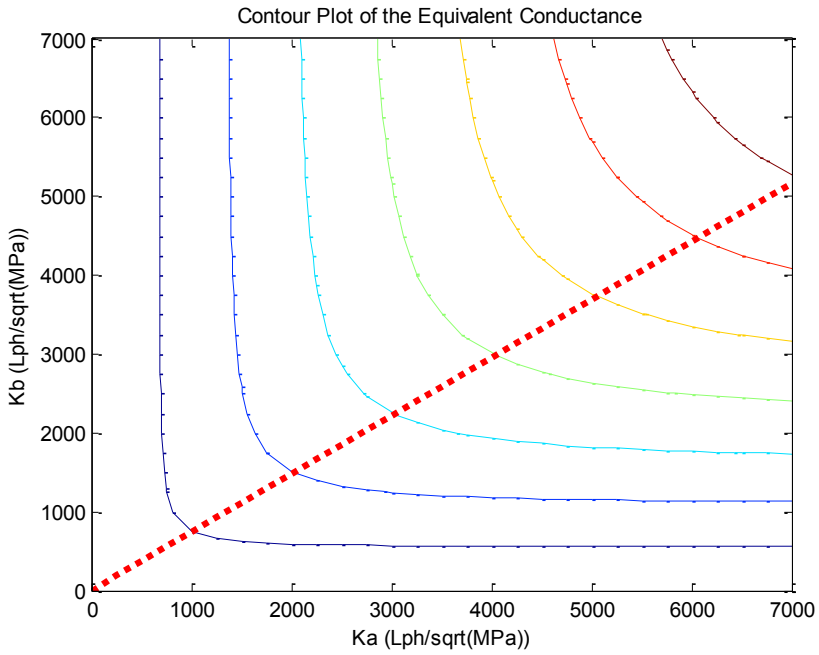

Figure 14. Contour plot of K_{eq} Vs K_a and K_b along with the optimal line

2.3.2 Physical Valve Limitations

There is a limit on how much we can open the valves on both the inlet and the outlet, if we look at figure 15, we see the limits of K_{out_max} and K_{in_max} when completely open represented by the vertical line for K_{in} and the horizontal line for K_{out}. Assuming our K_{eq} is represented by the curve shown, we now know only the values of K_a and K_b that lie within the box formed by the axes K_{in_max} and K_{out_max} can be used, which limits our choices of K_a and K_b [45].

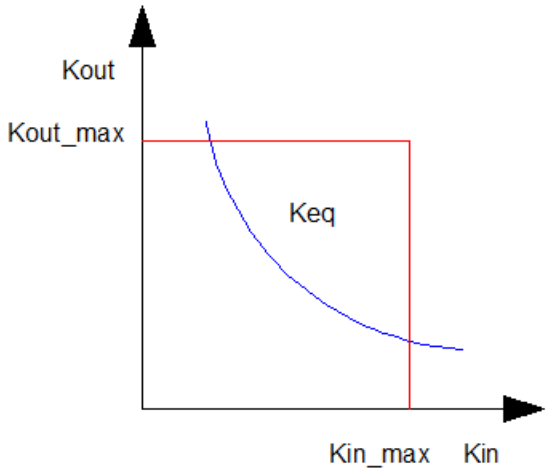

Figure 15. The valve control plot and the physical limitations of the valve openings.

2.3.3 Work Port Pressure Control

The goal of the controller is to provide the required flow to the piston in order to drive it at the desired speed while operating in the region that is least sensitive to error in terms of K_a and K_b, yet there is another concern , which is keeping the pressure in both cylinder chambers above cavitation pressure.

Cavitations occurs when the load acting on the cylinder causes one chamber to be filled with oil at a rate less than its expansion rate. If cavitation occurs, the equations are no longer valid, so to keep the controller working, cavitation must not occur. The methods used to prevent cavitation will be discussed later. There is also a maximum pressure limit on the work ports which is determined by piping and parts strength or else these parts will fail. Both maximum and minimum pressure for the chamber must be specified for the actuator. One advantage of the two degrees of freedom is the ability to control the outlet pressure for energy saving. The minimum pressure for chambers A and B will be called threshold pressure and will be denoted by P_{tha} and P_{thb} respectively. These threshold pressures are represented on the control valve plot by horizontal and vertical lines. The threshold pressures are expressed by previous equations as:

$$Kin_{th} = \frac{q_{in}}{\sqrt{\Delta P_{in}}} \tag{2.32}$$

$$Kout_{th} = \frac{q_{out}}{\sqrt{\Delta P_{out}}} \tag{2.33}$$

But there will be a slight variation depending on the metering mode [48,49].

2.3.3.1 Inlet Chamber Pressure Control

The threshold conductance coefficient can be written for every mode according to the threshold pressure at that chamber. The PE mode will be studied here in details and only the results will be presented for the rest of the modes [50]. For the inlet head chamber A:

$$Kin_{th} = Ksa_{th} = \frac{|\dot{x}|A_a}{\sqrt{P_s - P_{tha}}} \tag{2.34}$$

From this equation we notice that for a pressure above the threshold, one must maintain K above K_{sath} to prevent cavitation. This means we must keep the opening big enough to allow enough fluid to flow to fill the chamber at the required rate. This is shown in figure 16 on the valve control plot [45]:

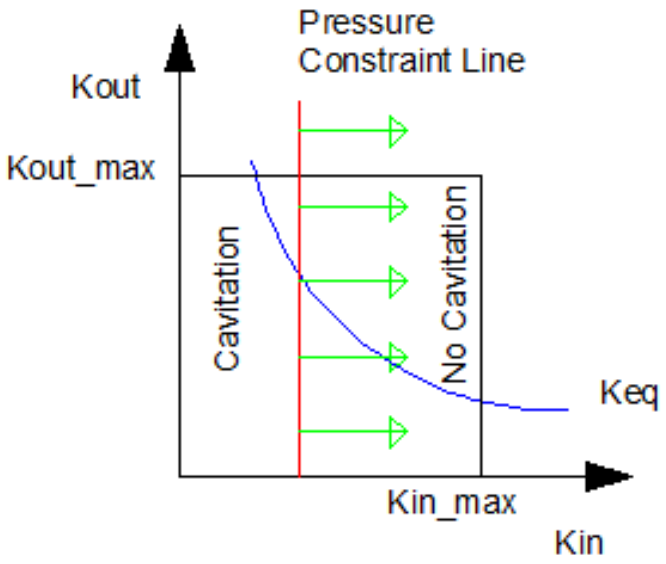

Figure 16. Minimum inlet valve opening corresponding to minimum pressure before cavitation occurs

On the high side, the inlet pressure must not go above the design limit determined by the piping and parts maximum stress, and the inlet pressure must be below that maximum pressure. This is explained in figure 17.

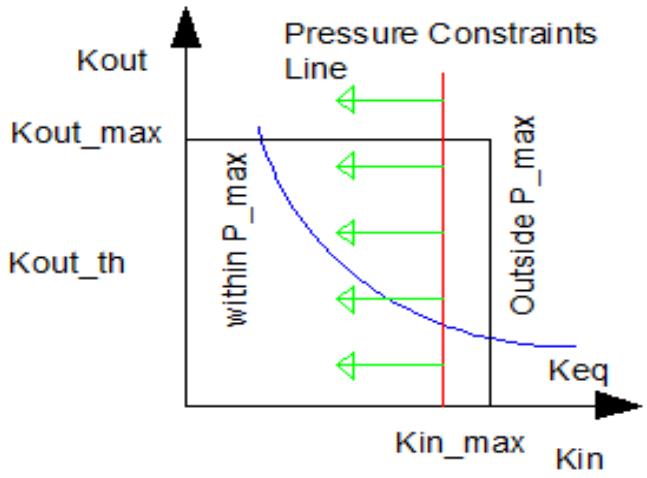

Figure 17. Maximum inlet valve opening corresponding to maximum pressure allowed.

This means that when the inlet valve opening is increased, less pressure drop occurs across the valve, which translates to higher pressure in the inlet chamber. On the other hand, if the inlet valve opening is reduced, more pressure drop occurs across the valve and less pressure at the inlet chamber [45].

2.3.3.2 Outlet Chamber Pressure Control

For the powered extension mode, the governing equation becomes:

$$Kout_{th} = Kbt_{th} = \frac{|\dot{x}|A_b}{\sqrt{P_{thb} - P_r}} \tag{2.35}$$

since in most cases the outlet chamber will be connected to the tank or to a relief valve which will be at low pressure, we will not worry about the minimum pressure to avoid cavitation. The maximum pressure that we should not exceed is the design pressure of the piping and parts. This means we must keep the outlet opening above K_{outth} as shown in the figure 18 [45].

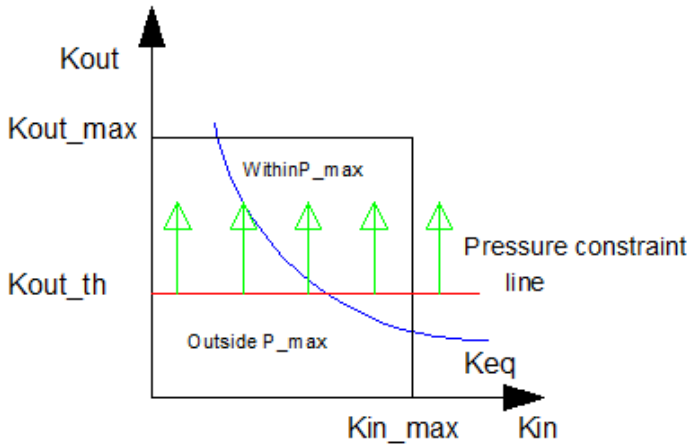

Figure 18. Maximum outlet valve opening corresponding to maximum design pressure.

Physically, this means that as we increase the outlet valve opening, there will be less pressure drop across the valve, and the outlet chamber pressure will not build up much higher than the return pressure.

2.3.4 Control Valve Summary

The velocity of the actuator is controlled by the flow rate in and out of the actuator inlet and outlet chambers. The flow is proportional to the pressure and the openings of the chambers K_a and K_b. These openings are proportional to the current commanded to the solenoids that move the poppets or spools. Unfortunately this current may not achieve the needed K_{eq} under all pressures and temperatures, so it is important to choose K_a and K_b where the current is least sensitive to errors in K_a and K_b which was shown in figure 11[47].

The second issue is making sure that cavitation does not occur in the inlet chamber. That is why a minimum pressure should be maintained and no pressure drop below it should be allowed [48].

Finally, there is a limit on the maximum pressure allowed which is determined by the design pressure of the piping and parts of the system, and this pressure should not be exceeded. One should know that there is a physical maximum opening for the inlet and outlet K_{in_max} and K_{out_max} that can be reached for a certain valve [50].

All four conditions are expressed as horizontal and vertical lines on the valve control plot (figure 19).

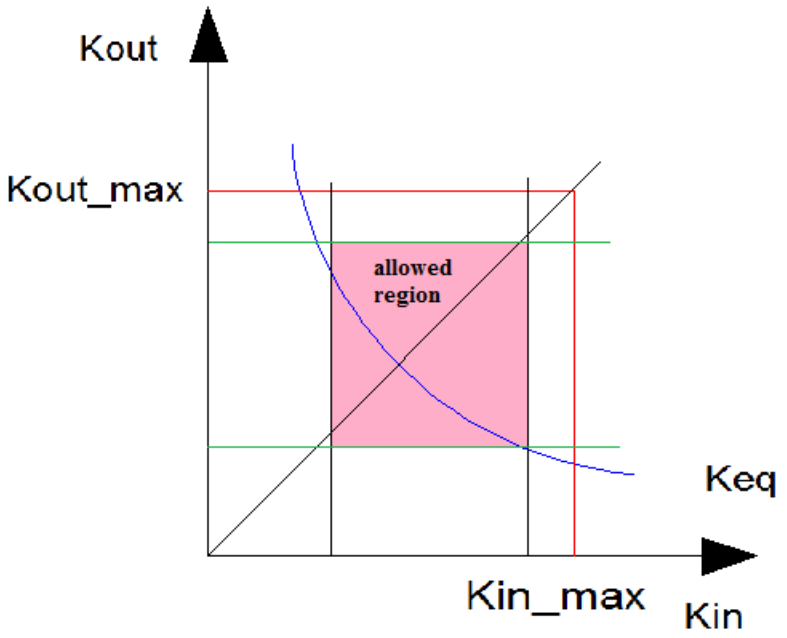

Figure 19. Limitations on valve openings

The IMV setup allows for controlling the actuator velocity while limiting the pressure in both chambers. The choice of the operating point should take into consideration the following physical limitations: work port pressure limitations, the actuator speed, and sensitivity to error. The next question becomes which of these parameters is more important?

It is clear that physical limitation is out of our control, so one should choose pressure in work ports to prevent cavitation on the low side and not exceed the design limitation on the high side. Then our goal is to achieve the desired speed of the actuator, and finally, the system should be operated at the least sensitive point to error if possible [45].

2.4 Supply Pressure Set Point

The source of the hydraulic power is the pump. The flow rate which determines the speed of the actuator, and the pressure which determines the maximum force will define the needed pressure required by the pump. Therefore we need to derive the equations of the supply pressure set point which is the pressure that must be supplied by the pump to move a certain load at a desired speed. Of course this supply pressure set point depends on the mode of operation.

2.4.1 Pressure Supply Set Point for Powered Extension Mode

It was found in equation 2.14, for PE mode that:

$$Keq = \frac{A_b \dot{x}}{\sqrt{P_{eq}}} = \frac{A_b \dot{x}}{\sqrt{(R P_s - P_r) + (-RP_a + P_b)}} \tag{2.36}$$

Replacing P_s by $P_{S,\,set\_point1}$ and squaring

$$Ps_{set-point1} = \frac{\dot{x}^2 A_b^2}{RK_{eq}^2} + \frac{(RP_a - P_b)}{R} + \frac{P_r}{R} \tag{2.37}$$

Electro-Hydraulic Poppet Valves require a minimum pressure drop across them for optimum performance, which must be supplied by the supply pressure set point, whether or not the velocity requirements demand such a set pressure. Figure 20 explains this point in more details [45,47,48].

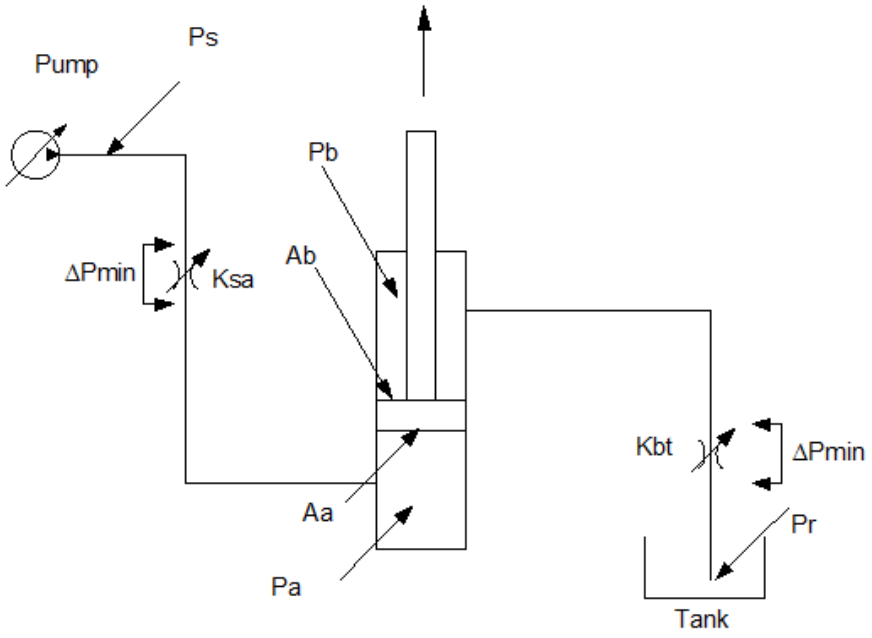

Figure 20. Minimum equivalent pressure including the minimum pressure drop across the valve.

The other minimum pressure requirement comes from the required equivalent pressure. Recall from equation 13 that:

$$P_{eq} = (RP_S - P_r) + (-RP_a + P_b) \tag{2.38}$$

$$Peq_{min} = (R+1)\Delta P_{min} \tag{2.39}$$

$$Ps_{set-point2} = \frac{Peq_{min}}{R} + \frac{(RP_a - P_b)}{R} + \frac{P_r}{R} \tag{2.40}$$

$$Ps_{set-point} = \max\left(Ps_{set-point1}, Ps_{set-point2}\right) \tag{2.41}$$

The same analysis applies to the rest of the modes, and the results are presented below.

2.4.2 Powered Retraction Mode

$$Ps_{set-point1} = \frac{\dot{x}^2 A_b^2}{K_{eq}^2} - RPa + Pb + RPr \tag{2.42}$$

$$Ps_{set-point2} = Peq_{min} - RPa + Pb + RPr \tag{2.43}$$

2.4.3 High Side Regeneration Extension Mode

$$Ps_{set-point1} = \frac{\dot{x}^2 A_b^2}{(R-1)K_{eq}^2} + \frac{(RPa - Pb)}{R-1} \tag{2.44}$$

$$Ps_{set-point2} = \frac{Peq_{min}}{R-1} + \frac{(RP_a - P_b)}{R-1} \tag{2.45}$$

2.4.4 Low Side Regeneration Modes

There is a supply pressure, yet a minimum pressure is needed for flow circulation. The return set point pressure needed is derived just like the supply pressure set point was derived:

$$Pr_{set-point1} = \frac{\dot{x}^2 A_b^2}{(R-1)K_{eq}^2} + \frac{(RPa - Pb)}{R-1} \tag{2.46}$$

$$Pr_{set-point2} = \frac{Peq_{min}}{R-1} + \frac{(RP_a - P_b)}{R-1} \tag{2.47}$$

$$Pr_{set-point} = \max\left(Pr_{set-point1}, Pr_{set-point2}\right) \tag{2.48}$$

In the case of low side regeneration retraction, the minimum value is P_r. In the case of the multi circuit system, each circuit is treated separately, and then the maximum supply pressure set point of all circuits is used as the supply pressure that must be supplied by the pump [48,50].

2.5 Anti-Cavitation Analysis

Cavitation occurs when the load causes one of the chambers to expand at a rate faster than oil can fill that space, which leads to negative or zero pressure in the inlet chamber. If this happens, control is lost, so cavitation must be prevented.

A minimum threshold pressure must be kept in the inlet chamber and the pressure must not go below it. This was shown as horizontal and vertical lines on the valve control plot, but how this relates to the load condition, and how to control the openings to avoid cavitation is explained next. The ratio of the valve opening $\alpha = K_a/K_b$ is the decisive factor for cavitation $F_{L,cav} = F\ (\alpha)$ and it depends on the mode of operation. If we have a load that acts under certain conditions and the cavitation occurs at a certain opening ratio, then the solution is to change this ratio to another value . Next we discuss the details for all modes [45].

2.5.1 Cavitation in Powered Extension Mode

Figure 21 shows PE mode under overrunning load, which means the cylinder is extending in the same direction the load is acting:

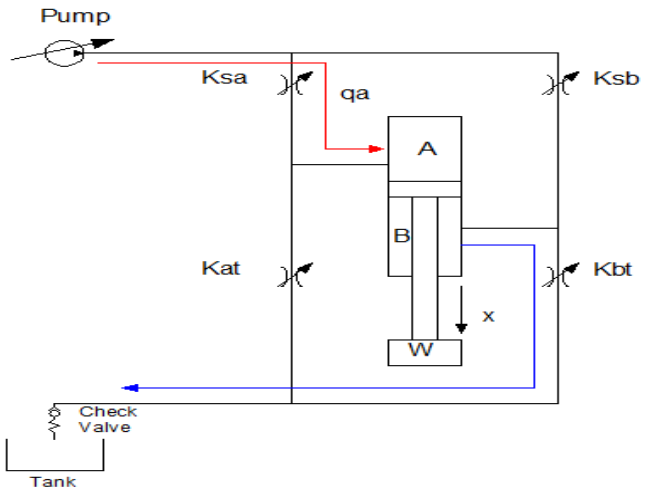

Figure 21. Overrunning load acting on a cylinder in powered extension mode.

$$F_{Hydraulic} = P_a A_a - P_b A_b = F_L - F_f \tag{2.49}$$

where the load force in this case is equal to the weight and F_f is the friction force. Rearrange this equation:

$$P_b = \frac{P_a A_a + F_L - F_f}{A_b} \tag{2.50}$$

From the flow equation:

$$q_a = A_a \dot{x} = K_{sa}\sqrt{\Delta P1} = K_{sa}\sqrt{P_s - P_a} \tag{2.51}$$

$$q_b = A_b \dot{x} = K_{bt}\sqrt{\Delta P2} = K_{bt}\sqrt{P_b - P_r} \tag{2.52}$$

Divide equation 51 by equation 52:

$$\frac{q_a}{q_b} = R = \alpha\sqrt{\frac{\Delta P_1}{\Delta P_2}} \tag{2.53}$$

Recall that $R = A_a/A_b$ and $\alpha = K_{sa}/K_{sb}$, square and rearrange:

$$\Delta P_2 = \left(\frac{\alpha}{R}\right)^2 \Delta P_1 \tag{2.54}$$

$$P_b - P_r = \left(\frac{\alpha}{R}\right)^2 (P_s - P_a) \tag{2.55}$$

$$P_b = \left(\frac{\alpha}{R}\right)^2 (P_s - P_a) + P_r \tag{2.56}$$

But equations 50 and 56 are equal, solving for P_a we get

$$P_a A_a + F_L - F_f = P_r A_b + \left(\left(\frac{\alpha}{R}\right)^2 P_s - \left(\frac{\alpha}{R}\right)^2 P_a\right) A_b \tag{2.57}$$

$$P_a \left[A_a + \left(\frac{\alpha}{R}\right)^2 A_b\right] = \left(\frac{\alpha}{R}\right)^2 A_b P_s - (F_L - F_f) + P_r A_b \tag{2.58}$$

$$P_a = \frac{\left(\frac{\alpha}{R}\right)^2 A_b P_s - (F_L - F_f) + P_r A_b}{\left[A_a + \left(\frac{\alpha}{R}\right)^2 A_b\right]} \tag{2.59}$$

Divide by A_b

$$P_a = \frac{\left(\frac{\alpha}{R}\right)^2 P_s - \frac{(F_L - F_f)}{A_b} + P_r}{\left[R + \left(\frac{\alpha}{R}\right)^2\right]} \tag{2.60}$$

The criterion for cavitation is that P_a must be positive or zero, for the limiting case where P_a=0

$$\left(\frac{\alpha}{R}\right)^2 A_b P_s + P_r A_b = \frac{(F_L - F_f)}{A_b} \tag{2.61}$$

$$F_L = \left(\frac{\alpha}{R}\right)^2 A_b P_s + P_r A_b + F_f \tag{2.62}$$

To illustrate using some real data we have the case of an actual tractor loader backhoe bucket cylinder. The parameters are as follow: R=1.658, A_b=4737mm^2, P_s=20MPa, P_r=0.7MPa, and F_f=0.

The optimum value of α occurs at $R^{3/4}$=1.461 and the corresponding load is 77KN. The results are plotted in figure 22.

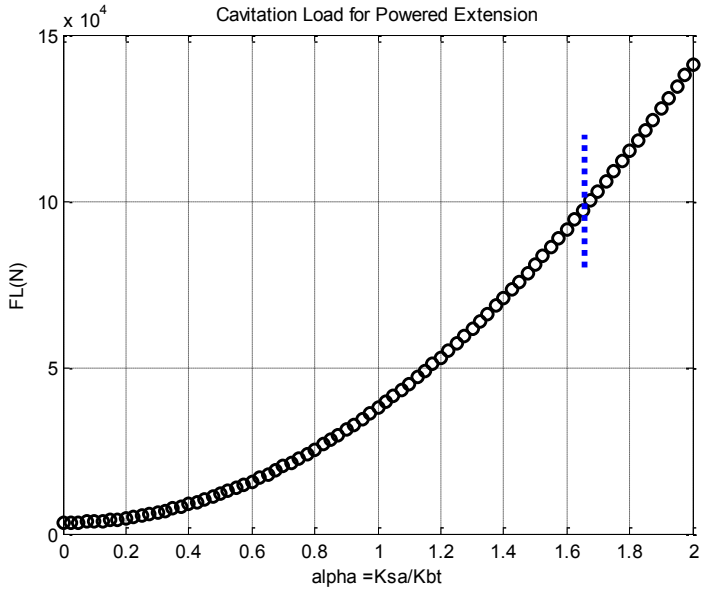

Figure 22. The cavitation load as a function of the valve ratio for PE mode.

How can this be useful? Recall that the controller has the values R, A_b, P_s, and P_r at our disposal. The friction either neglected or estimated as a function of pressure. Going back to the force equation:

$$F_{Hydraulic} = P_a A_a - P_b A_b = F_L - F_f \tag{2.63}$$

F_L becomes known, and the cavitation condition occurs at P_a=0 from equation 62 then:

$$\alpha = R \times \sqrt{\frac{F_L - F_f - P_r A_b}{P_s A_b}} \tag{2.64}$$

This means that any other value will not cause cavitation, which means higher loads can be moved by reducing the valve opening K_{bt} and increasing the valve opening K_{sa} [45].

2.5.2 Cavitation in Powered Retraction Mode

Figure 23 shows the powered retraction, the load is subjected to overrunning load.

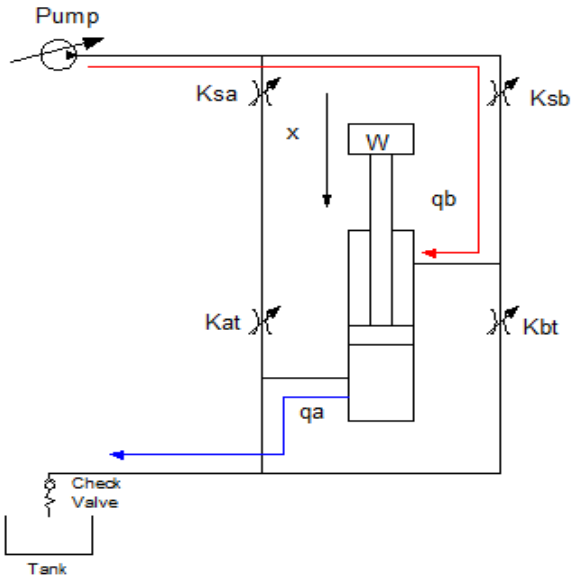

Figure 23. Overrunning load acting on a cylinder in PR mode.

$$P_a = \frac{P_b}{R} + \frac{(F_L - F_f)}{A_a} \tag{2.65}$$

$$P_a = \left(\frac{\alpha}{R}\right)^2 (P_s - P_b) + P_r \tag{2.66}$$

$$P_b = \frac{\left(\frac{R}{\alpha}\right)^2 P_s - \frac{F_L - F_f}{A_a} + P_r}{\frac{1}{R} + \frac{R}{\alpha}} \tag{2.67}$$

Cavitation condition require $P_b \leq 0$, substitute for $P_b = 0$ and solve for F_L:

$$F_L = \left(\frac{R}{\alpha}\right)^2 A_a P_s + A_a P_r + F_f \tag{2.68}$$

Going back to the same example as before, plotting F_L Vs α in figure 24. We find that at α_{opt} F_L=210 KN, which is the biggest load so far [45].

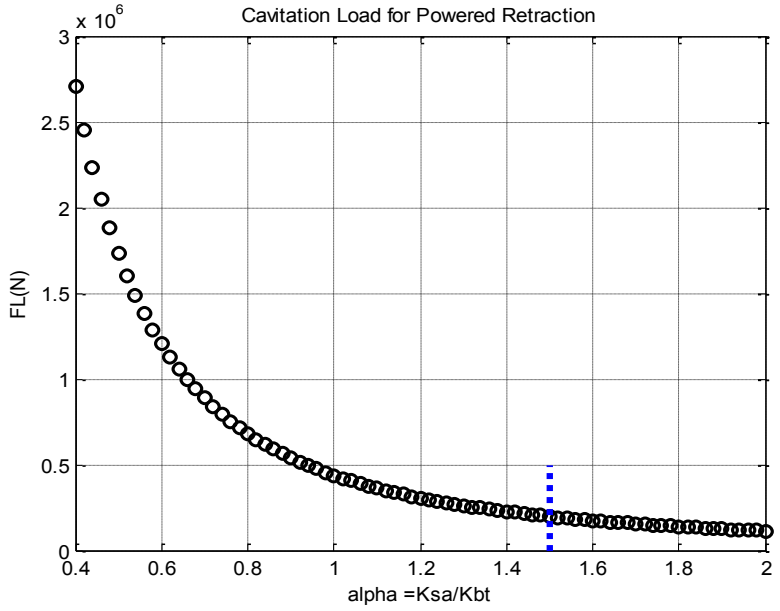

Figure 24. The cavitation load as a function of the valve ratio for PR mode.

2.5.3 Cavitation in High Side Regeneration Extension Mode

Figure 25 shows HSRE mode with overrunning load.

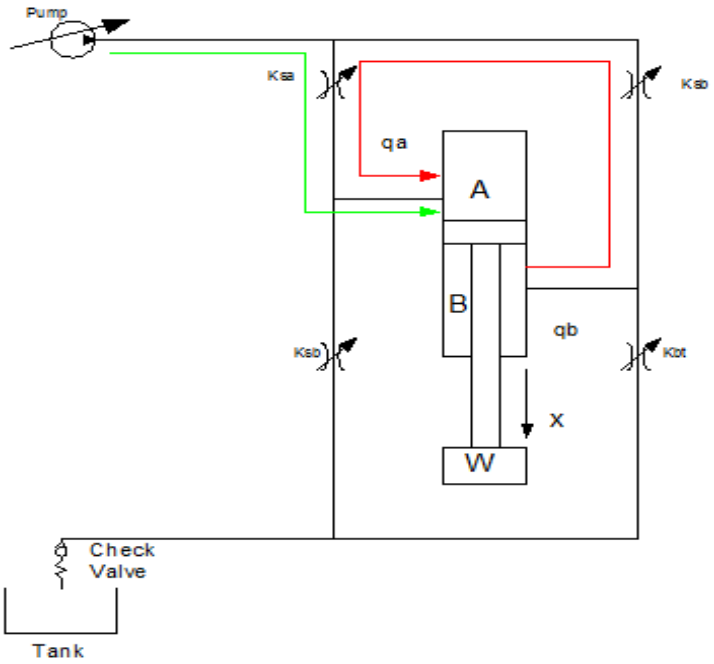

Figure 25. Overrunning load acting on a cylinder in HSRE mode.

Following the same analysis we get:

$$P_b = \left(\frac{\alpha}{R}\right)^2 (P_s - P_a) + P_s \tag{2.69}$$

$$P_a = \frac{[1+\left(\frac{\alpha}{R}\right)^2]P_s - \frac{(F_L - F_f)}{A_b}}{\left[R+\left(\frac{\alpha}{R}\right)^2\right]} \tag{2.70}$$

$$F_L = [1 + \left(\frac{\alpha}{R}\right)^2]A_b P_s + F_f \tag{2.71}$$

Again, plotting F_L Vs α, we get figure 26:

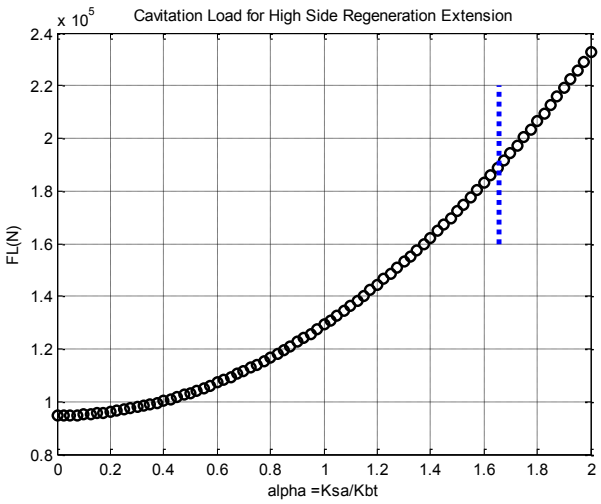

Figure 26. The cavitation load as a function of the valve ratio for HSRE mode.

For the values of the previous example; F_L =168KN. This means we can operate to move much higher loads in HSRE mode without cavitation in comparison with PE mode [45].

2.5.4 Cavitation in Low Side Regeneration Extension Mode

Figure 27 shows LSRE under overrunning load. The deficiency of flow is assumed to be supplied at zero pressure and hence does not affect cavitation.

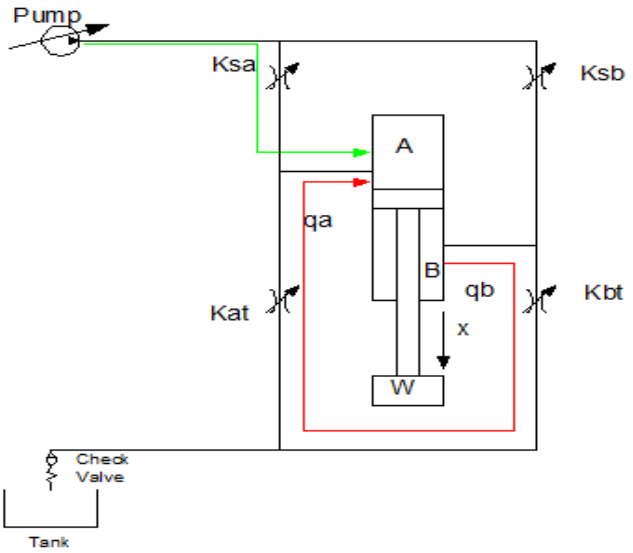

Figure 27. Overrunning load acting on a cylinder in LSRE mode.

$$P_b = RP_a + \frac{F_L - F_f}{P_b} \tag{2.72}$$

$$P_a = \frac{[1+\left(\frac{\alpha}{R}\right)^2]P_r - \frac{(F_L - F_f)}{A_b}}{\left[R+\left(\frac{\alpha}{R}\right)^2\right]} \tag{2.73}$$

$$F_L = [1 + \left(\frac{\alpha}{R}\right)^2]A_b P_r + F_f \tag{2.74}$$

Going back to the same example as before, plotting F_L Vs α, at α_{opt}, F_L= 5.9 KN. This means cavitation can occur at a much lower load than PE or HSRE modes for the same value α. Again, plotting F_L Vs α, we get figure 28 [45]:

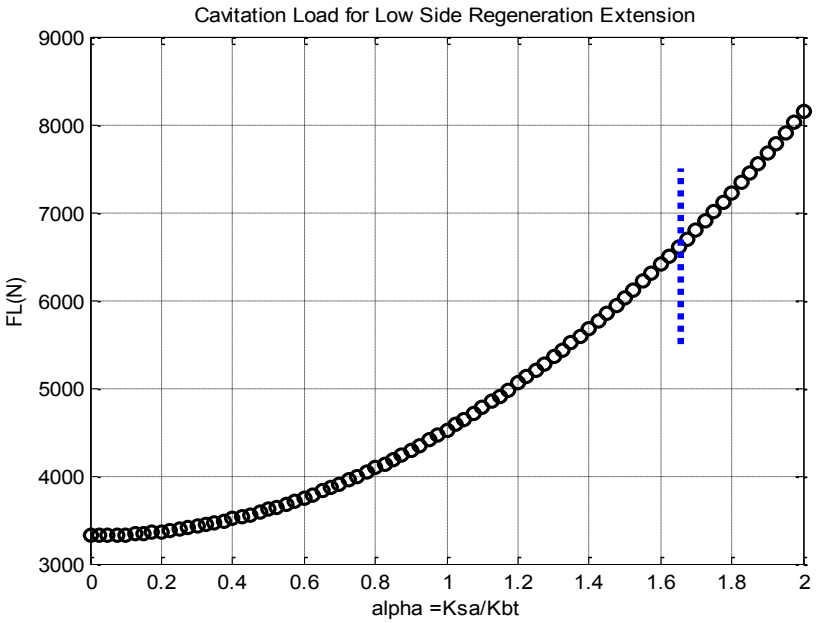

Figure 28. The cavitation load as a function of the valve ratio for LSRE mode.

2.5.5 Cavitation in Low Side Regeneration Retraction Mode

Figure 29 shows LSRR mode subjected to an overrunning load.

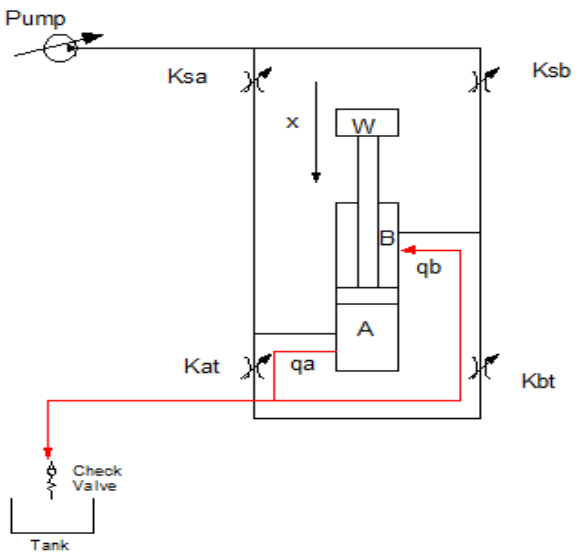

Figure 29. Overrunning load acting on a cylinder in LSRR mode.

$$P_a = \frac{P_b}{R} + \frac{(F_L - F_f)}{A_a} \tag{2.75}$$

$$P_a = \left(\frac{\alpha}{R}\right)^2 (P_r - P_b) + P_r \tag{2.76}$$

$$P_a = \frac{[1+\left(\frac{\alpha}{R}\right)^2]P_r - \frac{(F_L - F_f)}{A_b} + P_r}{\left[\frac{1}{R}+\left(\frac{\alpha}{R}\right)^2\right]} \tag{2.77}$$

$$F_L = [1 + \left(\frac{\alpha}{R}\right)^2]A_a P_r + F_f \tag{2.78}$$

Going back to the same example as before, plotting F_L Vs α, at α_{opt} F_L=12.5 KN, which is much lower than PR mode. Again, plotting F_L Vs α, we get figure 30:

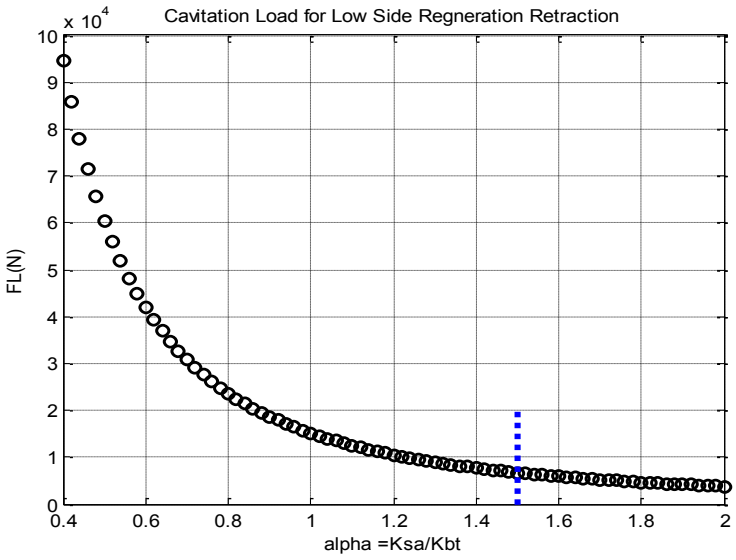

Figure 30. The cavitation load as a function of the valve ratio for PR mode.

From the previous analysis, we notice that HSRE mode is best for cavitation load, while LSRE was the worst. Low side regeneration extension and retraction were the critical cases where low loads can cause cavitation, but how does this relate to valve control plots? For PE $\alpha=K_a/K_b$ is a straight line whose slope is $K_b/K_a=1/\alpha$ as shown in figure 31 [45].

Assuming this is the critical ratio α_{crit} that would cause cavitation at the given load. The intersection of the line with the K_{eq} curve is our operating point for the desired speed. Any point to the right or below that line means higher than α_{cav} that would cause cavitation. By choosing higher α we decrease the slope and make cavitation worse, so the goal is to decrease α and increase the slope as much as possible.

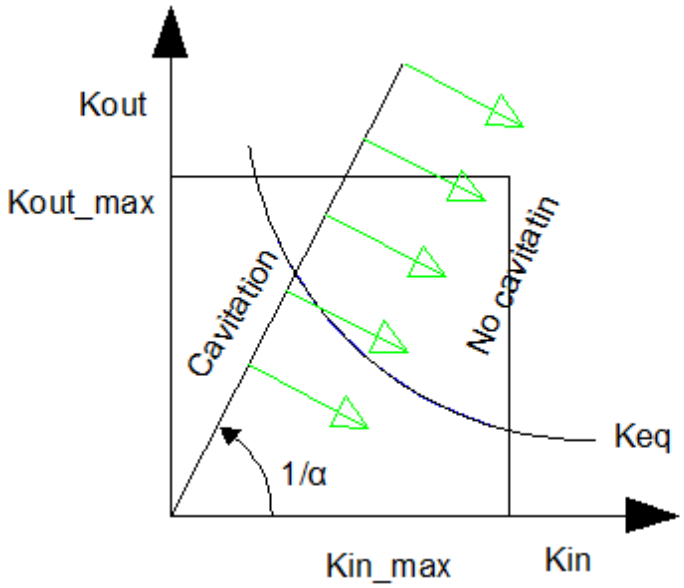

Figure 31. The valve ratio α as shown on the valve control plot.

Table 1. Cavitation load Comparison

	R = 1.658	A_b = 4737 mm^2	P_s = 20MPa	**P_r = 0.7MPa**	F_f = 0
Mode	PE	PR	HSRE	LSRE	LSRR
Cavitation Load (KN)	77	210	168	5.9	12.5

2.6 High Side Regeneration Retraction Mode

2.6.1 Introduction

In this section the HSRR is introduced as a concept and the equations are derived as was done to the five modes, this mode was not considered in previous work by Shenouda [45]. Opdenbosch

mentioned it as another IMV arrangement but did not discuss it further than that [36]. Here all the derivations concerning the equivalent pressure and equivalent conductance are derived, then the pressure supply set point, which is the return pressure in this case, is then found, next the cavitation equations are visited and the cavitation force is found.

The last part of this section presents a table that compares the new equations suggested here to the previous works.

2.6.2 Concept and Equivalent Circuit

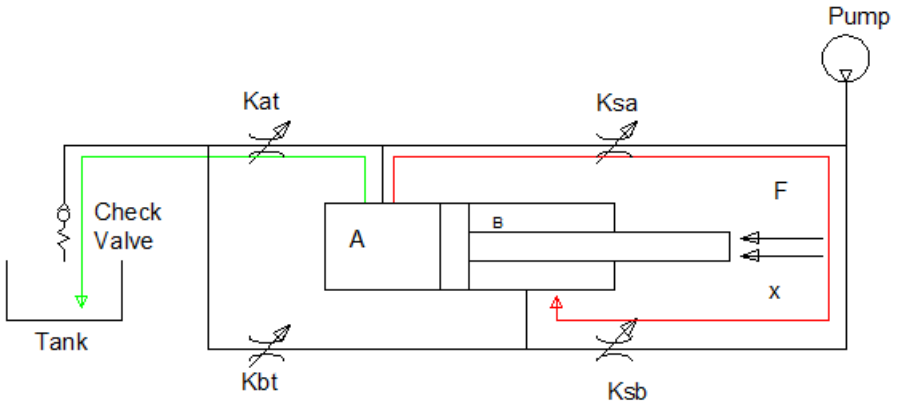

Figure 32. The concept of the HSRR.

$$P_{eq} = DR(P_r - P_A) + D(P_B - P_r) \tag{2.79}$$

$$P_r = \left((RP_a - P_b) - P_{eqmin}\right) \times 1/R - 1 \tag{2.80}$$

$$K_{eq} = \sqrt{{K_{sa}}^2 + {K_{sb}}^2} \tag{2.81}$$

The equations for all the modes become as shown in the table below, the equations derived in [45], are compared to the results and formulation of this research;

Table 2. New and previous formulation of the equivalent pressure.

Equivalent Pressure	Current Paper Formulation	Previous Works Formulation
PE	$DR(P_s - P_A) + D(P_B - P_r)$	$(RP_s - P_r) + (-RP_A + P_B)$
HSRR	$DR(P_s - P_A) + D(P_B - P_s)$	$(R-1)P_s + (-RP_a + P_b)$
LSRE	$DR(P_r - P_A) + D(P_B - P_r)$	$(R-1)P_r + (-RP_a + P_b)$
PR	$DR(P_r - P_A) + D(P_B - P_s)$	$(P_s - RP_r) + (-P_b + RP_a)$
HSRR	$DR(P_r - P_A) + D(P_B - P_r)$	----------
LSRR	$DR(P_r - P_A) + D(P_B - P_r)$	$-(R-1)P_r + (-P_b + RP_a)$

2.6.3 Cavitation Derivation

The same procedure is repeated for this mode as for the other modes

$$F_{Hydraulic} = P_a A_a - P_b A_b = F_L - F_f \tag{2.82}$$

where the load force in this case is equal to the weight and F_f is the friction force. Rearrange this equation:

$$P_b = \frac{P_a A_a + F_L - F_f}{A_b} \tag{2.83}$$

From the flow equation:

$$q_a = A_a \dot{x} = K_{sa}\sqrt{\Delta P1} = K_{sa}\sqrt{P_a - P_r} \tag{2.84}$$

$$q_b = A_b \dot{x} = K_{bt}\sqrt{\Delta P2} = K_{bt}\sqrt{P_r - P_b} \tag{2.85}$$

Divide equation 84 by equation 85:

$$\frac{q_a}{q_b} = R = \alpha\sqrt{\frac{\Delta P_1}{\Delta P_2}} \tag{2.86}$$

Recall that $R = A_a/A_b$ and $\alpha = K_{sa}/K_{sb}$, square and rearrange:

$$\Delta P_2 = \left(\frac{\alpha}{R}\right)^2 \Delta P_1 \tag{2.87}$$

$$P_r - P_b = \left(\frac{\alpha}{R}\right)^2 (P_r - P_a) \tag{2.88}$$

$$P_b = \left(\frac{\alpha}{R}\right)^2 (P_r - P_a) + P_r \tag{2.89}$$

But equations 82and 88 are equal, solving for P_a we get

$$P_a A_a + F_L - F_f = P_r A_b + \left(\left(\frac{\alpha}{R}\right)^2 P_s - \left(\frac{\alpha}{R}\right)^2 P_a\right) A_b \tag{2.90}$$

$$P_a \left[A_a + \left(\frac{\alpha}{R}\right)^2 A_b\right] = \left(\frac{\alpha}{R}\right)^2 A_b P_r + (F_L - F_f) + P_r A_b \tag{2.91}$$

$$P_a = \frac{\left(\frac{\alpha}{R}\right)^2 A_b P_r + (F_L - F_f) + P_r A_b}{\left[A_a + \left(\frac{\alpha}{R}\right)^2 A_b\right]} \tag{2.92}$$

Divide by A_b

$$\Rightarrow P_a = \frac{\left(\frac{\alpha}{R}\right)^2 P_r + \frac{(F_L - F_f)}{A_b} + P_r}{\left[R + \left(\frac{\alpha}{R}\right)^2\right]} \tag{2.93}$$

The criterion for cavitation is that P_a must be positive or zero, for the limiting case where P_a=0

$$\left(\frac{\alpha}{R}\right)^2 A_b P_r + P_r A_b = \frac{(F_L - F_f)}{A_b} \tag{2.94}$$

$$\Rightarrow F_L = P_a A_a - \left(\left(\frac{\alpha}{R}\right)^2 A_b (P_r - P_a) + P_r A_b + F_f\right) \tag{2.95}$$

Table 3. Cavitation load Comparison

	R = 1.658	A_b = 4737 mm^2	P_s = 20MPa	**P_r = 0.7MPa**	F_f = 0	
Mode	PE	PR	HSRE	HSRR	LSRE	LSRR
Cavitation Load (KN)	77	210	168	5.9	5.9	12.5

3 IMV BASED HYDRAULIC SYSTEM MODELING

The five modes of IMVs are different in terms of their equations and pressure set point, but it is necessary to unify all of them in a general format to make it more systematic for analysis. That is why the idea of valve switching function is introduced by Shenouda [45]. A simplified second order dynamic model of the poppet valves is introduced and validated for the individual valves; and then a state space representation is provided [33,41,45].

3.1 Valve Switching Functions

Previously we derived the equations for each mode along with its pressure set point, its equivalent conductance, equivalent pressure, cavitation condition, etc. The process of analyzing and controlling the model of the system must be repeated for each mode. That is why the valve switching function unifies all five modes.

We start by defining universal parameters for the IMVs. Looking at figure 32, we notice that the head chamber A has two valves K_{sa} and K_{at}, which we will call branch A. The same is true for rod chamber B, with valves K_{sb} and K_{bt}, which we will call branch B [1,2].

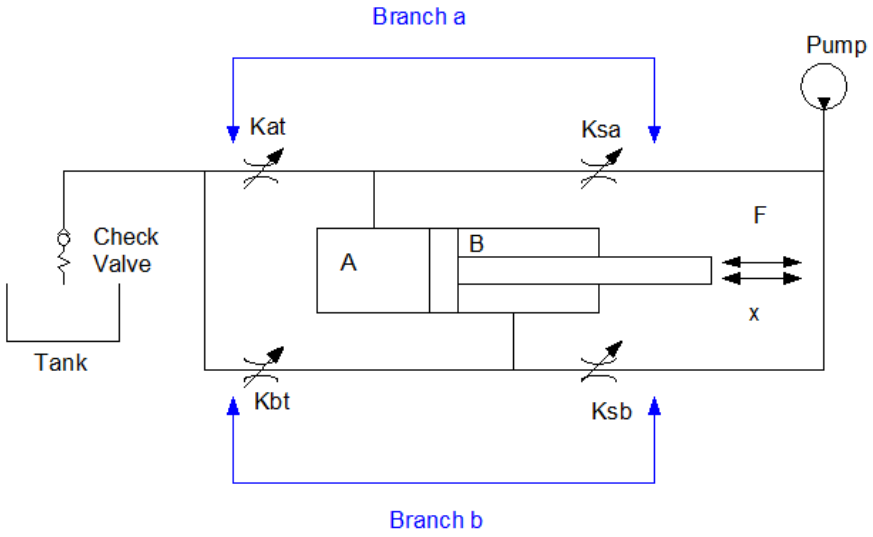

Figure 33. Schematic of valve switching function.

Then we define the following switching functions of the valves.

$$S_a = \begin{cases} 1 & when\ K_{sa}\ is\ open \\ -1 & when\ K_{at}\ is\ open \end{cases}$$

$$S_b = \begin{cases} 1 & when\ Ksb\ is\ open \\ -1 & when\ Kbt\ is\ open \end{cases}$$

Since the actuator can be either extending or retracting, we must define a parameter to express this motion, so we define the direction $D = 1$ for extension, and $D = -1$ for retraction. This enables us to define any mode by the following space (S_A, S_b, and D) as follows:

Table 4. Switching function representation.

	Valve mode	Switching Pattern
1	Powered Extension (PE)	[1,-1, 1]
2	Powered Retraction (PR)	[-1, 1,-1]
3	High Side Regeneration Extension (HSRE)	[1, 1, 1]
4	Low Side Regeneration Extension (LSRE)	[-1, -1, 1]
5	Low Side Regeneration Retraction (LSRR)	[-1,-1,-1]

3.1.1 Flow Equations

Next we define universal equations for the supply and return flow for all five modes as

$$Q_s = \frac{S_a+1}{2} q_a - \frac{S_b+1}{2} q_b \tag{3.1}$$

$$Q_r = \frac{S_a-1}{2} q_a - \frac{S_b-1}{2} q_b \tag{3.2}$$

To verify our proposed function

For PE: $Sa = 1,$ $S_b = -1,$ $\Rightarrow Q_s = q_a$ and $Q_r = q_b$

For HSRE: $Sa = 1,$ $Sb = 1,$ $\Rightarrow Qs = qa - qb$ and $Qr = 0.$

3.1.2 Equivalent Conductance

The valve switching function also sets a unified representation of the valve opening and pressure drop across the valves for all five modes as follows:

$$K_a = \frac{S_a+1}{2} K_{sa} - \frac{S_a-1}{2} K_{at} \tag{3.3}$$

$$K_b = \frac{S_b+1}{2} K_{sb} + \frac{1-S_b}{2} K_{bt} \tag{3.4}$$

$$K_{eq} = \frac{K_a K_b}{\sqrt{K_a^2 + R^3 K_b^2}} \tag{3.5}$$

K_a and K_b represent the conductance coefficients at the head chamber and rod chamber respectively. They can be the conductance coefficient to the pump side or to the tank side. K_{eq} is the equivalent conductance for the combination of both valves used in the circuit that achieve the desired flow under the loading condition of the system.

3.1.3 Equivalent Pressure

Now the flow into the head chamber A becomes:

$q_a = Ka\sqrt{\Delta P1}$ Where ΔP_1 is defined as:

$$\Delta P_1 = \begin{cases} P_s - P_a & in\ PE\ mode \\ P_a - P_r & in\ PR\ mode \\ P_s - P_a & in\ HSRE\ mode \\ P_r - P_a & in\ LSRE\ mode \\ P_a - P_r & in\ LSRR\ mode \end{cases}$$

Using the valve switching function to express ΔP_1 we get the following equation:

$$\Delta P_1 = D\left[\frac{S_a+1}{2}(P_s - P_a) - \frac{S_a-1}{2}(P_r - P_a)\right] \quad (3.6)$$

the same way we have:

$$\Delta P_2 = \begin{cases} P_b - P_r & in\ PE\ mode \\ P_s - P_b & in\ PR\ mode \\ P_b - P_s & in\ HSRE\ mode \\ P_b - P_r & in\ LSRE\ mode \\ P_r - P_b & in\ LSRR\ mode \end{cases}$$

$$\Delta P_2 = D\left[\frac{S_b+1}{2}(P_b - P_s) + \frac{1-S_b}{2}(P_b - P_r)\right] \quad (3.7)$$

now the equivalent pressure can be expressed by:

$$P_{eq} = R\Delta P_1 + \Delta P_2 \quad (3.8)$$

finally, the pressure set point for all five modes becomes:

$$PS_{setpoint} = \frac{\Delta P_{min}}{\frac{S_a+1}{2}R - \frac{S_a+S_b}{2}} + \frac{\frac{S_a+1}{2}(RP_a - P_b) + \frac{S_a-1}{2}(RP_a - P_b)}{\frac{S_a+1}{2}R - \frac{S_a+S_b}{2} + \frac{1-S_a}{2}} + \frac{\frac{1-S_a}{2}R + \frac{1-S_b}{2}}{\frac{1-S_b}{2}R + \frac{1-S_a}{2} + \frac{S_a+S_b}{2}} P_r \quad (3.9)$$

Due to using the valve switching function and the unified equations, it becomes much easier to represent the system and to manipulate it.

3.2 Electrohydraulic Poppet Valve Modeling

As mentioned before, the INCOVA consists of five EHPVs, so it is important to understand, model, and validate how the EHPVs work. Much research was conducted on them, but the most accurate model was developed by Opdenbosch [33-38]. The work conducted by Opdenbosch is based on a second order dynamic model that accurately represents the valve and to perform online correction and estimation of the valves' conductance coefficient as a function of a commanded current input. Next we present the results [33].

3.2.1 Analysis and Operation of EHPVs

The structure of EHPV is shown in figure 33:

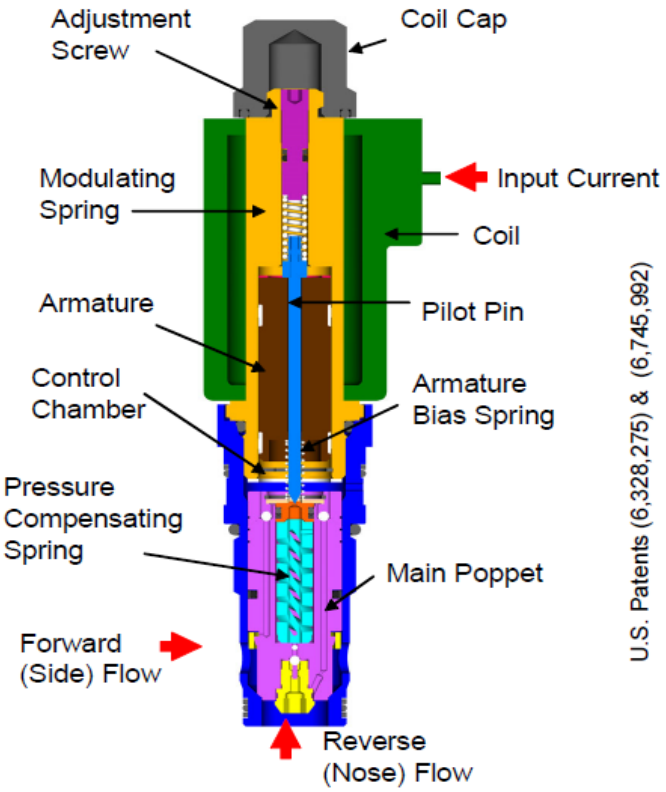

Figure 34. Structure of the EHPV.

The principle of how EHPV works is explained in details in references [33-39]. The EHPV consists of two stages; the first stage consists of a main poppet and pressure compensation mechanism. The pressure compensation mechanism has a compensating piston and spring. The second stage houses the armature and the housing pilot pin with a pressure control chamber that separates the two stages.

The goal is to achieve the desired flow through the valve. The high pressure flow from the main poppet is passed to the central chamber through a small passage of the main poppet. When the current is passed through the coils, the solenoid is activated, which moves the pilot pin. This allows the fluid to flow from the control pressure chamber to the low pressure side through a piston and tubular spring, and this will cause a drop in the control chamber pressure. The pressure difference on both sides of the main poppet will move it from the main valve seat, which creates a passages between the inlet and outlet of the valve. The EHPV is bidirectional because the control chamber can receive the high pressure flow from either port.

3.2.2 Second Order Model of EHPV

The valve is modeled as a linear second order model with nonlinear gain that represents the steady state response. the parameters that control the nonlinear gains are the input current to the solenoid, the pressure drop across the valve, and the direction of the flow (forward or reverse).

$f\ (i_{sol}, \Delta P, \Phi)$. $\Phi\ =\ +1$ when the valve is in forward flow mode, and $\Phi\ =\ -1$ when the valve is in reverse flow mode.

Other parameters like the oil temperature have little effect and will be ignored here. Our input will be the solenoid current and the output will be the valve flow conductance parameter K_v, so the simplified second order dynamic model becomes [33,45]:

$$\ddot{K}_v + 2\zeta\omega_n \dot{K}_v + \omega_n^2 K_v = \omega_n^2 f(i_{sol}, \Delta P, \Phi) \tag{3.10}$$

3.2.3 Experimental Validation

Experiments were conducted to find the optimum parameter coefficients of the linear model, then non linear gains are obtained from the steady state data, different currents were commanded to the solenoids of the EHPVs and data was collected for each commanded current, the figure below shows K_v for steady state current response in milli ampere and pressure drops over a wide range, this was done for both forward and reverse flows [38]. Notice that K_v is only dependent the current for pressure drop less than 0.4 MPa, below that both pressure and current play a role, so if we keep ,ΔP above 0.4 MPa then K_v is not a function of the pressure drop.

$$\ddot{K}_v + 2\zeta\omega_n \dot{K}_v + \omega_n^2 K_v = \omega_n^2.\ f(i_{sol}, \Phi) \tag{3.11}$$

from the experimental data it was determined that ω_n = 72.05 *rad/s* and damping ratio is found to be ζ = 1.25. The model is then subjected to a step response and the data was collected and compared to the model to validate it at different currents for both forward and reverse flows. Of course a low pass filter with 25 Hz cutoff frequency was used to eliminate noise [36,37].

3.3 Modeling the Actuator

In this section we develop a mathematical model for our actuator, which is the cylinder. Hydraulic systems are inherently nonlinear and the fluid used can be compressible. We use the conservation laws of mass and momentum to find the differential equations of our system, but first we must define our system and impose some restrictions; the assumptions and restrictions are [45]:

1. Sharp edge orifices of the poppet valves.
2. Inviscid simple flow through the valve where $Q = K\sqrt{\Delta P}$ applies.
3. Time delay from the moment the pressure is commanded to the flow change is neglected.
4. Small fluid inductance due to relatively short wide pipes are used.
5. Oil hydraulic bulk modulus is constant through the entire pressure range.
6. Isothermal process of the oil, which eliminates the energy equation.
7. Small hydraulic losses in the lines.

3.3.1 Mathematical Modeling

Figure 35 represents our simplified system. The pump pressurizes the fluid which flows to the valves where it is controlled and directed to the cylinder which has different pressures in its chambers, and load acting on the rod end of the cylinder [36,45].

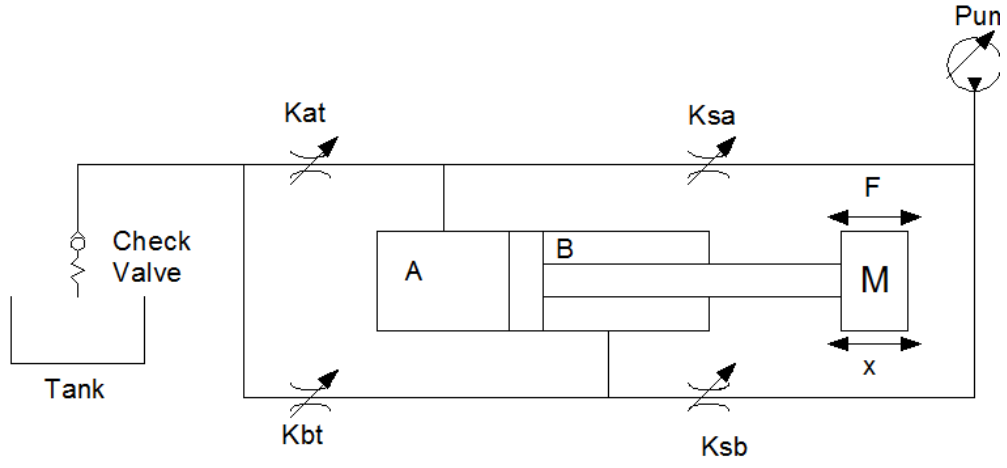

Figure 35. Hydraulic cylinder control using IMV assembly

All these components in addition to the lines, the poppet valves, the chambers of the cylinder under variable flows, volumes, and loads need to be modeled. We already found the equations for the valves, and after the model is created, it will be simulated. The control input will be the opening of the valves.

3.3.1.1 Flow through the Orifices

According to Merrit [29], the flow will be turbulent and the flow relationships will be expressed as:

$$Q_{sa} = K_{sa}\sqrt{|P_s - P_a|}sgn(P_s - P_a)$$
$$Q_{sa} = K_{sa}\sqrt{|P_s - P_a|}sgn(P_s - P_a)$$
$$Q_{sb} = K_{sb}\sqrt{|P_s - P_b|}sgn(P_s - P_b)$$
$$Q_{at} = K_{at}\sqrt{|P_a - P_r|}sgn(P_a - P_r)$$
$$Q_{bt} = K_{bt}\sqrt{|P_b - P_r|}sgn(P_b - P_r) \quad (3.12)$$

3.3.1.2 Compressibility

$$Q_{ca} = \frac{CV_a}{B_e}\dot{P}_a$$
$$Q_{cb} = \frac{CV_b}{B_e}\dot{P}_b$$
$$CV_a = V0_a + A_a x$$
$$CV_b = V0_b - A_b \quad (3.13)$$

V_{0a} is the initial volume of head chamber (a), and V_{0b} is the initial volume of rod Chamber (b)

3.3.1.3 Conservation of Mass

$$Q_{sa} - Q_{at} - Q_L = Q_{ca} + A_a\dot{x}$$
$$Q_{sb} - Q_{bt} + Q_L = Q_{cb} - A_b\dot{x} \quad (3.14)$$

Where Q_L is the leakage from chamber A to chamber A_b, which can be very small and neglected.

Substitute for Q_{sa}, Q_{at}, Q_{ca}, Q_{cb}, Q_{sb}, and Q_{bt} from equations 12, 13, and 14 we get:

$$K_{sa}\sqrt{|P_s - P_a|}\ sgn(P_s - P_a) - K_{at}\sqrt{|P_a - P_r|}\ sgn(P_a - P_r) = \frac{CV_a}{B_e}\dot{P}_a + A_a\dot{x} \quad (3.15)$$

$$K_{sb}\sqrt{|P_s - P_b|}\ sgn(P_s - P_b) - K_{bt}\sqrt{|P_b - P_r|}\ sgn(P_b - P_r) = \frac{CV_b}{B_e}\dot{P}_b - A_b\dot{x} \quad (3.16)$$

3.3.1.4 Conservation of Momentum

$$P_a A_a - P_b A_b = M\ddot{x} + F + F_f \quad (3.17)$$

where F is the external force (the load), and F_f is the friction force inside the cylinder.

3.4 Friction Estimation

There is no exact formula for calculating the friction, but lots of research was conducted to accurately estimate it, due to advances in technology and strict requirements on the error range. It should be noted that changing the mode of operation and the pressure will change the friction, Bonchis and others found that the friction is highly dependent on the pressure in the chambers, an empirical formula was developed

$$F_f = a_1 e^{a_2 v} + a_3(P_a - P_b) + a_4 P_b + a_5 v \quad (3.18)$$

where F_f is the friction force acting on the piston, a_1-a_5 are coefficients to be determined, P_a and P_b are the pressures in the head and rod chambers, and *v* is the piston speed. Bonchis then found that the velocity has little effect and refined his formula to:

$$F_f = a_1(P_a - P_b) + a_2 P_b + Cv \quad (3.19)$$

where a_1,a_2, and the viscous friction parameter C are experimentally determined [36,37].

3.5 State Space Representation

The system will be considered as a multi input system because we have four valves to be controlled, so we put the equations in state space format :

$$\dot{x} = f(x,u) \tag{3.20}$$

Our variables are the actuator position, speed, inlet chamber pressure, and the outlet chamber pressure [45].

$$\begin{aligned}
x_1 &= x \\
x_2 &= \dot{x} \\
x_3 &= P_a \\
x_4 &= P_b \\
\dot{x_1} &= x_2 \\
\dot{x}_2 &= -F_{ext} - \frac{Cx_2}{M} + \frac{(A_a - a_1)}{M} x_3 + \frac{(a_1 - a_2 - A_b)}{M} x_4 \\
\dot{x}_3 &= \frac{B_e}{CV_a}\left[K_{sa}\sqrt{P_s - x_3} - K_{at}\sqrt{x_3 - P_r} - A_a x_2\right] \\
\dot{x}_4 &= \frac{B_e}{CV_b}\left[K_{sb}\sqrt{P_s - x_4} - K_{bt}\sqrt{x_4 - P_r} - A_b x_2\right]
\end{aligned} \tag{3.21}$$

The supply pressure was found for all modes as the set point pressure:

$$Ps_{setpoint} = \frac{\Delta P_{min}}{\frac{S_a+1}{2}R - \frac{S_a+S_b}{2}} + \frac{\frac{S_a+1}{2}(RP_a - P_b) + \frac{S_a-1}{2}(RP_a - P_b)}{\frac{S_a+1}{2}R - \frac{S_a+S_b}{2} + \frac{1-S_a}{2}} + \frac{\frac{1-S_a}{2}R + \frac{1-S_b}{2}}{\frac{1-S_b}{2}R + \frac{1-S_a}{2} + \frac{S_a+S_b}{2}} P_r \tag{3.22}$$

4 ENERGY SAVING ANLYSIS

4.1 Conventional Load Sensing Pump Control

In pressure compensated load sense, the controller commands the pump to provide a certain pressure margin Pm after measuring the pressure in the hydraulic cylinder inlet chamber; the goal is to keep a fixed pressure drop across the valve, which means a linear relationship between the spool position and the flow rate through the valve.

The comparison between PE and PR with IMV modes will be presented here, with the basic assumptions of quasi static behavior. Compressibility effects and capacitance variation are neglected. In addition the valve dynamics are neglected.

4.1.1 Powered Extension Mode

Figure 36 shows schematic of the PE mode [45]. The fluid flows through valve K_{sa} to chamber A, and out of valve K_{bt} to the tank, the flow equations are:

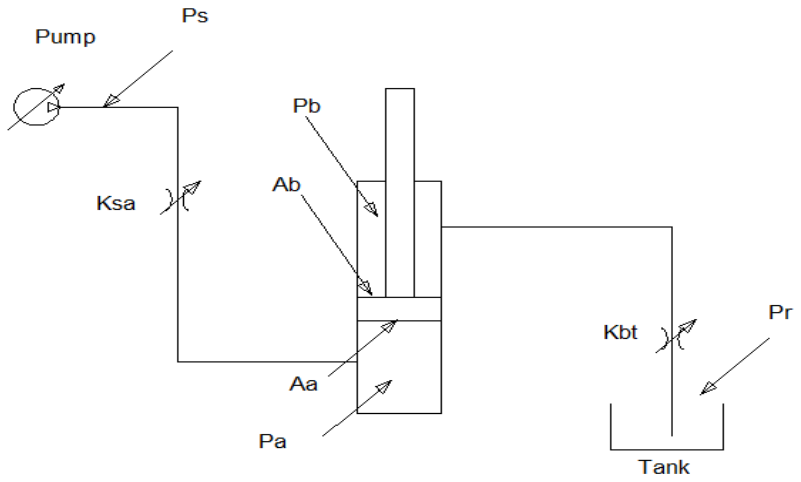

Figure 36. Schematics of the PE mode.

$$q_a = K_{sa}\sqrt{\Delta P_1} = K_{sa}\sqrt{P_s - P_a} = A_a.\dot{x} \quad (4.1)$$

$$q_b = K_{bt}\sqrt{\Delta P_2} = K_{bt}\sqrt{P_b - P_r} = A_b.\dot{x} \quad (4.2)$$

Divide equation 1 by 2 we get:

$$\frac{q_a}{q_b} = R = \alpha\sqrt{\frac{P_s - P_a}{P_b - P_r}} \quad (4.3)$$

Rearrange:

$$P_s - P_a = \left(\frac{R}{\alpha}\right)^2 (P_b - P_r) \quad (4.4)$$

$$P_s = P_a + \left(\frac{R}{\alpha}\right)^2 P_b - \left(\frac{R}{\alpha}\right)^2 P_r \quad (4.5)$$

From Newton's Second Law for the hydraulic force:

$$F_{Hyd} = P_a A_a - P_b A_b \quad (4.6)$$

$$\Rightarrow P_a = \frac{F_{Hyd}}{A_a} + \frac{P_b}{R} = P_s - \left(\frac{R}{\alpha}\right)^2 P_b + \left(\frac{R}{\alpha}\right)^2 P_r \quad (4.7)$$

$$\Rightarrow \left[\frac{1}{R} + (\frac{R}{\alpha})^2\right] P_b = P_s - (\frac{R}{\alpha})^2 P_b + -(\frac{R}{\alpha})^2 P_r \quad (4.8)$$

$$\Rightarrow P_b = \frac{R}{1+\left(\frac{R^3}{\alpha^2}\right)} P_s - \frac{1}{1+\left(\frac{R^3}{\alpha^2}\right)} \frac{F_{Hyd}}{A_b} + \frac{R^3}{\alpha^2+R^3} P_r \quad (4.9)$$

$$\Rightarrow P_b = R\, P_a - \frac{F_{Hyd}}{A_b} = \left(\frac{\alpha}{R}\right)^2 P_s - \left(\frac{\alpha}{R}\right)^2 P_a + P_r \quad (4.10)$$

$$\Rightarrow \left[R + \left(\frac{\alpha}{R}\right)^2\right] P_a = \left(\frac{\alpha}{R}\right)^2 P_s + \frac{F_{Hyd}}{A_b} + P_r \quad (4.11)$$

$$\Rightarrow P_a = \frac{1}{1+\left(\frac{R^3}{\alpha^2}\right)} P_s - \frac{R^2}{\alpha^2+R^3} \frac{F_{Hyd}}{A_b} + \frac{R^2}{\alpha^2+R^3} P_r \quad (4.12)$$

The PCLS will be our choice to control the IMV system, and for the PE chamber A will be our input chamber:

$$P_s = P_a + P_m \quad (4.13)$$

Substitute in equation 12

$$\Rightarrow P_s = \frac{1}{1+\left(\frac{R^3}{\alpha^2}\right)} P_s - \frac{R^2}{\alpha^2+R^3} \frac{F_{Hyd}}{A_b} + \frac{R^2}{\alpha^2+R^3} P_r + P_m \quad (4.14)$$

$$\Rightarrow P_s \left[\frac{R^3}{\alpha^2+R^3}\right] = -\frac{R^2}{\alpha^2+R^3} \frac{F_{Hyd}}{A_b} + \frac{R^2}{\alpha^2+R^3} P_r + P_m \quad (4.15)$$

$$\Rightarrow P_s = \left[\frac{R^3+\alpha^2}{R^3}\right] P_m - \frac{1}{R} \frac{F_{Hyd}}{A_b} + \frac{1}{R} P_r \quad (4.16)$$

$$P_a = P_s - P_m \quad (4.17)$$

$$\Rightarrow P_a = \frac{\alpha^2}{R^3} P_m + \frac{1}{R} \frac{F_{Hyd}}{A_b} + \frac{1}{R} P_r \quad (4.18)$$

Or we can write equation 4 as:

$$P_{b=} \left(\frac{\alpha}{R}\right)^2 (P_s - P_a) + P_r \quad (4.19)$$

4.1.1.1 Back Pressure Limitations for PCLS

The previous derivation applies to both conventional and IMV systems, keeping in mind that the IMV system has two degrees of freedom, where the return chamber pressure P_b can be controlled to a certain value P_{b0}. Using the valve control plot, we express this desired outlet pressure as a horizontal line

that corresponds to the correct value of the opening that achieves this pressure. We choose the operating point to be the intersection between P_{b0} and the curve that represents K_{eq} corresponding to the desired speed as shown in figure 37.

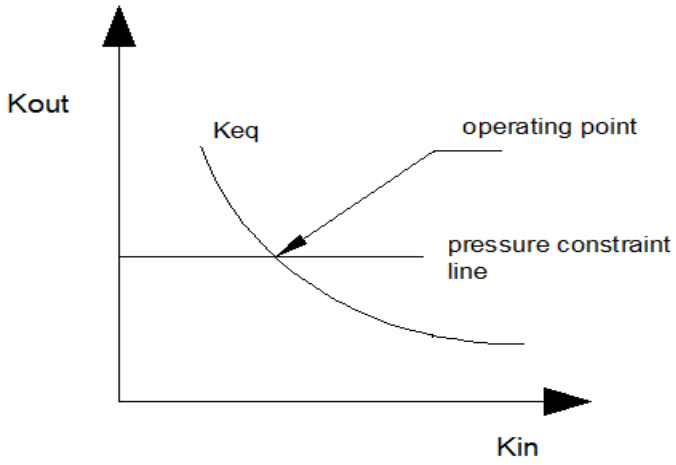

Figure 37. Back pressure limitations for PCLS control.

going below this line means lower pressure, so the controller must command a back or return pressure $P_b = P_{b0}$. Substitute in equation 19 we get:

$$P_0 = \left(\frac{\alpha}{R}\right)^2 (P_s - P_a) + P_r \tag{4.20}$$

Hence P_s becomes:

$$P_s = \left(\frac{\alpha^2}{R^3}\right) P_m + \frac{1}{R} P_r + \frac{1}{R}\frac{F_{Hyd}}{A_b} + P_m \tag{4.21}$$

$$P_s = \frac{1}{R}\left(\frac{\alpha^2}{R^2} P_m + P_r\right) + \frac{1}{R}\frac{F_{Hyd}}{A_b} + P_m \tag{4.22}$$

But $Pa = Ps - Pm$

$$\Rightarrow P_s = \left[\frac{1}{R} P_0 + \frac{1}{R}\frac{F_{Hyd}}{A_b} + P_m\right] \tag{4.23}$$

$$P_a = \left[\frac{1}{R} P_0 + \frac{1}{R}\frac{F_{Hyd}}{A_b}\right] \tag{4.24}$$

4.1.1.2 Pump Power Savings

In this section the power consumption by the pump of each system is compared, define the power.

$$Power = P_s \,.\, Q_s \tag{4.25}$$

For a system operating at the same speed and under the same load it must have the same flow rate, then the comparison becomes between the pressure needed by each system, and hence:

$$\Delta Power = \Delta P_s \,.\, Q_s \tag{4.26}$$

Equations 18 and 24 are the pressures for the two systems, then:

$$\Delta P_s = \left[\left(\frac{\alpha^2}{R^3}\right) P_m + \frac{1}{R}(P_r - P_{b0})\right] \tag{4.27}$$

denoting the supply pressure of the conventional system by P_s and the one for IMV system by *P's*

$$\Delta Power = P_s . Q_s - \dot{P}_s = \left[\left(\frac{\alpha^2}{R^3}\right) P_m + \frac{1}{R}(P_r - P_{b0})\right] . Q_s \tag{4.28}$$

this is true for the same load, and the same speed as mentioned before, also we are assuming same pressure drop across the inlet valve for now. The advantage of the IMV system lies in being able to control the outlet pressure, which means we can minimize the pressure losses and hence minimize the power consumption as shown in figure 38 [36,45]:

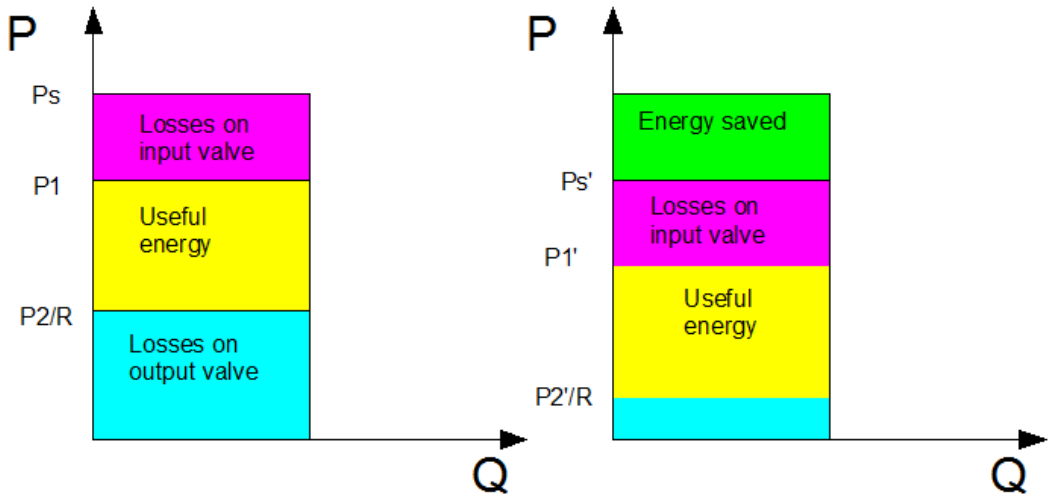

Figure 38. Energy saving for IMV and spool valve systems.

Take the example of the following system, $Pr = 0, R = 1.4, \alpha = 1.3, Pm = 1.7\ MPa$, and the controlled return pressure $P0 = 0.7\ MPa$.

$$\Delta P_s \approx 0.55\ MPa \tag{4.29}$$

$$Power\ Ratio = \frac{\Delta P'_s . Q_s}{\Delta P_s . Q_s} \approx 37\% \tag{4.30}$$

which will be the effect of varying the parameters P_m, R, P_0 on the supply pressure representing power savings. Next, the effect of changing these parameters is studied [45].

4.1.1.3 Energy Saving Variation

For the case of having the back pressure equal to P_r, the pressure difference will only depend on the valve opening ratio α and the pressure drop across the valve P_m. The pressure saved as a function of α and P_m is shown in figure 39 for the values of $P_m = 1, 2, 3\ MPa$, and $R = 1.658$.

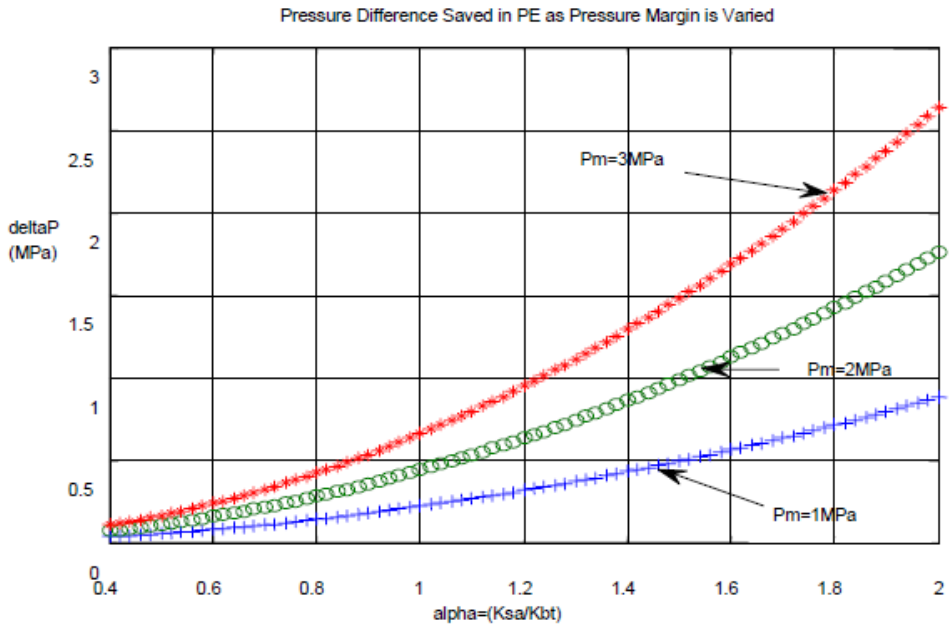

Figure 39. Pressure difference saving in PE mode as the margin pressure is changed.

It is clear that the energy saving is higher for high P_m; then the questions becomes how high can P_m be? the answer is that it depends on the maximum pressure allowed in the inlet pressure chamber.

The bigger the opening to chamber A, the higher the pressure in that chamber becomes and hence less losses, so increasing the pressure margin means higher energy savings. In figure 40 the pressure saving is studied as α and R are varied when P_m is constant, for $R = 1, 1.658$, and 2 at $Pm = 1MPa$. It is observed that energy saving is higher for smaller R [45].

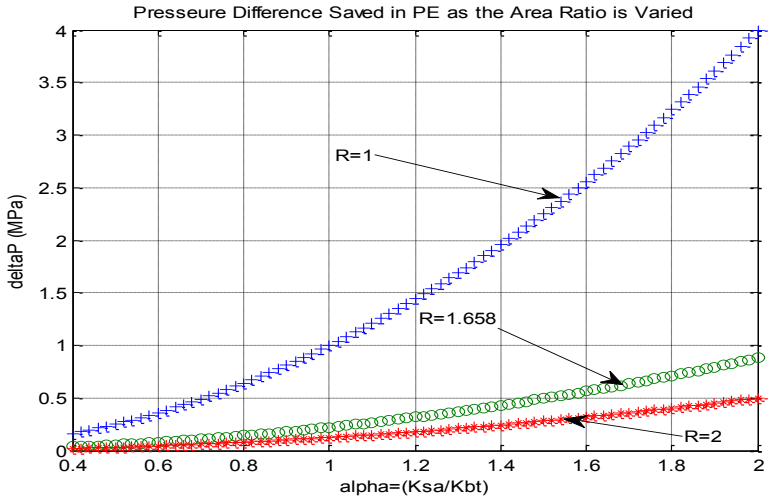

Figure 40. Pressure difference saving in PE mode as the area ratio is varied.

In figure 41, P_0 is varied to $P_0 = P_r$, $2P_r$, and $3P_r$ while P_m is fixed at 1 MPa, and R =1.658. It is observed that as P_{b0} gets closer to P_r the energy saving is higher, and in some cases for $P_0 > 3P_r$ pressure is being lost and hence power is lost [45].

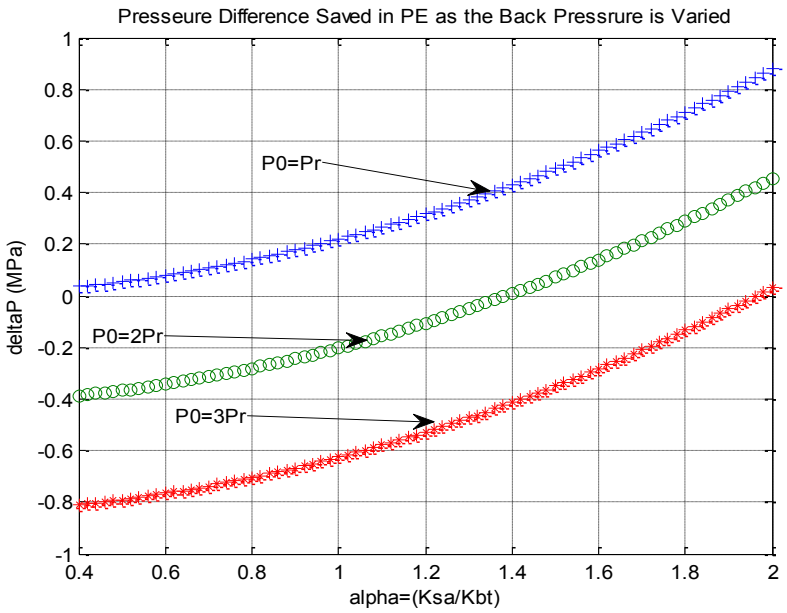

Figure 41. Pressure difference saving in PE mode as the back pressure is varied.

4.1.2 Powered Retraction Mode

4.1.2.1 Derivation

The same steps of the PE mode are repeated here with the same assumptions.

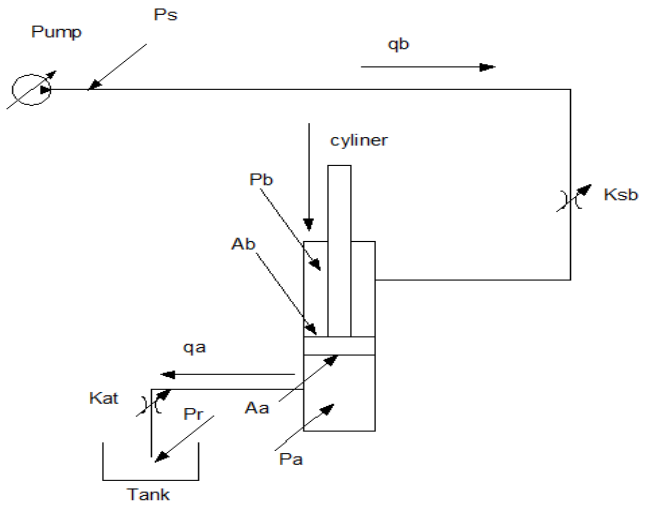

Figure 42. Schematics of the PR mode.

starting with the flow equations

$$q_a = K_{at}\sqrt{\Delta P_1} = K_{at}\sqrt{P_a - P_r} = A_a\dot{x} \quad (4.31)$$

$$q_b = K_{sb}\sqrt{\Delta P_2} = K_{sb}\sqrt{P_s - P_b} = A_b\dot{x} \quad (4.32)$$

divide equation 31 by 32:

$$\frac{q_a}{q_b} = R = \alpha\sqrt{\frac{P_a - P_r}{P_s - P_b}} \quad (4.33)$$

Newton second law:

$$F_{Hyd} = P_b A_b - P_a A_a \quad (4.34)$$

$$P_a - P_r == \left(\frac{R}{\alpha}\right)^2 (P_s + P_b) \quad (4.35)$$

for PR mode the input chamber is the rod chamber B, the PCLS system measures the pressure P_b and commands the pump to add the margin pressure P_m, and supply a pressure at $P_b = P_s - P_m$

substitute for P_b

$$P_s = \left[\frac{R^3}{\alpha^2} + 1\right] P_m + \frac{F_{Hyd}}{A_b} + RP_r \quad (4.36)$$

$$\Rightarrow P_b = \left(\frac{R^3}{\alpha^2}\right) P_m + \frac{F_{Hyd}}{A_b} + RP_r \quad (4.37)$$

to find P_a substitute in equation 34:

$$P_a = \left(\frac{\alpha}{R}\right)^2 (P_s - P_b) + P_r = \left(\frac{R}{\alpha}\right)^2 P_m + P_r \quad (4.38)$$

4.1.2.2 Back Pressure Limitations for PCLS

The back pressure P_a can be commanded to a specific valve P_0:

$$P_a = P_0 \quad (4.39)$$

using equation 38, P_0 can be written as:

$$P_0 = \left(\frac{R}{\alpha}\right)^2 P_m + P_r \quad (4.40)$$

The supply pressure becomes:

$$P_a = \frac{R^3}{\alpha^2} P_m + RP_r + P_m + \frac{F_{Hyd}}{A_b} \quad (4.41)$$

$$\Rightarrow P_s = RP_0 + P_m + \frac{F_{Hyd}}{A_b} \quad (4.42)$$

Hence P_b:

$$P_b = RP_0 + \frac{F_{Hyd}}{A_b} \quad (4.43)$$

4.1.2.3 Pump Power Savings

Once again we assume same load, same speed, and same area ratio, then the power saving becomes a matter of pressure saving between the two systems, equation 36 is the pressure needed by the conventional system while equation 42 is the pressure needed by the IMV system.

$$\Delta Power = \Delta P_s \,.\, Q_s \quad (4.44)$$

$$\Delta P_s = \left[\left(\frac{R^3}{\alpha^2} + 1\right) P_m + \frac{F_{Hyd}}{A_b} + RP_r\right] - \left[RP_0 + P_m + \frac{F_{Hyd}}{A_b}\right] \quad (4.44)$$

$$\Rightarrow \Delta P_s = \left[\left(\frac{R^3}{\alpha^2}\right) P_m + R(P_r - P_0)\right] \quad (4.45)$$

4.1.2.4 Power Saving Variation

The effect of changing the parameters P_m, R, and P_0 on power savings for PR mode is studied next. For the case of P_0=P_r, then ΔP_s depends on α and P_m.

In figure 43 P_m is varied to P_m=1, 2 and 3 MPa at R=1.658 [45].

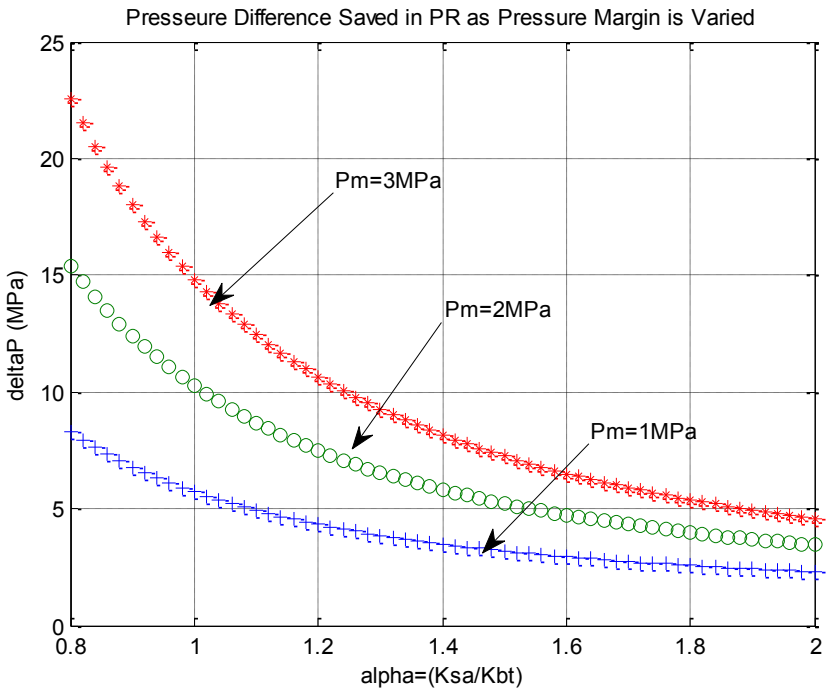

Figure 43. Pressure difference saving in PR mode as the margin pressure is varied.

At low valve coefficient, the savings are higher. In figure 44 R is varied to R=1, 1.658, and 2, while P_m is fixed to 1 MPa [45].

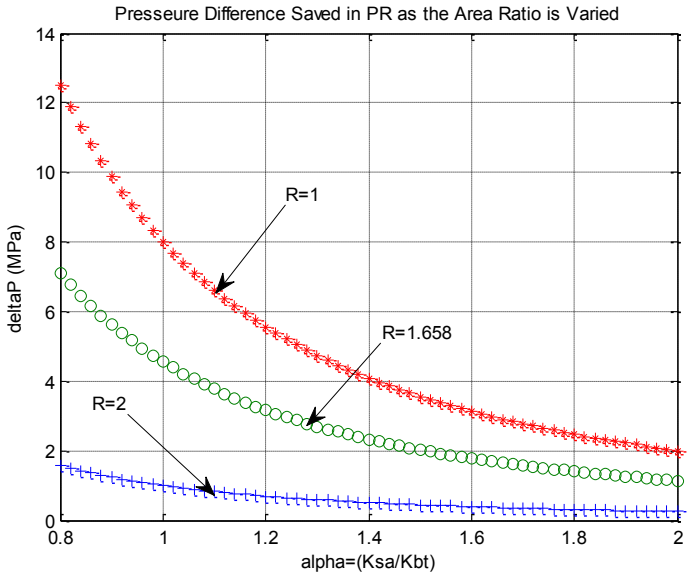

Figure 44. Pressure difference saving in PR mode as the area ratio is varied.

It is observed that higher pressure difference is higher for high values of R. In figure 45 P_0 is varied to $P_0=P_r$, $2P_r$, and $3P_r$ at P_m=1MPa and R=1.658.

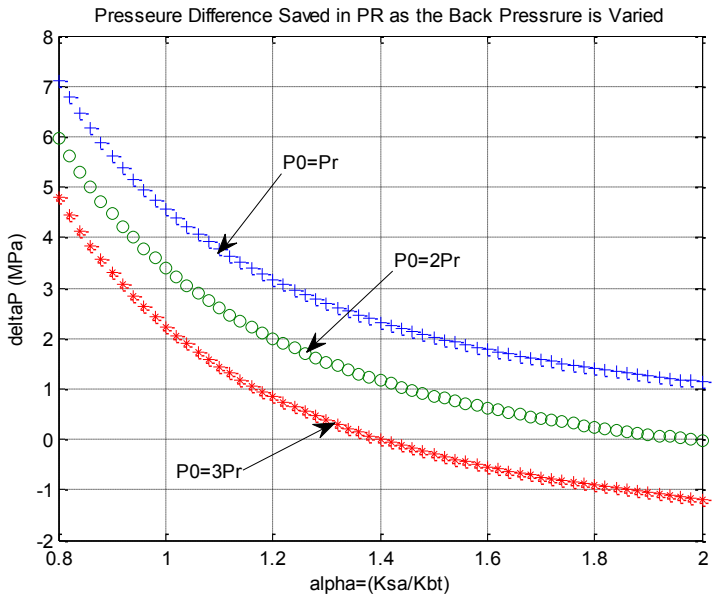

Figure 45. Pressure difference saving in PR mode as the back pressure is varied.

Here again more pressure saving is achieved around $P_0=P_r$ [45].

4.2 PE Supply Pressure Set Point Calculations

Going back to chapter two, the comparison here is done using derivation of the supply pressure set point for IMV system, instead of using PCLS. Recall that for IMV the cylinder can be extended in three different ways; PE, HSRE, and LSRE. Next the energy savings of the three modes will be compared for the same load speed to the case where the conventional PCLS system is used.

In chapter two we found two equations for the supply pressure set point for each mode, one came from the flow analysis, while the other came from force analysis, then the higher of the two used. Here the second pressure set point is used since in reality it is almost always higher [45].

$$\Delta Power = \Delta P_s \,.\, Q_s \tag{4.46}$$

$$\Delta P_s = \left[\left(\frac{\alpha^2+R^3}{R^3}\right)P_m + \frac{1}{R}\frac{F_{Hyd}}{A_b} + \frac{1}{R}P_r\right] - \left[\frac{Peq_{min}}{R} + \frac{(R\,P_a - P_b)}{R} + \frac{P_r}{R}\right] \tag{4.47}$$

$$Peq_{min} = (R+1)\,\Delta P_{min} \tag{4.48}$$

$$\Delta P_s = \left(\frac{\alpha^2+R^3}{R^3}\right)P_m - \frac{Peq_{min}}{R} \tag{4.49}$$

The power saving can be represented as a plot. Recall also that this power saving depends on P_m, R, and ΔP_{min} as seen from equation 49. Remember that EHPV needs ΔP_{min} to be maintained across the valve to ensure proper operation. Once again the effect of the three parameters on energy saving will be studied here.

In figure 46 the effect of P_m on ΔP_s and hence power saving is shown; P_m is the pressure margin across the inlet valve of a conventional spool valve controlled system. P_m is varied P_m=1, 2, 3 MPa at constant R=1.658 and ΔP_{min}=1MPa.

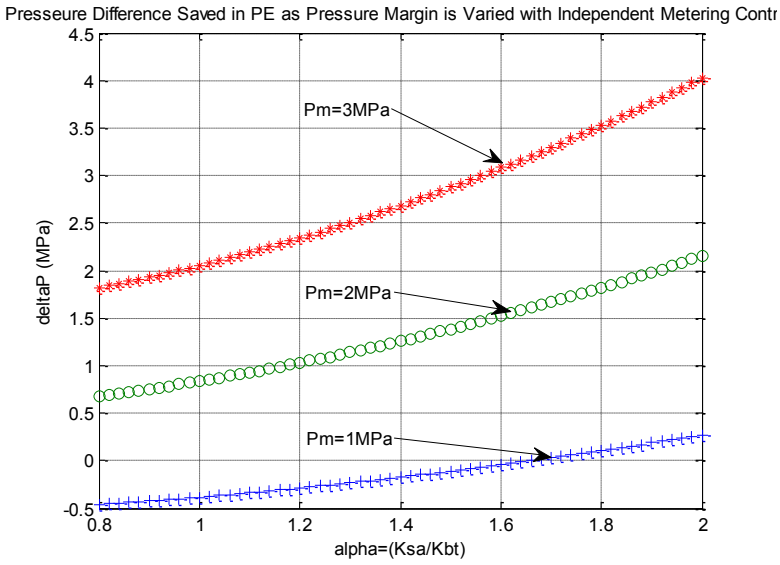

Figure 46. Pressure difference saving in PE mode as the pressure margin is varied. IMV control.

It is observed that for P_m=1 MPa and $\alpha < 1.6$ the pressure saving is negative, hence the conventional system is more efficient, but the savings get higher as P_m get higher.

In figure 47 the effect of changing R is studied, three values of R=1, 1.658, and 2 for P_m=1MPa, and ΔP_{min}=1MPa.

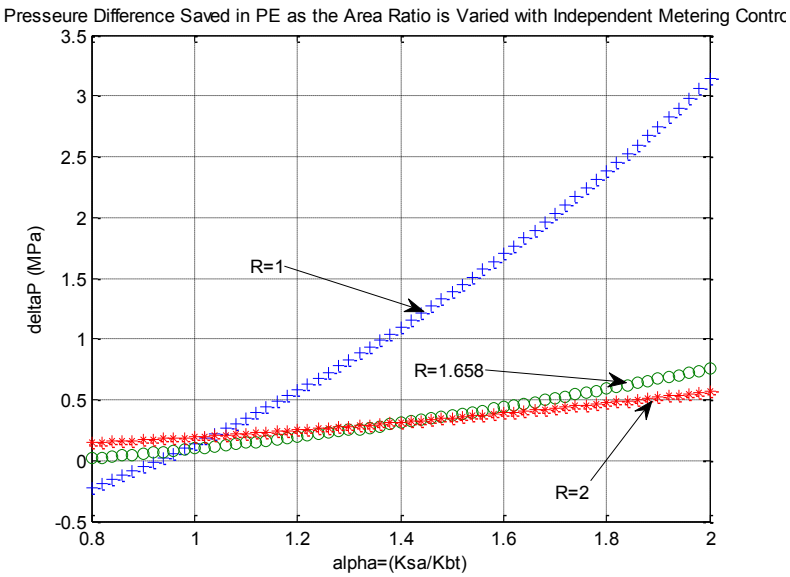

Figure 47. Pressure difference saving in PE mode as the back pressure is varied. IMV control.

It is observed that the smaller R is the higher the savings, but in some case cases for higher R the pressure becomes negative and hence more energy is required [45].

Finally, in figure 48 the effect of ΔP_{min} is varied to 0.5, 1, 1.5 MPa at constant R=1.658 and P_m=1 MPa.

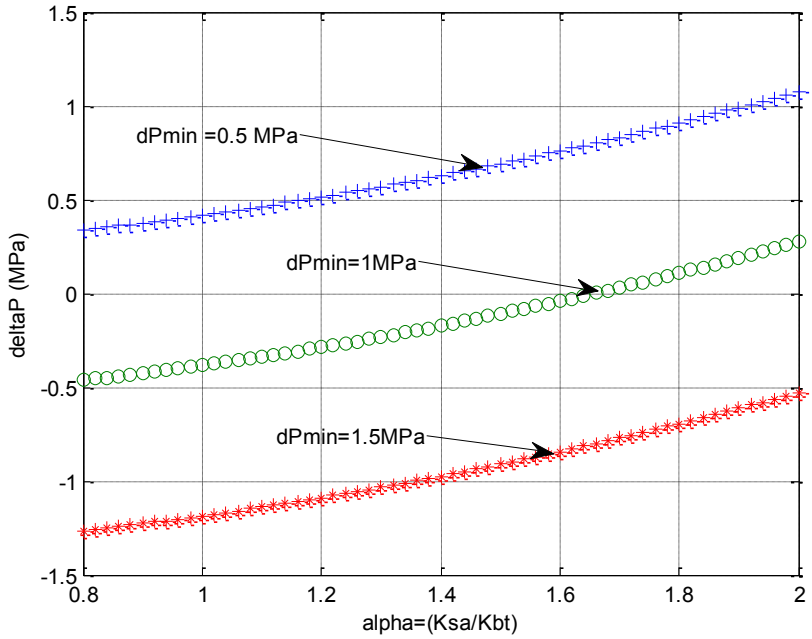

Figure 48. Pressure difference saving in PR mode as the back pressure is varied.IMV control.

By definition ΔP_{min} is the pressure lost across the valve for proper operation, so the higher the value the higher the losses [45].

In conclusion, to make sure that IMV system gives better performance than conventional spool valve system with PCLS, a small piston area ratio, smaller ΔP_{min} and high pressure margin P_m are needed.

4.3 Comparison of Regenerative Modes to Conventional Modes

4.3.1 HSRE Vs PE

Figure 49shows schematics of the two modes[45] ,

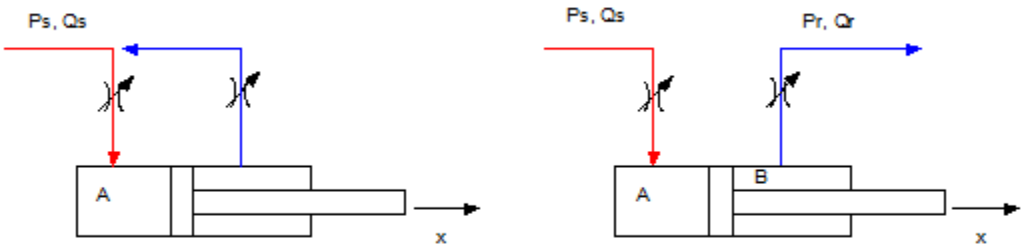

Figure 49. The maximum load that can be achieved assuming zero return pressure is

$$F_{maxPE} = P_s A_a \tag{4.50}$$

$$F_{maxHSRE} = P_s(A_a - A_b) \tag{4.51}$$

And the corresponding speed is:

$$\dot{x}_{PE} = \frac{Q_s}{A_a} \tag{4.52}$$

$$\dot{x}_{HSRE} = \frac{Q_s}{(A_a - A_b)} \tag{4.53}$$

It is observed that PE can achieve higher force, while HSRE can achieve higher speed. Another observation is that there are some loads that can be moved at the desired speed using either mode, while other loads can be driven at the desired speed by only one mode, this will be discussed in more details later. Moving to power saving we have

$$\Delta Power = P_{s,PE} \cdot Q_a - P_{s,HSRE} \cdot Q_r \tag{4.54}$$

$$Q_a = \left[\frac{Peq_{min}}{R} + \frac{(R\,P_a - P_b)}{R} + \frac{P_r}{R}\right] \tag{4.55}$$

$$Q_r = (A_a - A_b)\dot{x} \tag{4.56}$$

$$\Delta Power = \left[\frac{Peq_{min}}{R} + \frac{(R\,P_a - P_b)}{R} + \frac{P_r}{R}\right] A_a \dot{x} - \left[\frac{Peq_{min}}{R-1} + \frac{(R\,P_a - P_b)}{R-1}\right] A_r \dot{x} \tag{4.57}$$

$$Peq_{min} = (R+1)\,\Delta P_{min} \tag{4.58}$$

$$\Delta Power = \left(\left[\frac{Peq_{min}}{R} + \frac{(R\,P_a - P_b)}{R} + \frac{P_r}{R}\right] A_a - \left[\frac{Peq_{min}}{R-1} + \frac{(R\,P_a - P_b)}{R-1}\right] A_r\right) \dot{x} \tag{4.59}$$

$$\Delta Power = \Delta Force \,.\, \dot{x} \tag{4.60}$$

Since the speeds and loads are the same, the force difference will be zero, but in general the system is multi actuator system, where one actuator requires higher pressure, and other actuators may require lower pressures, but the high pressure available can save pump flow and hence power through using HSRE mode which requires less flow, rather than PE .

Figure 50 explains this point [45].

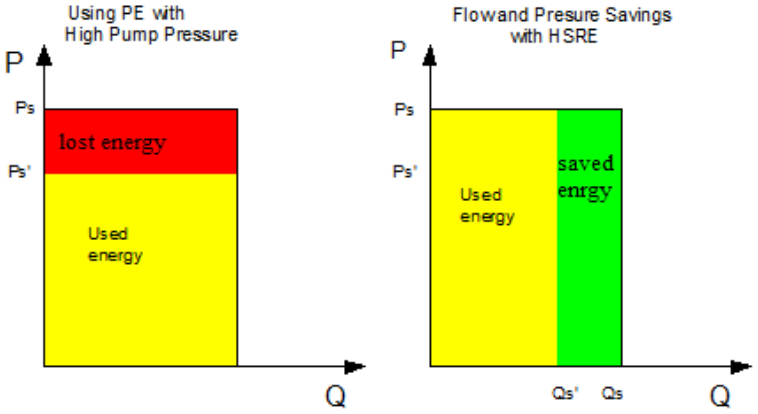

Figure 50. Flow savings in HSRE mode when the pressure is high enough.

For a supply pressure higher than needed by PE mode *P's*, power is lost, as shown by the red area in the figure. In case of HSRE, the high supply pressure Ps is used, but a fraction of the flow is needed which saves energy as shown by the green area.

4.3.2 LSRE Vs PE

The same comparison is done for LSRE as explained before; the regenerative flow is circulated through the low pressure line as shown in figure 51 [45]:

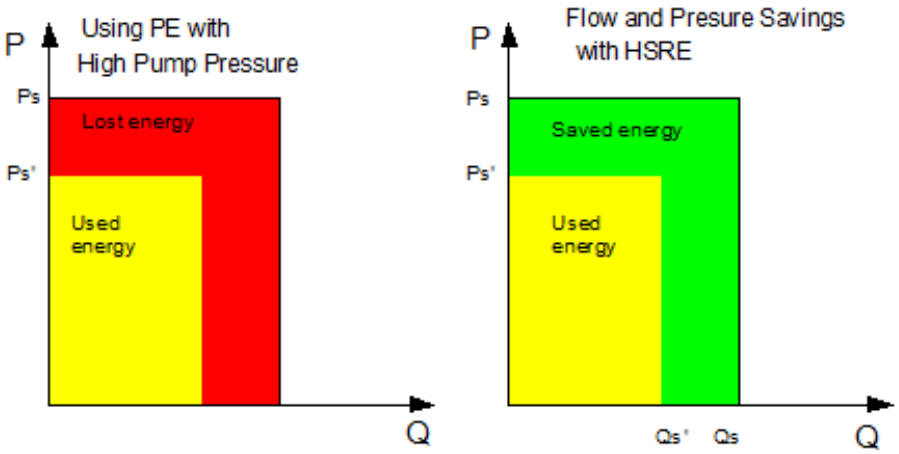

Figure 51. Flow saving in LSRE and hence power saving in comparison to PE.

Between Q_a and Q_b, so it saves power by saving both flow and pressure. LSRR does not require the pump to supply pressure or flow since it only uses the recirculation flow from the head chamber to the rod chamber, and the extra flow is vented to the tank, while PR requires the flow from the pump to move the load.

An important point here is that both LSRE and LSRR can only be used when there is gravity assistance, and these modes can only be achieved using IMV but not conventional system.

4.4 Inlet/Outlet Valve Power Losses Comparison

The power lost across the inlet and outlet valves is studied here for the PE, and the results are generalized. The flow equations are

$$q_a = K_{sa}\sqrt{\Delta P_a} = A_a\dot{x} \tag{4.61}$$

$$q_b = K_{bt}\sqrt{\Delta P_b} = A_b\dot{x} \tag{4.62}$$

$$q_a = Rq_b \tag{4.63}$$

$$\Rightarrow K_{sa}\sqrt{\Delta P_a} = RK_{bt}\sqrt{\Delta P_b} \tag{4.64}$$

Squaring

$$\Rightarrow {K_{sa}}^2\Delta P_a = R^2{K_{bt}}^2\Delta P_b \tag{4.65}$$

$$\Rightarrow \Delta P_a = R^2 \frac{{K_{bt}}^2}{{K_{sa}}^2} \Delta P_b \tag{4.66}$$

$$\Rightarrow \Delta P_a = \frac{R^2}{\alpha^2} \Delta P_b \tag{4.67}$$

The power lost is the pressure drop across the valve times the flow though it:

$$\mathbb{P}_a = q_a \Delta P_a \tag{4.68}$$

$$\mathbb{P}_b = q_b \Delta P_b \tag{4.69}$$

$$\mathbb{P}_a = q_a \Delta P_b \frac{R^2}{\alpha^2} = \frac{R^3}{\alpha^2} \mathbb{P}_b \tag{4.70}$$

$$\frac{\mathbb{P}_a}{\mathbb{P}_b} = \frac{R^3}{\alpha^2} \tag{4.71}$$

To generalize the results, substitute K_{sa} by K_a and K_{bt} by K_b, and to have equal losses in both valves the condition below must hold:

$$\frac{R^3}{\alpha^2} = 1 \tag{4.72}$$

The opening ratio of the valve gives Equal Throttling Power Loss

$$\alpha_{ETPL} = R^{\frac{3}{2}} \tag{4.73}$$

Recall that in chapter two the best opening ratio to reduce sensitivity to error was derived to be $\alpha_{opt}=R^{3/4}$, hence:

$$\alpha_{ETPL} = \alpha_{opt}^2 \tag{4.74}$$

The results are explained in figure 52 [45]:

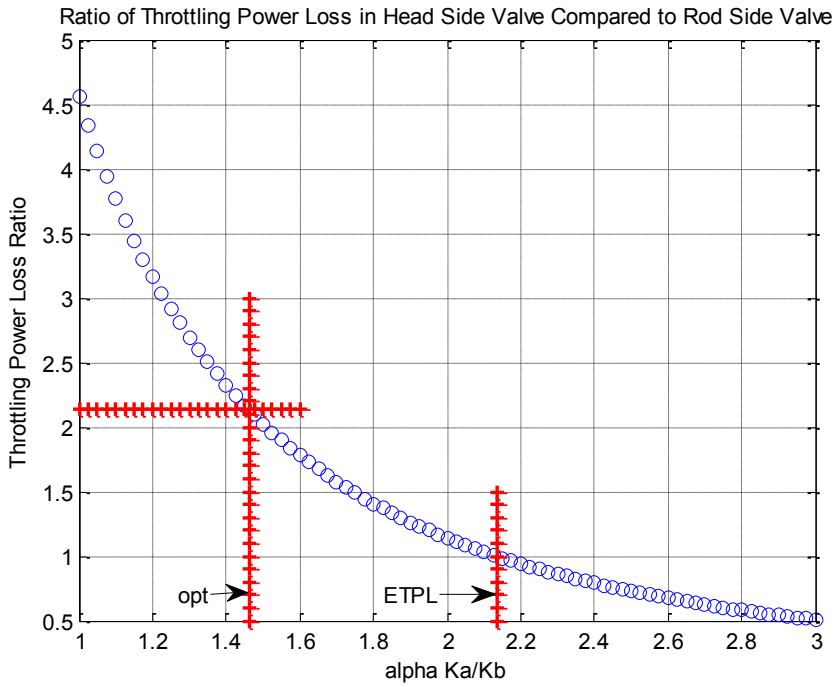

Figure 52. Throttling power loss ratio as a function of the valve opening ratio.

5 CONTINOUSLY VARIABLE MODES

5.1 Introduction

The five distinct modes are not a good way of control of hydraulic systems, because the opening and closing of the valves are not instantaneous, which means interruption of the flow and hence interruption of the flow velocity that causes vibration problems. The solution of this problem is to find a substitute for the five distinct modes, where there is no sudden change in the flow when transitioning from one mode to another, this solution is called the continuously variable mode (CVM). CVM uses three valves each at any instant of time to provide a path for the fluid flow and reduces the five distinct modes to three modes when only two valves are used. Another advantage of the CVM is the increased force speed capabilities over the five distinct modes, and it solves the vibration problem due to continuous flow path. The three modes used are:

1. Powered High Side Regeneration Extension (PHSRE).
2. Powered Low Side Regeneration Retraction (PLSRE).
3. Powered Low Side Regeneration Extension (PLSRE).
4. Powered High Side Regeneration Retraction(PHSRR).

The idea is to use three valves, and continuously switching between two distinct modes. The CVM have more speed force capabilities than distinct modes, but we should recalculate the supply pressure set point for CVM since it is will be different from the distinct modes [41,45].

5.1.1 Powered High Side Regeneration Extension Mode (PHSRE)

Figure 53 shows how this mode woks, with K_{sa}, K_{sb}, and K_{bt} as the three valves being used. Note here that two pumps are used to indicate that each chamber is connected to the power supply line, since three valves are involved at any instant of time.

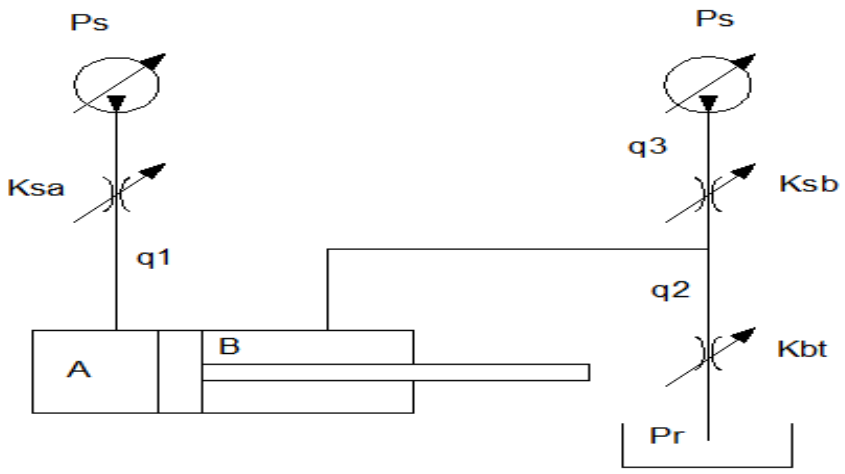

Figure 53. The concept of PHSRE CVM.

The hydraulic circuit of this mode is equivalent to an electric circuit that consists of a voltage source, a resistance, a transformer, and two other resistances with two other voltage sources. While the electrical circuits are linear by nature, hydraulic circuits are not, as seen by the relation $Q = K\sqrt{\Delta P}$. Since we have two valves involved in the rod side with one pressure P_b, the two valves K_{sb} and K_{bt} besides the supply and return pressures P_s and P_r, we must first reduce them to intermediate single valve that we call intermediate effective pressure P_{CVM_inter}, and intermediate effective valve conductance K_{CVM_inter}. Now if we look at the system it looks equivalent to PE mode and we can find the equivalent single pressure P_{CVM} and a single valve conductance K_{CVM} [41,45]. Figures 54 and 55 show the step by step reduction process of the system.

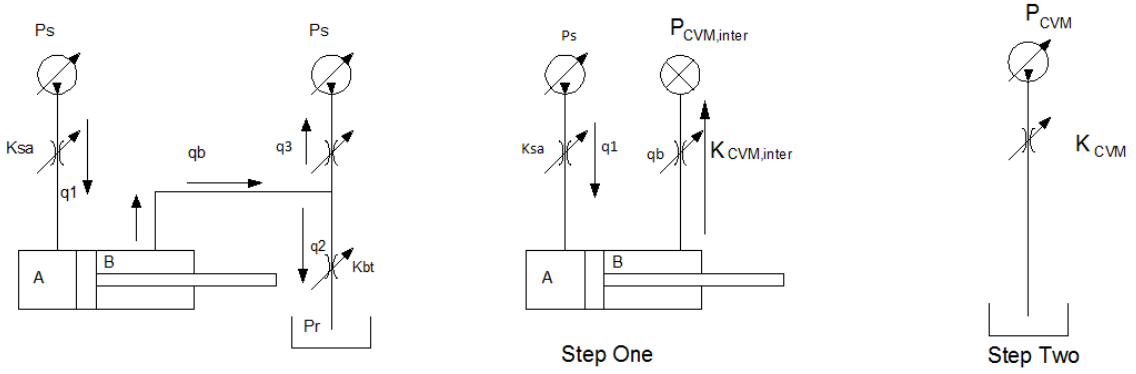

Figure 54. Schematic of the first step of PHSRE.

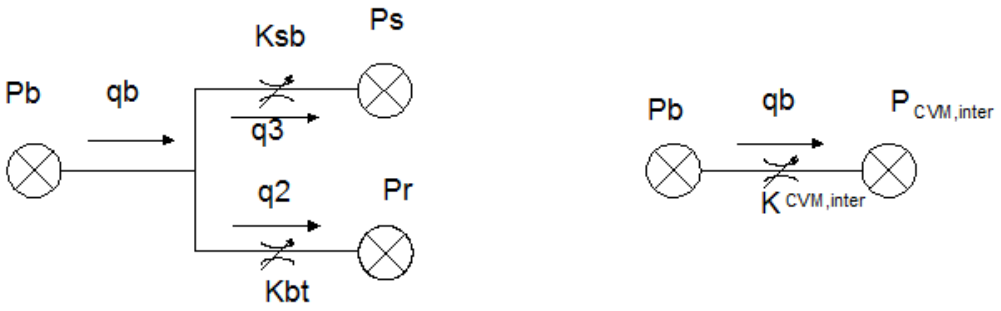

Figure 55. Schematic of the second step of the PHSRE.

In this analysis once again we are assuming quasi static system behavior and turbulent flow inside the system components.

$$q_b = q_2 + q_3$$

$$\Rightarrow K_{CVM,Inter}\sqrt{P_b - P_{CVM,Inter}} = K_{bt}\sqrt{P_b - P_r} + K_{sb}\sqrt{P_b - P_s} \quad (5.1)$$

$$\Rightarrow K_{CVM,Inter}^2\left(P_b - P_{CVM,Inter}\right) = {K_{bt}}^2(P_b - P_r) + {K_{sb}}^2(P_b - P_s) + 2K_{bt}K_{sb}\sqrt{(P_b - P_r)(P_b - P_s)}$$

$$\Rightarrow P_{CVM,Inter} \equiv \frac{{K_{bt}}^2 P_r + {K_{sb}}^2 P_s - 2K_{bt}K_{sb}\sqrt{(P_b - P_r)(P_b - P_s)}}{{K_{bt}}^2 + {K_{sb}}^2} \quad (5.1)$$

$$\Rightarrow K_{CVM,Inter} = \sqrt{{K_{bt}}^2 + {K_{sb}}^2} \quad (5.2)$$

From the intermediate values we move to the equivalent values for P and F, this is done the same way as for the normal PE mode where K_{sa} and K_{bt} are reduced to one effective pressure source and effective value of conductance. The final equivalent parameters become as follow:

$$P_{CVM} = R(P_s - P_a) + \left(P_b - P_{CVM,Inter}\right)$$

$$K_{CVM} = \frac{K_{sa}\,K_{CVM,Inter}}{\sqrt{{K_{sa}}^2 + R^3 {K_{CVM,Inter}}^2}} = \frac{K_{sa}\sqrt{{K_{bt}}^2 + {K_{sb}}^2}}{\sqrt{{K_{sa}}^2 + R^3\left({K_{bt}}^2 + {K_{sb}}^2\right)}} = \frac{\dot{x}A_b}{\sqrt{P_{CVM}}} \quad (5.3)$$

5.1.2 Powered Low Side Regeneration Extension Mode (PLSRE)

Figure 56 shows how this mode works; the valves used are K_{sa}, K_{at}, and K_{bt} [41,45].

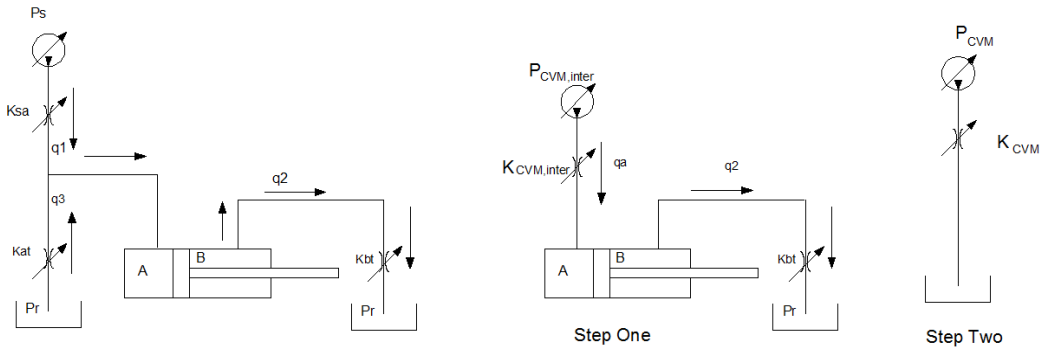

Figure 56. Schematic of the first step of the PLSRE.

Here again we will go through the same two steps as before, where in the first step we will reduce the head chamber two branches with the supply and return pressures P_s and P_r, the two valve conductance coefficients K_{sa} and K_{at} in addition to the chamber pressures P_a to intermediate pressure and conductance P_{CVM_inter} and K_{CVM_inter} [41,45]. Fig. 57 shows the second step of this process.

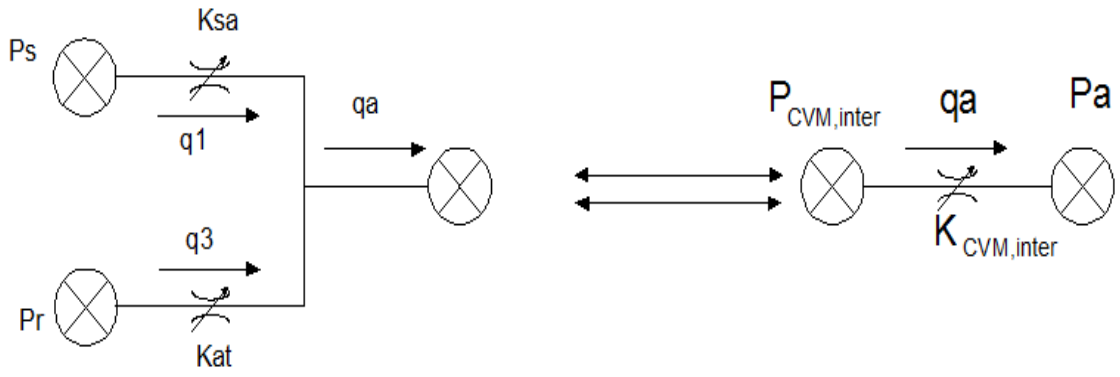

Figure 57. Schematic of the second step of the PHSRE.

$$q_a = q_1 + q_3$$

$$\Rightarrow K_{CVM,Inter}\sqrt{P_{CVM,Inter} - P_a} = K_{sa}\sqrt{P_s - P_a} + K_{at}\sqrt{P_r - P_a}$$

$$\Rightarrow K_{CVM,Inter}^2\left(P_{CVM,Inter} - P_a\right) = {K_{sa}}^2(P_s - P_a) + {K_{at}}^2(P_r - P_a) + 2K_{sa}K_{at}\sqrt{(P_s - P_a)(P_r - P_a)}$$

$$\Rightarrow K_{CVM,Inter}^2\, P_{CVM,Inter} - K_{CVM,Inter}^2 P_a =$$

$$-\left({K_{sa}}^2 + {K_{at}}^2\right)P_a + {K_{at}}^2 P_r + {K_{sa}}^2 P_s + 2K_{bt}K_{sb}\sqrt{(P_r - P_a)(P_s - P_a)} \quad (5.4)$$

$$\Rightarrow P_{CVM,Inter} \equiv \frac{{K_{at}}^2 P_r + {K_{sa}}^2 P_s + 2K_{at}K_{sa}\sqrt{(P_s - P_a)(P_r - P_a)}}{{K_{sa}}^2 + {K_{at}}^2} \quad (5.5)$$

$$\Rightarrow K_{CVM,Inter} \equiv \sqrt{{K_{sa}}^2 + {K_{at}}^2} \quad (5.6)$$

the second step is the same as used for PE except we replace P_a and K_{sa} by P_{CVM_inter} and K_{CVM_inter} along with P_b and K_{bt}

$$P_{CVM} = R\left(P_{CVM,Inter} - P_a\right) + (P_b - P_r)$$

$$K_{CVM} = \frac{K_{bt}\, K_{CVM,Inter}}{\sqrt{{K_{CVM,Interat}}^2 + R^3\left({K_{bt}}^2\right)}} = \frac{K_{bt}\sqrt{{K_{sa}}^2 + {K_{at}}^2}}{\sqrt{{K_{sa}}^2 + {K_{at}}^2 + R^3\left({K_{bt}}^2\right)}} = \frac{\dot{x}A_b}{\sqrt{P_{CVM}}} \quad (5.7)$$

5.1.3 Powered Low Side Regeneration Retraction Mode (PLSRR)

Figure 58 shows how this mode works, the three valves used are K_{at}, K_{sb}, and K_{bt} [41,45].

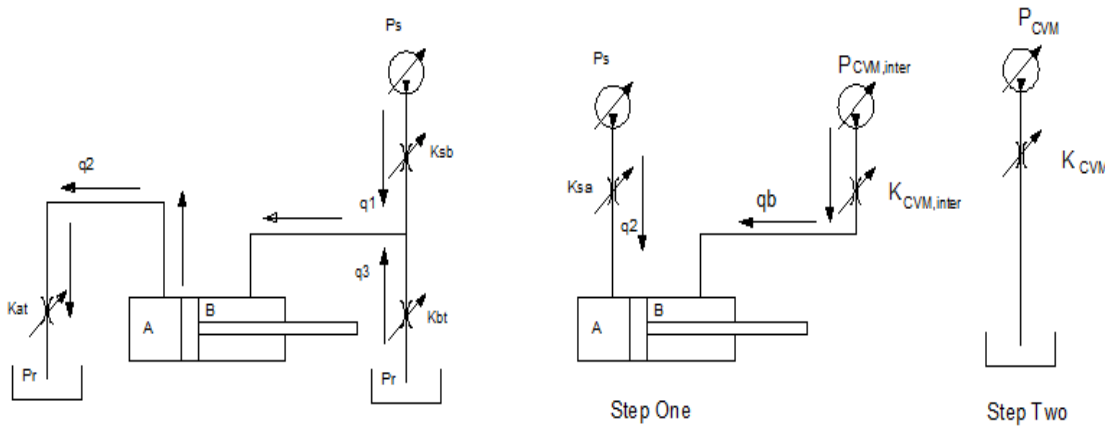

Figure 58. Schematic of the first step of PLSRR.

Here again we will go through the same two step as done for PHSRE, in the first step we reduce the two branches of the rod side to one and find the intermediate pressure and valve conductance, then we reduce the entire circuit to equivalent pressure and conductance.

Figure 59 show the first step which reduces the rod pressure P_b of the two valves K_{sb} and K_{bt} in addition to supply and return pressures P_s and P_r to P_{CVM_inter} and K_{CVM_inter} [41,45].

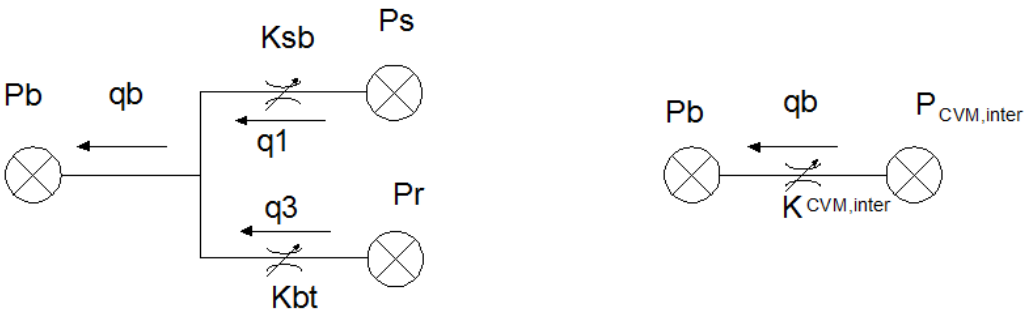

Figure 59. Schematic of the second step of the PLSRR.

$$q_b = q_1 + q_3$$

$$\Rightarrow K_{CVM,Inter}\sqrt{P_{CVM,Inter} - P_b} = K_{bt}\sqrt{P_r - P_b} + K_{sb}\sqrt{P_s - P_b}$$

$$K_{CVM,Inter}^2\left(P_{CVM,Inter}-P_b\right)=K_{bt}{}^2(P_r-P_b)+K_{sb}{}^2(P_s-P_b)+2K_{bt}K_{sb}\sqrt{(P_r-P_b)(P_s-P_b)}$$

$$K_{CVM,Inter}^2\,P_{CVM,Inter}-K_{CVM,Inter}^2\,P_b\;=$$
$$-\left(K_{bt}{}^2+K_{sb}{}^2\right)P_b+K_{bt}{}^2P_r+K_{sb}{}^2P_s+2K_{bt}K_{sb}\sqrt{(P_r-P_b)(P_s-P_b)} \quad (5.8)$$

$$\Rightarrow P_{CVM,Inter}\equiv\frac{K_{bt}{}^2P_r+K_{sb}{}^2P_s+2K_{bt}K_{sb}\sqrt{(P_r-P_b)(P_s-P_b)}}{K_{bt}{}^2+K_{sb}{}^2} \quad (5.9)$$

$$\Rightarrow K_{CVM,Inter}\equiv\sqrt{K_{bt}{}^2+K_{sb}{}^2} \quad (5.10)$$

The second step is the same as used for PR except we use the intermediate value instead of the rod side value for pressure and conductance.

$$P_{CVM}=R(P_a-P_r)+\left(P_{CVM,Inter}-P_b\right)$$

$$K_{CVM}=\frac{K_{at}\,K_{CVM,Inter}}{\sqrt{K_{at}{}^2+R^3K_{CVM,Inter}{}^2}}=\frac{K_{at}\sqrt{K_{bt}{}^2+K_{sb}{}^2}}{\sqrt{K_{at}{}^2+R^3\left(K_{bt}{}^2+K_{sb}{}^2\right)}}=\frac{\dot{x}A_b}{\sqrt{P_{CVM}}} \quad (5.11)$$

5.1.4 Powered High Side Regeneration Retraction

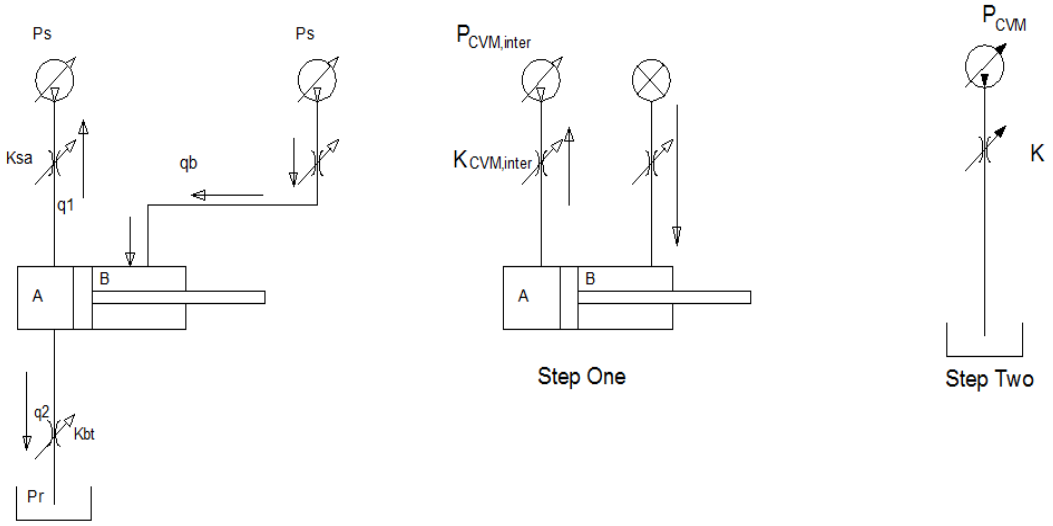

Figure 60. Schematic of the first step of PHSRR.

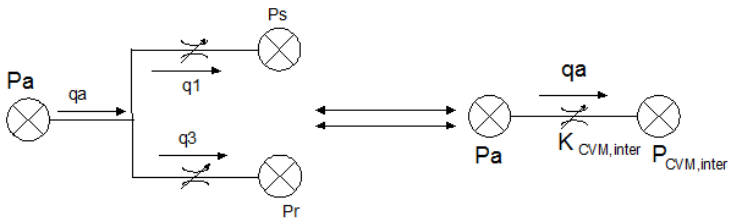

Figure 61. Schematic of the second step of the PHSRR.

$$q_a = q_1 + q_3$$

$$K_{CVM,inter}\sqrt{P_a - P_{CVM,inter}} = K_{sa}\sqrt{P_a - P_s} + K_{at}\sqrt{P_a - P_r}$$

$${K_{CVM,inter}}^2\left(P_a - P_{CVM,inter}\right) = {K_{sa}}^2(P_a - P_s) + {K_{at}}^2(P_a - P_r) + 2K_{sa}K_{at}\sqrt{(P_a - P_s)(P_a - P_r)}$$

$$P_{CVM,inter} = \frac{{K_{sa}}^2 P_s + {K_{at}}^2 P_r - 2K_{sa}K_{at}\sqrt{(P_a - P_s)(P_a - P_r)}}{{K_{sa}}^2 + {K_{at}}^2} \quad (5.12)$$

$$K_{CVM,inter} = \sqrt{{K_{sa}}^2 + {K_{at}}^2} \quad (5.13)$$

$$P_{CVM} = R\left(P_a - P_{CVM,inter}\right) + (P_s - P_b) \quad (5.14)$$

$$K_{CVM} = \frac{K_{sb}\, K_{CVM,inter}}{{K_{sb}}^2 + R^3 {K_{CVM,inter}}^2} \quad (5.15)$$

5.2 Mode Capabilities of CVM in Comparison to Distinct Modes

As an example we will explore the capabilities of the PHSRE CVM and compare it to PE and HSRE modes. PE and HSRE modes are considered special cases of PHSRE which means it will definitely have the same force speed capabilities of both, furthermore, the change of K_{sb} and K_{bt} ratio will result in improved envelop of performance for the PHSRE. It is clear that the speed depends on the flow rate supplied by the pump, while the force of the actuator depends on two things; the load itself and the maximum pressure the pump can supply. The equations below are derived for the actuator speed in the PHSRE CVM [41,45].

$$F = P_a A_a - P_b A_b \quad (5.16)$$

$$\dot{x}_{PHSRE} = \frac{K_{CVM}\sqrt{(RP_s - P_{CVM,Inter}) + (-RP_a + P_b)}}{A_b} \quad (5.17)$$

$$\dot{x}_{PHSRE} = \frac{K_{CVM}\sqrt{\left(RP_s - \frac{F}{A_b} - P_{CVM,Inter}\right)}}{A_b} \quad (5.18)$$

The pump capacity in terms of the flow rate and pressure determines the maximum power available and hence the output force and speed of the actuator

$$Power = P.Q = F.\dot{x} \quad (5.19)$$

$$P_s.Q_{PHSRE} = F_{max}.\dot{x}_{PHSRE} = (P_s A_a - P_{CVM,Inter} A_b)\dot{x}_{PHSRE} \quad (5.20)$$

$$\Rightarrow Q_{PHSRE} = \frac{(P_s A_a - P_{CVM,Inter} A_b)\dot{x}_{PHSRE}}{P_s} \quad (5.21)$$

Now if the calculated Q_{PHSRE} is greater than Q_{max} then $\dot{x}_{PHSRE}$ is limited to that of Q_{max}.

$$\dot{x}_{PHSRE} = \frac{Q_{max} P_s}{(P_s A_a - P_{CVM,Inter} A_b)} \quad (5.22)$$

For the example of the telehandler extender cylinder, we assume maximum opening of valve K_{sa}, while we vary K_{sb} and K_{bt} by α where $0 \leq \alpha \leq 1$. Such that:

$$K_{bt} = \alpha K_{max}$$

$$K_{sb} = (1 - \alpha) K_{max} \quad (5.23)$$

Notice that if α =1 then K_{bt} is closed while K_{sb} is completely open, which means operating under PE mode, which is a special case of the PHSRE. To explore the capabilities of PHSRE we vary α from zero to one. Figure 62 shows the force speed capabilities of the telehandler extender subjected to 0-100KN load, with a maximum pump flow of 5520LPH.

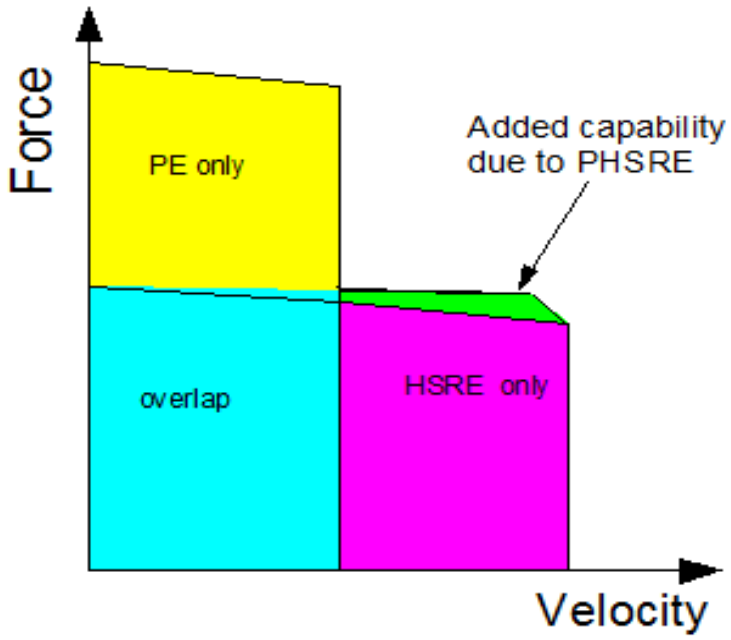

Figure 62. The force-speed capability curves of PHSRE.

Notice that as α changes so does the force speed curve of the PHSRE between PE and HSRE modes. Also notice the small region added to the curve of the PHSRE that could not be achieved by any of the distinct modes alone. The PHSRE can push loads at speeds that could not be done by PE or HSRE alone, in the blue triangular region of the capability envelop, this removes some of the limitations on moving some loads at certain speeds, for example, we could not move a force of 50.3 KN at a commanded speed of 0.7 m/s, but we can now using PHSRE [45].

The other significant achievement of PHSRE is the removal of switching point, because it keeps the three valves open almost all the time, and so the problem of discontinuity due to opening one valve and closing another is no longer an issue, which means smooth transition from one mode region to another, this will improve velocity and vibration performance of the system greatly.

5.3 PLSRE CVM Valve Control

We will take this case as an example of how to control an individual valve in CVM. The desired actuator speed required a specific value of K_{CVM}, and this can be achieved by finding one of the individual values of the openings, which can be done through the command from the operator using a joystick.

Since we have three valves involved in CVM, the control process becomes more complex; also recall that we have both P_{CVM_inter} and PCVM which depend on the valve openings. For a desired commanded speed we can find K_{CVM} to be:

$$K_{CVM} = \frac{A_b\ \dot{x}_{com}}{\sqrt{P_{CVM}}} = \frac{A_b\ \dot{x}_{com}}{\sqrt{R(P_{CVM,Inter} - P_a) + (P_b - P_r)}} \tag{5.24}$$

$$P_{CVM,Inter} = \frac{{K_{at}}^2\ P_r + {K_{sa}}^2\ P_s + 2K_{at}K_{sa}\sqrt{(P_s - P_a)(P_r - P_a)}}{{K_{sa}}^2 + {K_{at}}^2} \tag{5.25}$$

$$K_{CVM} = \frac{K_{bt}\sqrt{{K_{sa}}^2 + {K_{at}}^2}}{\sqrt{{K_{sa}}^2 + {K_{at}}^2 + R^3{K_{bt}}^2}} \tag{5.26}$$

From these equations it is apparent that both intermediate and equivalent pressures depend on K_{at} and K_{sa} in addition to the supply and return pressures and off course on the load. Figure 63 show the variation of both the intermediate and equivalent pressures with the change in K_{at} and K_{sa} as surfaces [45].

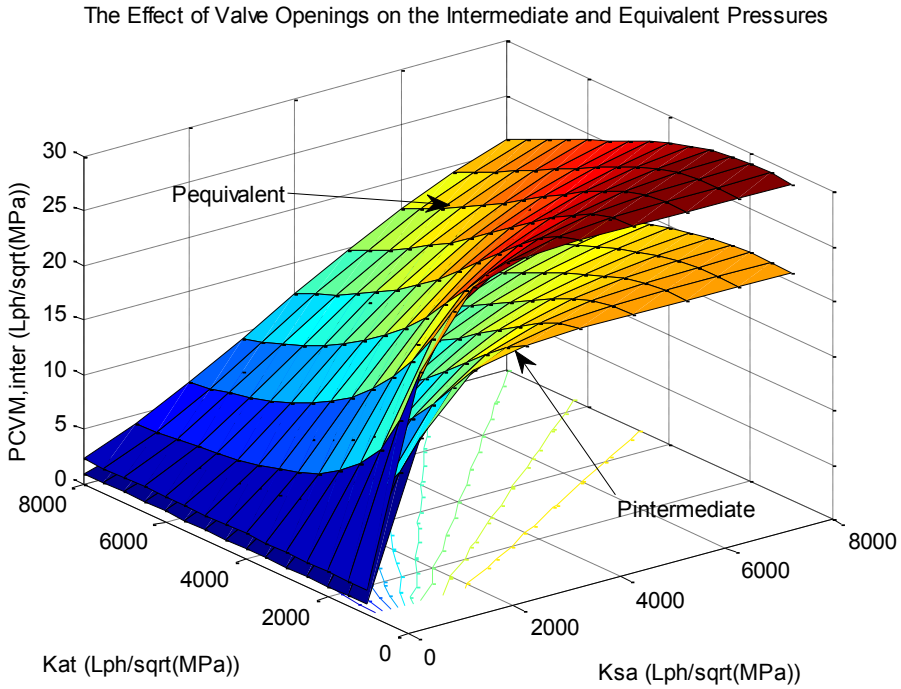

Figure 63. 3D surface of the equivalent and intermediate pressures as Kat and Ksa are varied.

Notice that for one value of K_{CVM_inter} there is an infinite number of combinations of K_{sa} and K_{at} to achieve this value, from equation 23 if we set K_{sa} to zero then we end up with the same equation for LSRE in the distinct mode as seen before and in comparison to figure 10, keeping in mind that this is a special case of PLSRE and that in general K_{sa} is not equal to zero. Figure 64 shows few surfaces describing the variations of K_{sa} and K_{bt} for the values of K_{sa}=0, 2000, 4000, 6000, and 8000 LPH/MPa^0.5 [45] .

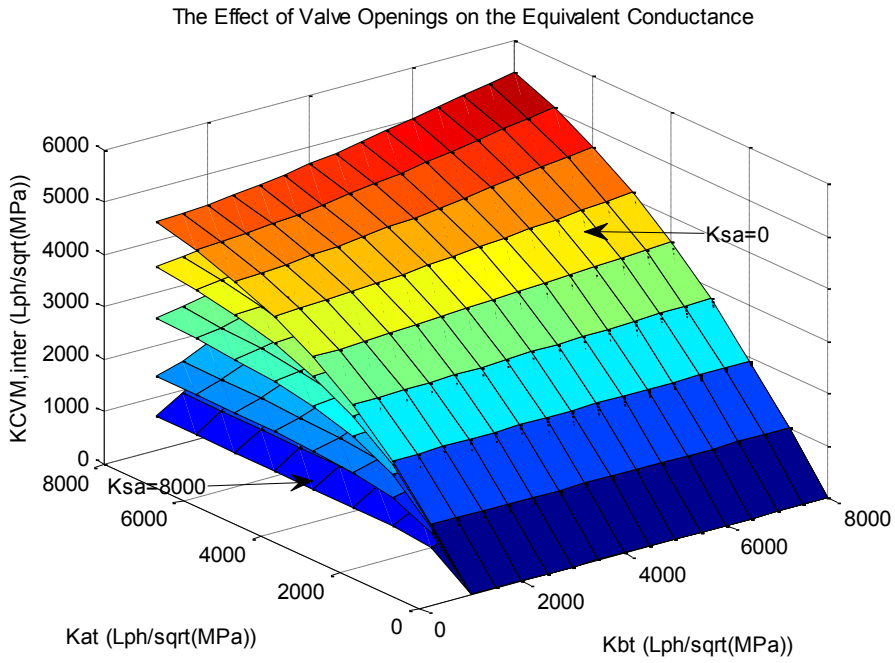

Figure 64. 3D surface of the equivalent conductance for different values of Ksa.

Comparing the case of K_{sa}= 0 to LSRE, we expect them to be identical, but they are not. The effect of K_{sa} can be viewed clearly in figures 65 and 66 for K_{sa} value of 3000 LPH/MPa^0.5 , and 5000 LPH/MPa^0.5 [45].

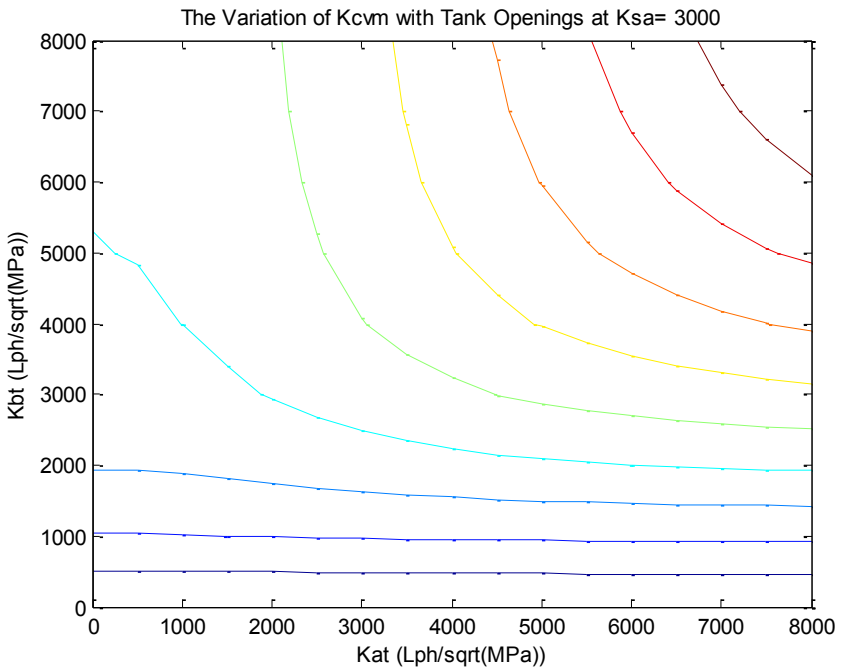

Figure 65. Contour plot of the equivalent conductance for Ksa =3000.

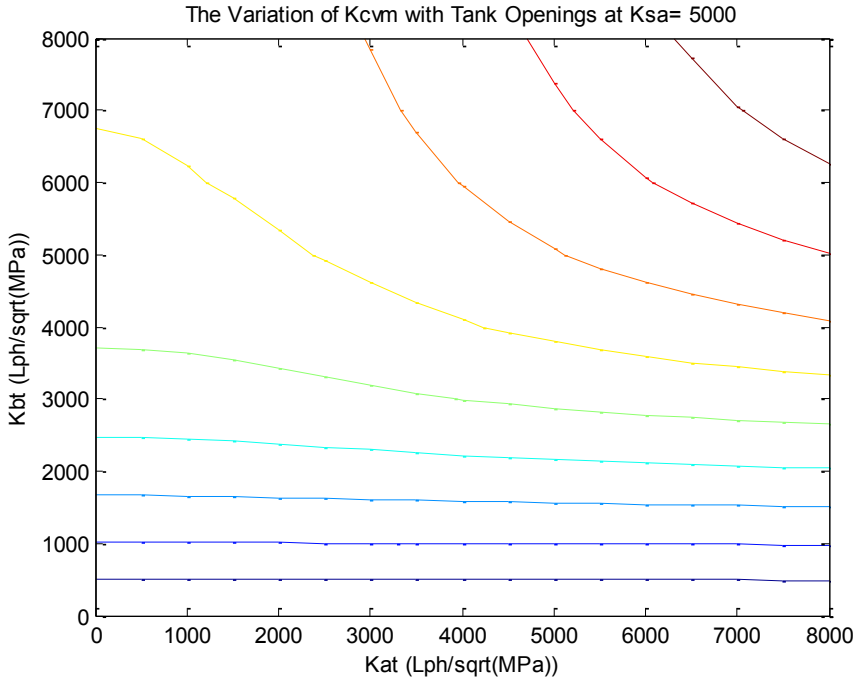

Figure 66. Contour plot of the equivalent conductance for Ksa =5000.

Notice that for low values of K_{CVM} e.g. 500, 1000 the curve is very much linear, which means that the effect of K_{at} is very limited and any value of K_{at} will achieve the same value of K_{CVM} with negligible error. This means that the important parameters are K_{bt} and K_{sa}, for example, for K_{sa} = 3000 and K_{bt} =1000, the variation of K_{at} from zero to 8000 will only result in a variation in KCVM from 888.2 - 983.9, but what does this mean physically? A small value of K_{CVM} means small commanded speed which means small flow in and maximum flow is circulated to the tank through the K_{at}, if K_{at} is opened beyond this amount it will make no difference since the needed flow is already reached [39,41].

Now as K_{CVM} is getting bigger, i.e. 2000, we get closer and closer to LSRE distinct mode behavior, but the only difference will be an upward shift of the surface. This shift upwards will interfere with sensitivity and it will reduce it, so one must chose smallest K_{at} which means low regeneration flow and lower energy saving, so one must prioritize the goals of the system parameters beforehand. Figure 66 shows the same behavior for K_{sa}=5000. Notice that large values of K_{at} are still in effect [39].

5.4 Valve Control Strategy

The goal is to find how much each of the three involved valves must be opened for a given supply and return pressures, a load, and commanded speed [41].

Let's define a new variable $\gamma=K_{sa}/K_{at}$ or $K_{sa}=\gamma K_{at}$, and substitute for K_{CVM_inter}:

$$K_{CVM,Inter} = \sqrt{{K_{sa}}^2 + {K_{at}}^2} = \sqrt{\gamma^2 {K_{at}}^2 + {K_{at}}^2} = \sqrt{\gamma^2 + 1}\ K_{at} \quad (5.27)$$

if K_{bt} is the value that achieves minimum losses across the outlet valve then the desired chamber pressures $P_{b,\,Des}$ and $P_{a,\,Des}$ for a given load and commanded speed are given by:

$$P_{b,Des} = \frac{(\dot{x}_{com} A_b)^2}{{K_{bt}}^2} + Pr \quad (5.28)$$

$$P_{a,Des} = \frac{F}{A_a} + \frac{P_{b,Des}}{R} \quad (5.29)$$

Substitute in 10 we find P_{CVM_inter}:

$$P_{CVM,Inter} = \frac{{K_{at}}^2\ P_r + \gamma^2 {K_{at}}^2\ P_s + 2\gamma {K_{at}}^2 \sqrt{(P_s - P_{a,Des})(P_r - P_{a,Des})}}{\gamma^2 {K_{at}}^2 + {K_{at}}^2} \quad (5.30)$$

Divide by K_{at}^2

$$P_{CVM,Inter} = \frac{P_r+\gamma^2 P_s+2\gamma\sqrt{(P_s-P_{a,Des})(P_r-P_{a,Des})}}{\gamma^2+1} \quad (5.31)$$

So for a given value γ one can find P_{CVM_inter} from equation 4.29 for a certain load, P_s, and P_r which means we can find P_{CVM}:

$$P_{CVM} = R\left(P_{CVM,Inter} - P_{a,Des}\right) + \left(P_{b,Des} - P_r\right) = RP_{CVM,Inter} - \frac{F}{A_b} - P_r \quad (5.32)$$

Since we know P_{CVM} now, we can translate the commanded speed $\dot{x}_{com}$ into corresponding K_{CVM} for the value of $P_{a,\,Des}$ based on the chosen value of K_{bt}

$$K_{CVM} = \frac{\dot{x}_{com}A_b}{\sqrt{P_{CVM}}} \quad (5.33)$$

Again, the idea of controlling PLSRE is to find the K_{CVM} that corresponds to a desired commanded speed and to find the individual valve openings K_{sa}, K_{at} and K_{bt} that make up this value of K_{CVM}:

$$K_{CVM} = \frac{K_{CVM,Inter}K_{bt}}{\sqrt{K^2{}_{CVM,Inter}+R^3{K_{bt}}^2}} = \frac{\sqrt{\gamma^2+1}K_{at}K_{bt}}{\sqrt{(\gamma^2+1){K_{at}}^2+R^3{K_{bt}}^2}} \quad (5.34)$$

$${K_{CVM}}^2\left[(\gamma^2+1){K_{at}}^2 + R^3{K_{bt}}^2\right] = (\gamma^2+1){K_{at}}^2{K_{bt}}^2 \quad (5.35)$$

$${K_{at}}^2 = \frac{R^3{K_{CVM}}^2{K_{bt}}^2}{(\gamma^2+1)\left[{K_{bt}}^2-{K_{CVM}}^2\right]}$$

$$K_{at} = \frac{R^{3/2}K_{CVM}K_{bt}}{\sqrt{(\gamma^2+1)\left[{K_{bt}}^2-{K_{CVM}}^2\right]}} \quad (5.36)$$

To sum up the strategy, given the load, the supply and return pressures, the input and output opening ratio γ, we choose a value for K_{bt} that satisfy the desired chambers pressures, and using equation 31 to find K_{CVM} and then equation 33 to find K_{at}. We then multiply K_{at} by γ to get K_{sa} which determines all three valve openings K_{sa}, K_{at}, and K_{bt} for a commanded speed. The choice of γ is very important and it holds some implications on the PLSRE, if γ is high then K_{sa}/K_{at} is high which mean high force and low speed capability compared to low γ. In comparison to distinct mode method, this is not completely identical, for distinct mode K_{eq} represents all possible solutions that can achieve a desired speed for a specific load at a given supply and return pressures, this is because P_{eq} is constant for a given load and it is independent of the chamber pressures [41].

In PLSRE CVM, the P_{CVM} depends on the chambers pressures due to its dependence on P_{CVM_inter}. This means that K_{CVM} does not represent the surface of solutions, but a curve in 3D of the valve openings K_{sa}, K_{bt}, and K_{at} depending on the chamber pressure Pa [45].

As mentioned before, the two factors that determine the supply pressure by the pump are the load, and pressure drop across the valve. The supply pressure set point will be different for each of the three CVMs. An example of the derivation will be presented here for PHSRE and the results for the other two cases are listed. Figure 67 represents the hydraulic circuit for PHSRE 41,45].

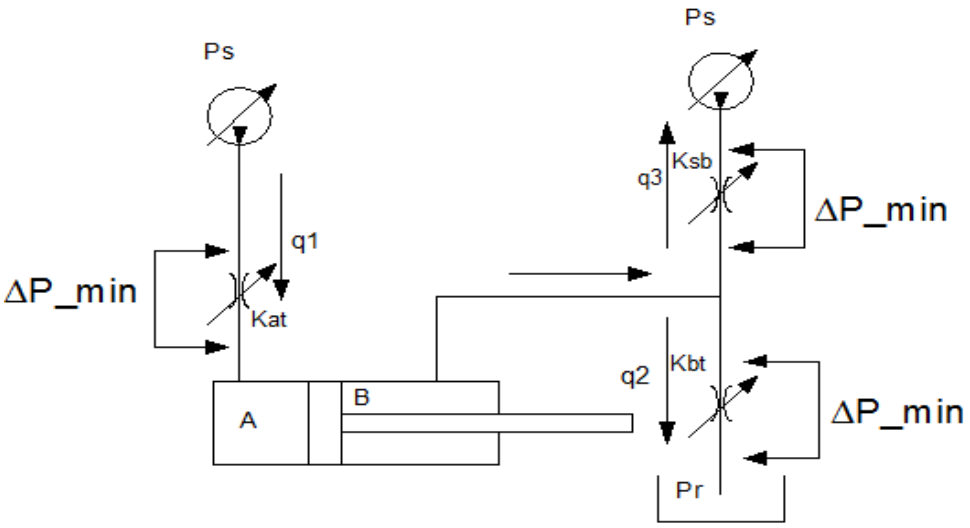

Figure 67. Schematic of the pressure set point for PHSRE.

The force equation is:

$$P_s A_a - P_r A_b - P_s A_b = \Delta P_1 A_a + (P_a A_a - 2P_b A_b) + A_b \Delta P_2 + A_b \Delta P_3 \quad (5.37)$$

Where we define:

$$\Delta P_1 = P_s - P_a$$

$$\Delta P_2 = P_b - P_r$$

$$\Delta P_3 = P_b - P_s$$

$$\Rightarrow (R-1)P_s - P_r - RP_a + 2P_b = R\Delta P_1 + \Delta P_2 + \Delta P_3 \quad (5.38)$$

Recalling that the EHPV requires a minimum ΔPmin across them to perform correctly, and the supply Pressure set point must keep this minimum pressure even if no such pressure is needed for load or speed requirements. Replacing ΔP_1, ΔP_2, ΔP_3 by ΔP_{min} and solving for P_s we get:

$$\Rightarrow P_{S\ set-point} = \frac{(R+2)\Delta P_{min}}{R-1} + \frac{RP_a - 2P_b + P_r}{R-1} \quad (5.39)$$

Following the same methodology we get the results for PLSRR

$$P_{S\ set-point} = (R+2)\Delta P_{min} - RP_a + 2P_b + (R+1)P_r \quad (5.40)$$

for PLSRE

$$P_{S\ set-point} = \frac{(2R+1)\Delta P_{min}}{R} + \frac{2RP_a - P_b - (R-1)P_r}{R} \quad (5.41)$$

for PHSRR

$$P_{s,setpoint} = \frac{(2R+1)\Delta P + RP_r - RP_a + P_b}{1-R} \quad (5.42)$$

6 CLOSED LOOP CONTROL OF AN ELECTROHYDRAULIC SYSTEM

6.1 System Description

The system to be controlled here is an IMV arrangement that consist of four -two stage servo valves to control the flow from the pump to the head chamber and the rod chamber of the actuator, as well as the flow to the tank from the two chambers [12]. Some minor simplifications are assumed about the system such as ignoring the leakage effect which is very safe to assume, and neglecting the effect of the relief valves, in addition to the assumption of a perfect performance of the pump .

The pump used is a fixed displacement pump with fixed flow rate due to the constant speed of the driving electric motor. The relief valve opens instantaneously when there is an excessive flow from the pump, and it is circulated to the tank, so when the pump pressure is less than the relief valve set pressure, the relief valve will remain closed and it will open if the pump pressure exceeds this set pressure limiting the pump pressure to this maximum set pressure, this is done by and instantaneous opening of the valve and dumping the excess flow to the tank. The mathematical model of the relief valve and the fluid compressibility of this section of the system is limiting the maximum pressure setting of the pressure integration. A traditional system used in [12] is used as a reference to the IMV system to be modeled and controlled in this section.

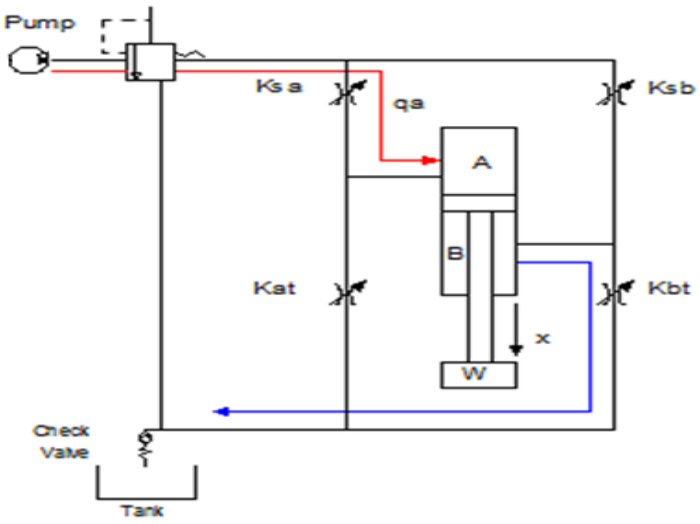

Figure 68. Hydraulic system description.

6.2 Mathematical Modeling

The mathematical model of the pump passing by the relief valve, the servo valve and the compressibility effect in this section of the system is given by the following equations [29]:

$$Q_p(t) = D_p(t).w_{shaft}(t) \tag{6.1}$$

for $p_p < p_{max}$

$$\frac{dp_p(t)}{dt} = \frac{\beta}{V_{hose,pv}}\left(Q_p(t) - Q_v(t)\right) \tag{6.2}$$

$$Q_r(t) = 0$$

else if $p_p > p_{max}$

$$Q_r(t) = (Q_p(t) - Q_v(t)) \tag{6.3}$$

$$p_p(t) = p_{max}$$

$Q_p(t)$ is the total flow out of the pump, while $Q_v(t)$ represents the flow rate from the pump to the cylinder which can be to the head side in extension $(Q_{pa}(t))$ or to the rod side in retraction $(Q_{pb}(t))$.

Each port of the cylinder is assumed to use a two stage servo valve, the first stage is a flapper nozzle, while the second stage is a spool type, so the four ports are using four independent valves that connect each chamber to the pump from one side and to the tank from the other side [12]. The flow through these valves is proportional to the pressure differential across it, and the position of the spool in the second stage, which move due to the torque exerted on the spool by the current commanded to the servo valve.

A first order filter is used as a model of the current amplifier and the electrical dynamics of the servo valve in response to the commanded current, and the torque is modeled as a linear relation of the current, while the torque to spool position is modeled as a second order mass force system, and the natural frequency of this model is dependent on the spool position and on the location of the spool travel to the maximum spool travel distance, which in turn is a function of the commanded current to the maximum commanded current. The details of this model can be found in reference[12]. The formulas here have been modified to fit the IMV format, yet the dynamics of the valves have not been changed, the idea is to only replace the dynamics of the valve and the approach will still be valid for any

electrohydraulic system with it has one or two degrees of freedom, and this is the main contribution of this thesis. The mathematical relations among the various parts of the systems are given in the equations below:

$$\frac{di}{dt} = K_a \times \frac{1}{\tau_a} \times (i - i_{cmd}) \tag{6.4}$$

$$T_v = K_T \times i \tag{6.5}$$

If $\frac{x_v}{x_{vmax}} \leq 0.4$

$$\omega_n = 2\pi \times 75 \tag{6.6}$$

else

$$\omega_n = 2\pi \times (75 - ((\text{x\_v/x\_vmax}) - 0.4) \times ((75 - 25)/(1.0 - 0.4))) \tag{6.7}$$

$$(dx\_v)/dt = v_v \tag{6.8}$$

$$\frac{dv_v}{dt} = (-2 \times c_v \times \omega_n \times v_v) - ({\omega_n}^2 \times x_v) + \left(\frac{x_v}{T_{vmax}}\right) \times {\omega_n}^2 \times T_v \tag{6.9}$$

If $x_v \geq 0$

$$Q_{pa} = C1 \times |x\_v| \times \sqrt{p_p - p_a} \tag{6.10}$$

$$Q_{bt} = C1 \times |x\_v| \times \sqrt{p_b - p_t} \tag{6.11}$$

$$Q_v = Q_{pa} \tag{6.12}$$

$$\frac{dp_a}{dt} = \frac{\beta}{V_{hose\_va} + y\, A_a}\left(Q_{pa} - y' \times A_a\right) \tag{6.13}$$

$$\frac{dp_b}{dt} = \frac{\beta}{V_{hose\_va} + (l_{cyl} - y)\, A_a}(-Q_{bt} + y' \times A_b) \tag{6.14}$$

else

$$Q_{at} = C1 \times |x\_v| \times \sqrt{p_a - p_t} \tag{6.15}$$

$$Q_{pb} = C1 \times |x\_v| \times \sqrt{p_p - p_b} \tag{6.16}$$

$$Q_v = Q_{pb} \tag{6.17}$$

$$\frac{dp_a}{dt} = \frac{\beta}{V_{hose\_va} + y\, A_a}(-Q_{at} - y' \times A_a) \tag{6.18}$$

$$\frac{dp_b}{dt} = \frac{\beta}{V_{hose\_va} + (l_{cyl} - y)\, A_a}(Q_{pb} + y' \times A_b) \tag{6.19}$$

end

$$\frac{dy}{dt} = v \tag{6.20}$$

$$\frac{dv}{dt} = \frac{1}{m_p + m_l} - c_v \times y' + p_a \times A_a - p_b \times A_b - F_{load} \tag{6.21}$$

where $C1 = \frac{Q_{rv}}{x_{vmax}\sqrt{p_r}}$

The first three equations for the current of the valve, the position of the second stage spool, and the velocity of the spool are repeated for each valve in the case of the independent metering valve model, and only once for traditional valves.

These equations are the same as those derived in chapters two and three for electrohydraulic poppet valves, with the exception of the dynamics of the valves, that is replacing the terms C1* $|x_v|$ by *Ka* or *Kb* will give identical equations [45].

The control approach used here is to use the simplest control algorithm that can meet the requirements of the system, so the first controller that comes to mind is the PID controller in the simplest form which is the P controller, keeping in mind that for this case the inlet and outlet are decoupled, so a PID control gains should be applied to each valve independent of the other. Here the results are presented for both cases the traditional valve, and the IMV valve using the same approach [30].

6.3 Control Strategy

The control strategy is based on dealing with each valve as an independent system that needs its own controller, this section discusses only one mode which is the powered extension mode as a proof of the validity of the method, it is compared to the traditional two stage electrohydraulic servo valve with one degree of freedom, then the results are compared. This is the same strategy used by Cetinkunt for the traditional electrohydraulic system with a two stage servo valve [12]. The three programs used to model and control the system have been modified to describe the new IMV system.

6.3.1 The Dynamics Function

Despite the high nonlinearity in the equations that result from the variable volume of the regions between the valve and the chambers and between the tank the chambers, the square root of the pressure difference, and the natural frequency that depend on the spool position, a PID controller is proposed due to its wide use, simplicity, and reliability [26]. First, a PID controller is used to control the traditional system with the same valve dynamics, and the gains are found to meet the system requirements, which is the desired position of the cylinder arm in this case, then the model for the IMV is included for each valve in the new system that has two degrees of freedom. This IMV system requires a signal to be sent to each valve, so the state equations of the systems are modified such that the equations describing the dynamics of the each valve are augmented into the system equations, this step will result in increasing the state variables, and hence, the system equations by three. The new augmented set of nonlinear equations are simultaneously solved in a function file, this function file is programmed to describe the dynamics of augmented system.

6.3.2 The Controller Function

In the controller function file, a PID controller is coded such that it continuously defines the desired position in time over four different intervals; first, the desired position of the hydraulic piston is located 0.2 meters for the first second, the following interval is the extension of the arm at a given rate for the next second until it reaches the desired position point or the fully extended arm at 0.7 meters, when this is achieved the cylinder is expected to stay at this desired position for one second to make sure it has enough time to damp out any oscillations and compensate for any delays, by the end of this process any manufacturing process is assumed to take place , finally, the retraction of the arm is started at the beginning of the fourth second with a rate that can be the same as the extension rate or different from it back to the 0.2 meter position, in our case we have the same retraction rate, and when the cylinder is back to this position, the system waits for another second before starting another cycle [12].

The controller then reads the actual position, in addition to the actual velocity, and calculates the error in the position, velocity and the integral of position. These values are then used to calculate the commanded current signal after giving them the proper gains.

This process is repeated for both valves where the gains are defined in the main program and passed to the controller to compute the commanded current, and it is very important to mention that both control signals are totally independent from each other, so each one can any combination of the

PID control elements that give the desired output. In the case of independent powered extension mode shown below the first valve uses the PD controller, while the second valves uses PID controller [12].

6.3.3 The Main Program

The main program consists of several sections; the first is the parameters definitions, and the initializing of the variables that are used to define the system and the controller, some of the values are defined once and they remain constants throughout the code, while others are just initialized and will be updated with time for each time step [12].

The second section of the main program is the time loop, where the calculation of the states of the system are calculated and solved for, and the controller is applied to those states at each time step. The time is divided to small steps and the controller is applied to both valves at each step and the commanded signal is used to correct for the deviation between the desired states and the actual states. At each corresponding time the dynamics of the systems are calculated from the differential equations described above and the initial conditions used are the states of the previous step, this process continues throughout the time interval.

The dynamics function used to find the differential equations is applied at each time step to find the rate of the states, then the ODE45 function built in Matlab is used to solve for these set of equations, the solved equations give the current states as an array over the time, the last row of the states are then saved to represent the current state, and to be used as initial conditions to the next step, in addition to update the next error signal based on the difference between them and the desired states.

The third section of the main program is the data analysis, where all the data calculated over the various time intervals are stored in one array, which is the output array. This output array is used to separate all the states throughout the running time.

In this section the plots of the various states and parameters are generated to monitor and analyze the system performance, in this section four types of plot are created, the first shows the flow paths through the system for different pressures, while the second describes the pressure variation from the pump in the cylinder chambers, the third plot explains the relation between the commended current signal and the response of the spool to it, and last and most important the position response under the influence of the controller compared to the desired position [12].

6.4 Results and Discussion

6.4.1 Traditional System

As mentioned earlier the traditional electrohydraulic valve has one degree of freedom, it is more robust and very reliable due to the coupling of the inlet and outlet openings, but the problem is that no regeneration can be used for the system in which it is used, so there is no energy saving.

The controller used for this case is just a PI controller with the gains of $K_p = 4$, and $K_i = 0.4$. The output position of the hydraulic cylinder in comparison to the desired position is shown below in response to the aforementioned PI controller, which represents the combination of various gains that gave the best tracking output. It is noticed that the response is very acceptable with very small error shown as small deviation between the blue line which represents the actual output and the straight black lines that represent the desired position. This response is a typical response with small overshoot and few oscillations that damp out both at the end of the extension stroke and the retraction stroke as seen at times equal to two seconds and four seconds.

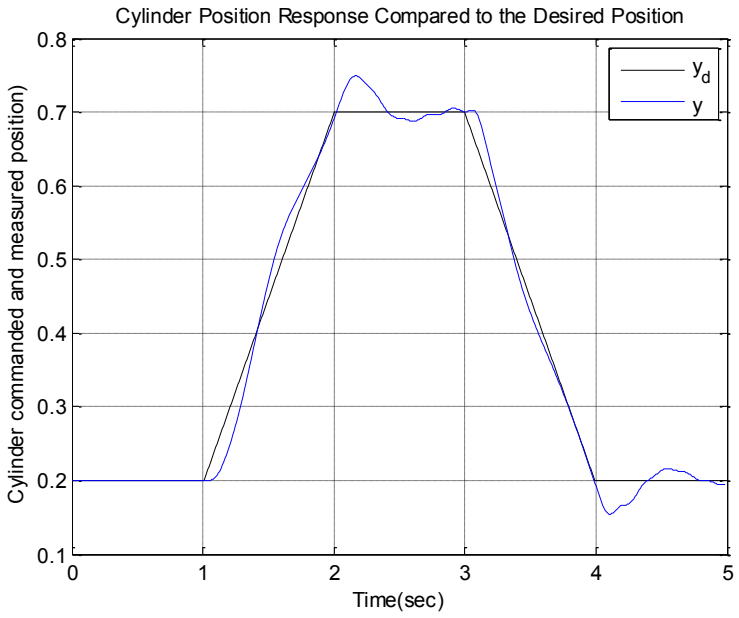

Figure 69. Position response for traditional system.

The second important state is the position of the spool of the second stage of the electrohydraulic servo valve in response to the commanded current, it can be seen that there is a near complete alignment between the two after substituting a gain factor to the current which is 10.

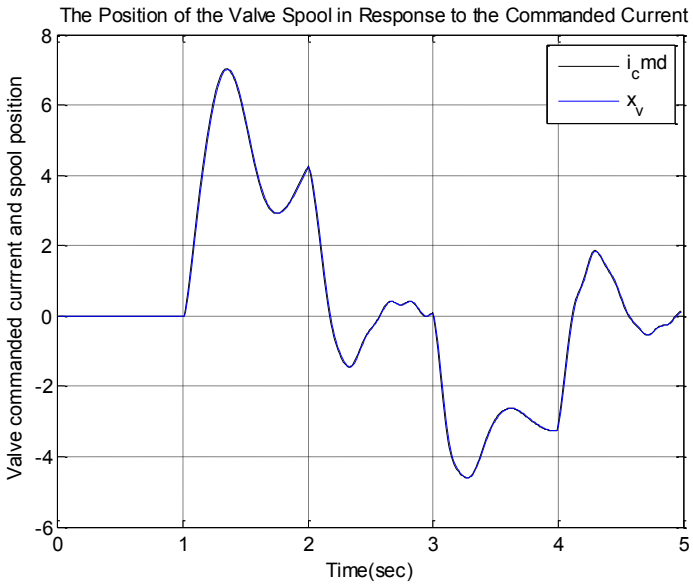

Figure 70. Spool position response to commanded current.

The last parameters to investigate is the flow path from the pump, to the cylinder or to the tank. It is shown that the flow from the pump is constant at 10 liters per second, the green curve is the flow to the cylinder, while the magenta is the flow through the relief valve back to the tank , and the sum of the two is total flow as can be seen at any point.

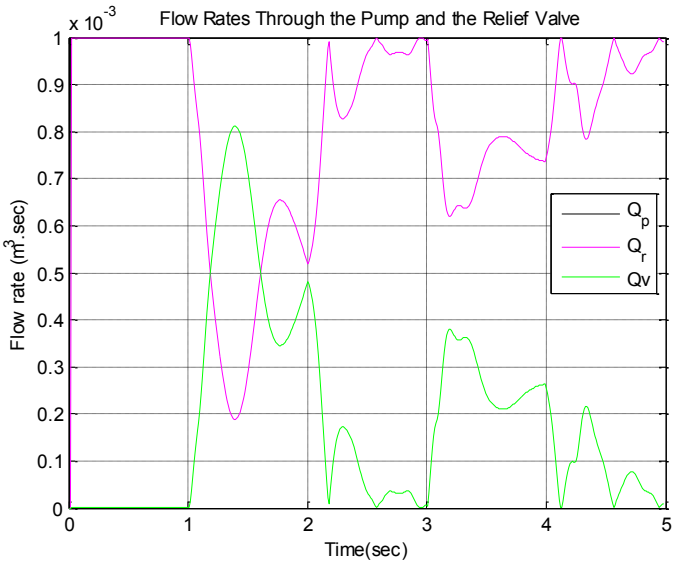

Figure 71. Flow rates of the system.

6.4.2 IMV System

The same analysis for the traditional valve is done for the IMV , with the difference that the new valve has two degrees of freedom, and the opening of the valve inlet port is decoupled from the opening of the valve exit port. Each valve has its own controller, for this case of powered extension using the IMV the first valve is used to control the flow from the pump to head chamber of the cylinder, and a PD controller is applied to it, the gains are K_p1=2.5 and K_d1=0.03, while the second valve connects the rod chamber to the tank with a PID controller applied to it, the gains are K_p2=4,K_i2=.05, and K_d2=.01. The response obtained here is better than that for the traditional valve in terms of the transients, but it seems to be further away from the desired position by a constant value, the overshoot and the oscillations here are eliminated and a smooth curve is obtained.

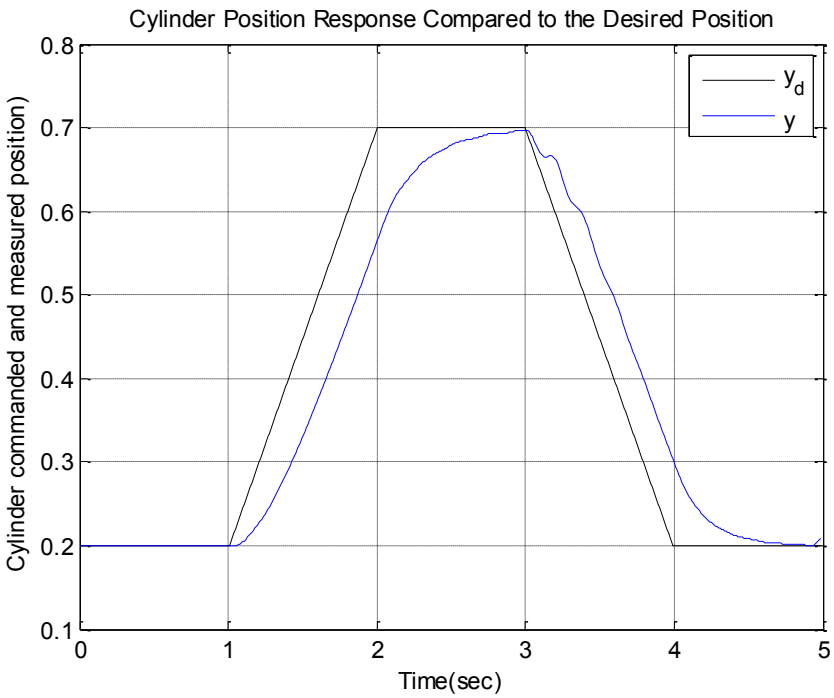

Figure 72. Position response for IMV system.

The second important state is the position of the spool of the second stage of the electrohydraulic servo valve in response to the commanded current, it can be seen that there is a near complete alignment between the two after substituting a gain factor to the current which is a factor of 10. In this case there should be two figures one for each valve, the figure shows the response of the first valve only.

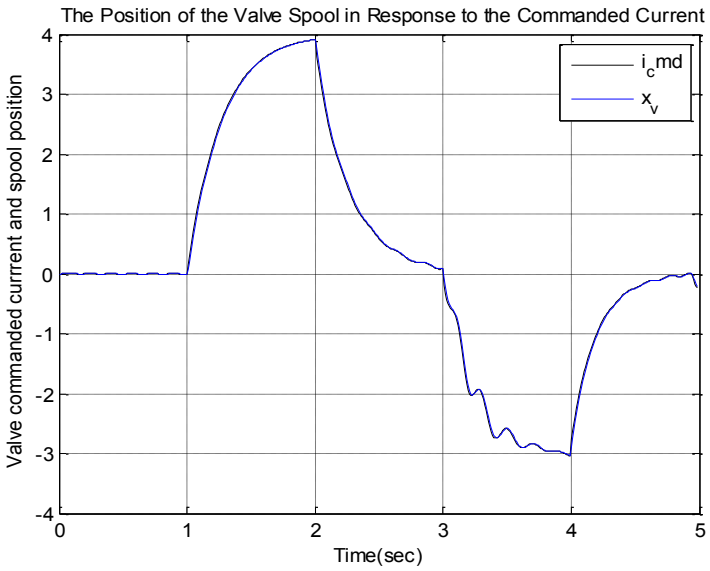

Figure 73. Spool position response of the IMV system.

7 AN EXPERIMENTAL APPROACH TO MODELING AND OPEN LOOP CONTROL OF ELECTROHYDRAULIC SYSTEMS.

7.1 Introduction

Hydraulic power is widely used in applications that require high power, rugged environment, and accurate control capabilities; the best example on such systems is construction and earth moving equipments [15]. The problem with using hydraulic power is its' complexity due to the highly nonlinear behavior of the system, and the inherent control problems of such a system [29]. Sources of nonlinearities include friction, orifice flow equation, hysteresis, overlapping of the valve lands, etc. This issue makes the mathematical modeling of such a complex system very difficult, prone to approximation, and very hard to control using traditional control algorithm [56].

Current modeling and control techniques are highly complicated and require complex control algorithms; many papers are published using these techniques such as fuzzy control and adaptive control [57]. Husco International developed a more complex control system to their highly flexible and complex valve " INCOVA" and patented this approach [41].

This chapter proposes an experimental approach that considers the hydraulic system as a black box with control signal going in and desired state outputs leaving this box. First, a brief description of the systems under study along with the components used in the lab is presented.

7.2 System Definition and Theoretical Approach

The system used in this paper is a basic hydraulic experimental setup. The system consists of a pump system that supplies a fluid flow at a constant pressure of 350 psi, the pump is then connected to a traditional electro hydraulic valve [12] . The cylinder is a basic hydraulic cylinder in a horizontal position that extends or retracts in response to the control signal from the electro hydraulic valve, is equipped with a LVDT position sensor . Finally, the rod end is connected to a variable load that is hanging by a pulley system that can make the load act in the direction of the extension or retraction direction. [10]. The theoretical approach is based on modeling every single component separately as a set of differential and algebraic equations. The differential equations of the various components and the overall system are provided here for the sake of completeness.

7.2.1 Valve Modeling

The second component to be modeled is the valve, it is the brain of the hydraulic system that operates the rest of the system. Traditional modeling of hydraulic systems are based on the famous orifice equation that is found in all hydraulic and fluid mechanics books, Merrit published these equations as shown in equation 3.12 [29] . The equations are listed for all the components in chapter three.

7.2.2 Cylinder Modeling and Response

The equations for thy cylinder under the influence of the load are derived again by Merrit [29], where extensive math and highly nonlinear equations are obtained. These equations were modified for the IMV system in used in [45].

7.2.3 Compressibility Effect

Three locations contribute to the compressibility of the fluid in the system. The first equation describes the compressibility between the pump and valve including the piping between the two. The second describes the compressibility between the valve and the head chamber A including the piping between them, and the third one is for the compressibility between the valve and the rod chamber B including the piping between them [29].

7.2.4 Conservation of Mass

These are the equations that quantify the flow among the various components of the system, that is the flow from the pump to both chambers, from both chamber to the tank, from the pump to the tank, and the leakage of the flow between these components as shown by equations 3.14 [45].

7.2.5 Conservation of Momentum

This section models the dynamics of the cylinder with the loads acting on it in addition to the friction force model inside the cylinder, equations 3.15 give the mathematical model [45].

7.2.6 State Space Representation

The system at hand is a single input system and the best representation of the equations is the state space format

$$\dot{x} = f(x, u)$$

Our variables are the actuator position, speed, inlet chamber pressure, and the outlet chamber pressure

$$x_1 = x$$
$$x_2 = \dot{x}$$
$$x_3 = P_a$$
$$x_4 = P_b$$

The derivation, solution, and control of such highly nonlinear complex system require special mathematical skills, control experience, and sophisticated control algorithms.

7.3 Experimental Approach

The approach used is the black box approach described by the figure below. Given the inputs which are the supply pressure from the pump and the commanded voltage, one should be able to predict the full states of the system, i.e.; cylinder position, cylinder velocity, pressure in the head chamber, and the pressure in the rod chamber, all this must be measured for different loads, then based on the data collected general formulas should be obtained to provide the desired response for other situations where the inputs are varied. The experimental setup consists of the position sensor that is connected to a Tektronix oscilloscope, which in turn is connected to a laptop that can collect the data from the sensor in real time, simultaneously, the readings of the pressure gauges of both chambers of the hydraulic cylinder are recorded during each run.

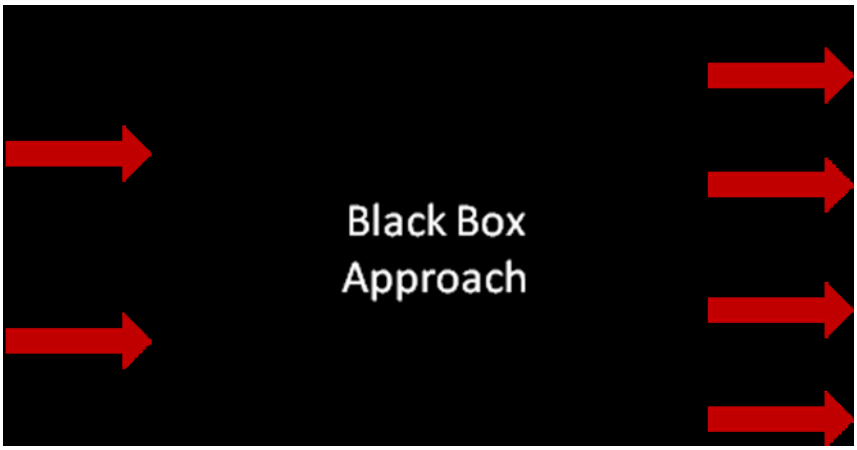

Figure 74. Experimental Approach illustration.

7.3.1 Sensor Calibration and Modeling

This sections introduces the procedure used to model and calibrate the sensor used in this approach. Although the calibration chart of the LVDT position sensor is provided by the manufacturer, the decision is made to follow a standard approach to create our own calibration relation .

The first step was to determine the input voltage needed to operate the sensor and range of signal output in response to the cylinder extension. Figure 78 show the experimental data obtained for the setup.

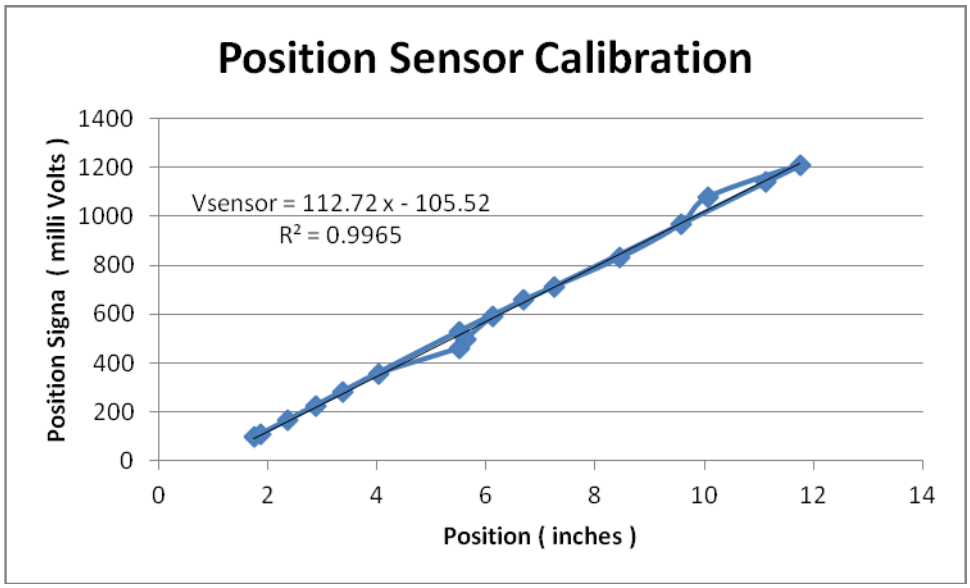

Figure 75. Sensor calibration and sensor modeling.

7.3.2 Valve Modeling

The experimental approach proposed here does not even bother about any equation since the dynamics of the valve are automatically found. The valve operation signal is first determined, which is

the voltage needed to activate the valve, it was found that this voltage is about 12.5 volts. The next step was to find the input signals required to extend and retract the cylinder. Keeping in mind that electro hydraulic valves have saturation limits, this must be taken into consideration, in other words, the valve will open in response to the signal strength to a certain value, after that if the signal is increased there will be no increase in the opening of the valve [12]. The starting point was at six volts, where no response was obtained, then the voltage was increased to nine volts and there was an extension. There was no load exerted on the cylinder at this point, and the input voltage was to be varied several times to find the limits of operation of this valve.

The logical next thing to do is to find the limits of operation, a variation of voltages were used to determine these limits, and after many attempts it turned that there are four limits, two for extension and two for retraction, the valve extended in response to voltages between 6.25 volts and 12 volts, while it retracted in response to voltages between 1.75 volts and 5.5 volts.

Two important observations are that the higher the voltage for the extension range the faster the cylinder extended, and the lower the signal the slower the extensions happened, on the other end of the retraction side, the higher the voltage on the retraction range the slower the extension occurred while the lower the voltage the faster the cylinder retracted. This indicate that the rate of motion is proportional to the difference between the signal and a reference signal value, and the bigger this difference the faster the motion was.

7.3.3 Cylinder Modeling

The experimental approach takes a shortcut and avoids all this messy mathematics, so the next step is to determine model the dynamics of the next component which is the hydraulic cylinder. The cylinder represents the muscle of the hydraulic system, up to this point the analysis of the valve was qualitative to some extent, in this section a quantitative approach is introduced. The load is introduced and the effect of this load on the response, and the required input voltage to achieve a desired speed and position is studied in details. The system setup is based on a load in the retraction mode, where a load is exerted on the cylinder as a weight that must be pulled in the
retraction stroke of the cylinder, for this purpose a weight is attached to the piston rod through a pulley, this load is left hanging under its own weight and it was made flexible to change the weight according to the desired force to be studied. Figure 79 shows the system setup.

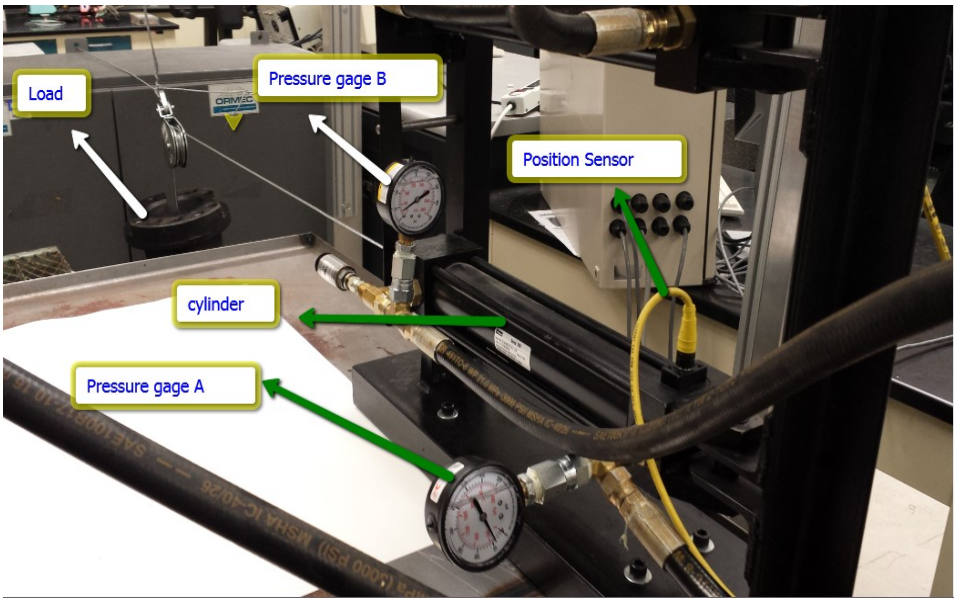

Figure 76. The cylinder setup with variable loading conditions.

The response of the cylinder is measured by installing two pressure gauges on the head chamber and the rod chamber, the ideal choice would be an electrohydraulic pressure gauge that would collect continuous pressure data, but due to funding limitations dial pressure gauges with pressure limit of 500 psi were installed.

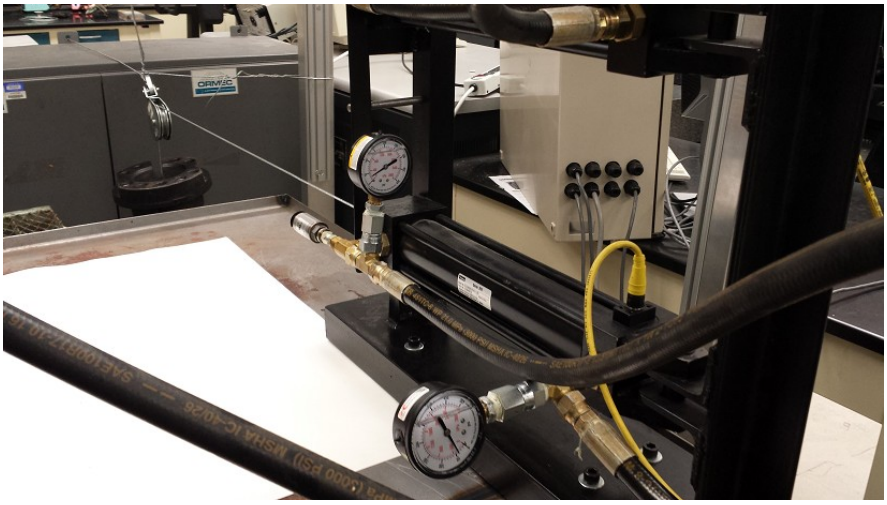

Figure 77. The experimental setup of the hydraulic cylinder with gage pressure meters.

The oscilloscope is capable of taking and storing 2500 data points for each run, which is more than enough for collecting accurate data for our experimental runs. The data is stored in a spreadsheet data file to be processed at a later time, where in each run the voltage corresponding to the position of the cylinder is recorded versus the time, this means that we have accurate data for the position and velocity of the cylinder, on the other hand it was noticed that both pressures for chambers A and B were constant for each run, these pressures were recorded and tabulated for further analysis.

The data acquisition was set up so that five different loads are applied to the system, corresponding to 0,20,40,60, and 80 pounds of weight, then for each load different commanded voltages over the range of the linear response were commanded both for extension and retraction. The full states then were recorded to establish formulas for future references, the position, the calculated velocity and the tabulated pressures were then used to predict the desired loads and velocities in response to a certain commanded voltage or the opposite, i.e., to calculate the desired commanded voltage needed to move a certain load at a desired velocity or to a desired position and the pressure difference between the two chambers.

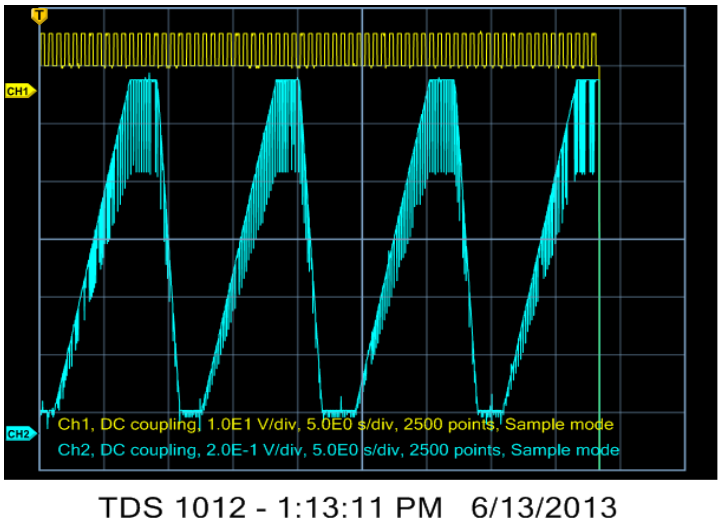

Figure 78. The oscilloscope screen of the cylinder in extension at seven volts and zero loads.

Figure 79 shows a sample data acquired for the extension stroke of the hydraulic cylinder in response to a seven volt command signal with zero load. As one can see from the oscilloscope there are four extensions at different times for the same voltage and load. This data is stored in an excel spread sheet and the four extensions are processed and the position with time is found as shown in figure 78.

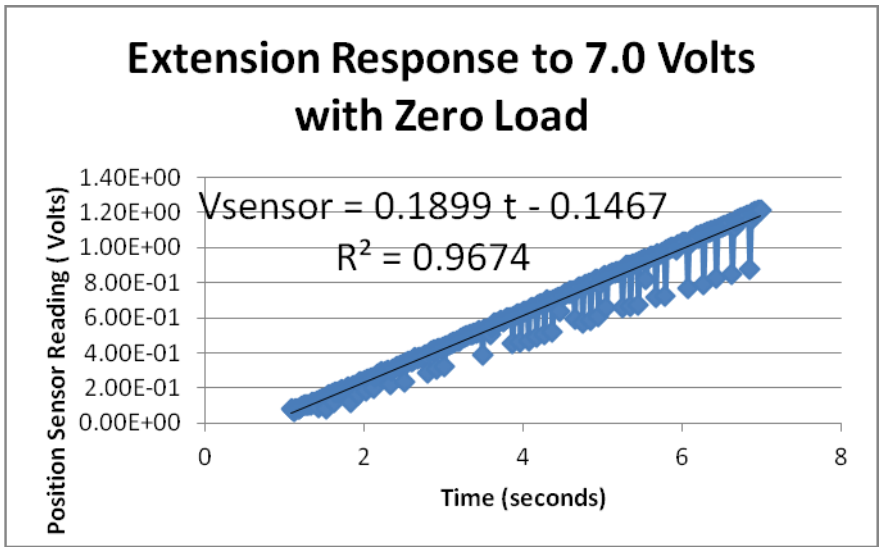

Figure 79. Extension at seven volts and zero loading.

Figure 79 shows the first extension response to a seven volt command signal at zero load, the sensor voltage is then translated into position which means a relationship between the position and time is available, and velocity in turns is then known.

7.4 Results and Discussion

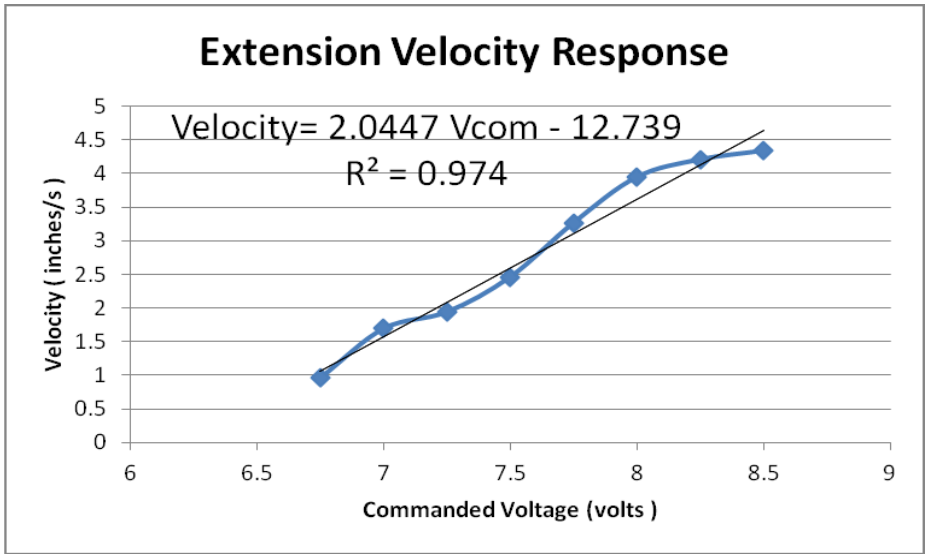

Figure 80. Velocity response of the cylinder to different commanded voltages in extension.

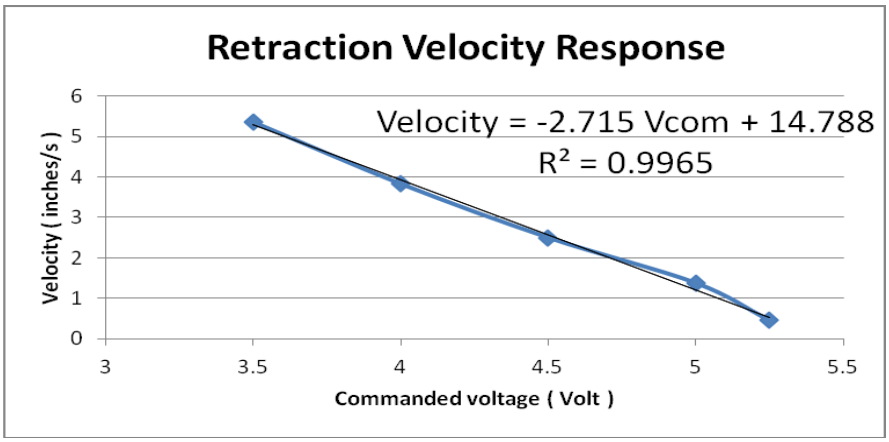

Figure 81. Velocity response of the cylinder to different commanded voltages in retraction.

Figure 78 shows the screen snapshot of the oscilloscope for an extension test at commanded voltage of 7 volts and zero load, it can be seen that there are three extensions with the signal and sensor

volatages as PWM voltage signals against the time. This data is exported to an excel sheet for each trial and the velocity for each scenario is calculated. A relationship for the velocity vs the commanded voltage is then obtained for the extension and retraction trials, each one at different loading condition, so in order to achieve a certain desired velocity at a certain loading condition the formula is used. For the extension case the result obtained is :

$$V_{elocity} = 2.045V_{com} - 12.74 \quad (7.1)$$

and for the retraction the formula is:

$$V_{elocity} = -2.715V_{com} + 14.79 \quad (7.2)$$

It is clear from figure 80 that the relationship is linear, it represents the position vs time multiplied by some factor, so to get the position the velocity relation is integrated with respect to time, and since the relation is linear the position is just the velocity by time.

Table 5.Pressure response to commanded voltage at different load in extension.

Vcom (volts)	Load ((lbs)	Pa (psi)	Pb (psi)	Velocity (in/s)	Q (GPM)
7.5	0	115	110	2.398	1.103
7.5	20	110	110	2.451	1.127
7.5	40	103	110	2.433	1.118
7.5	60	98	110	2.431	1.118
7.5	80	93	110	2.471	1.136

Table 6. Head chamber pressure response to commanded voltage in extension.

Load (lbs)→	0	20	40	60	80
V com ↓	Pa(psi)	Pa(psi)	Pa(psi)	Pa(psi)	Pa(psi)
6.75	155	145	140	135	130
7	125	120	115	110	105
7.25	120	115	110	102	95
7.5	115	110	103	98	93
7.75	113	108	100	93	92
8	110	105	100	95	90
8.25	105	100	95	90	85
8.5	95	90	85	80	75
8.75	95	90	80	72	65
9	80	75	70	65	60

Table 7. Rod chamber pressure response in extension

Load (lbs)→	0	20	40	60	80
V com ↓	Pb(psi)	Pb(psi)	Pb(psi)	Pb(psi)	Pb(psi)
6.75	160	160	160	160	160
7	130	130	130	130	130
7.25	120	120	120	120	120
7.5	110	110	110	110	110
7.75	105	105	105	105	105
8	100	100	100	100	100
8.25	90	90	90	90	90
8.5	80	80	80	80	80
8.75	70	70	70	70	70
9	60	60	60	60	60

Table 8. Head chamber response to commanded voltage in retraction.

Load (lbs)→	0	20	40	60	80
V com ↓	Pa(psi)	Pa(psi)	Pa(psi)	Pa(psi)	Pa(psi)
2.5	120	120	115	115	115
3	130	125	120	120	115
3.5	170	170	165	160	155
4	180	175	170	170	165
4.5	190	185	180	175	170
5	210	205	195	190	185
5.25	215	210	200	195	190

Table 9. Rod chamber response to commanded voltage in retraction.

Load (lbs)→	0	20	40	60	80
V com ↓	Pb(psi)	Pb(psi)	Pb(psi)	Pb(psi)	Pb(psi)
2.5	150	160	160	170	170
3	160	160	170	175	180
3.5	220	220	230	230	230
4	230	230	230	240	240
4.5	240	240	240	245	245
5	260	260	260	260	260
5.25	265	265	265	270	270

Tables 6 and 7 show the pressure response to different commanded signals and different loads in both chambers; head chamber A, and rod chamber B. The two tables can be interpolated or extrapolated for any other conditions other than the data points that were tested with high accuracy, a clear pattern for both chambers in for the two cases of extension and retraction can be observed and used to predict the desired conditions.

From table 5 it is noticed that the velocity of extension is independent of the loading condition for a certain commanded voltage, this is not what expected about the response, where the velocity is supposed to increase as the load is increased in traditional electrohydraulic valve. This problem seemed as a glitch in the approach, so the manual of the valve was studied and it was found that the valve is a flow compensated valve, which means that the valve opening is adjusted to allow a ceratin amound of flow regardless of the loading condition, this turns to porve the validity of the approach.

8 Conclusions and Future Work

The equations for the equivalent pressure and the supply pressure set point for the HSRE and LSRE are the same with some advantages for using the HSRE for the regeneration mode in extension. The first is that the control of the supply pressure P_s is much easier than the control of the return pressure P_r, and the cavitation load of the HSRE is much higher than that of the LSRE, which means it is safer to operate with the first mode. The same discussion applies to using the LSRR and HSRR; that is the equivalent pressures, the supply pressure set point, and the cavitation load. It is suggested then to reduce the six distinct modes to only four modes that can be used to achieve all possible combinations, and to focus only on those four modes. This finding was made obvious due to the new formulation of the equations as listed in tables two and three. A quick glance at the tables proves the validity of this suggestion. In addition to the theoretical work of previous research is the introduction and the derivation of the fourth CVM, which is the PHSRR mode. Based on previous analogy, it is suggested that the focus should be on two CVM's: PHSRE and PLSRR.

The second contribution of this thesis is the introduction of a truly independent controller to each valve used. The valves openings are then related to each other by some proportionality constant, so the same controller was used for the valves used in any mode. In this research the PE mode is used to prove that a simple controller such as the PID controller can be applied to each valve independent of the others. The results presented in chapter six show the two simple yet totally different PID gains used to control the two valves involved in powered extension under the IMV mode. The method used compared the system response of an electrohydraulic system with a traditional valve to the response of the same system using IMV. It was shown that the IMV has more flexibility despite its complexity; it even gave better results than the traditional system at certain regions of the desired position curve.

The third and final contribution of this thesis is the introduction of an experimental approach to model and control electrohydraulic systems when there is no enough data available. Like many discoveries in science and engineering, this was proposed when the original plan did not go as planned. The original plan was to verify the mathematical model of the system in the lab so it can be controlled using full state feedback. When the work started to model the system, there were few parameters missing and needed high performance equipment to measure. Due to the absence of funding, it was necessary to use only what is available in the lab, so the idea was to come up with a method where a

signal is sent to the system and a response is registered. Then to study the relation between the two under different conditions, and the rest of the details are presented in chapter seven. The method works for any system and under any conditions.

There are many venues to be explored in the future. Currently the research is undergoing on two fronts; the first one is the mathematical and modeling of the system, and the second is the experimental and practical front. Finding a linear model of this highly nonlinear system is the first recommendation. A good amount of work has been conducted in this field, and results are about to be obtained in the next few weeks. This will allow the use of more control strategies since the system can be turned to a state space format. A proposed controller will be a full state feedback controller, pole placement method, and integral control, which are all with reference input.

The most important work to be conducted in the near future is apply the control algorithm proposed here to the IMV system and compare the results to the traditional system. An experimental setup is being prepared at Birzeit University to achieve this goal.

A third proposal for future work is to improve the experimental approach using electrohydraulic pressure gages instead of the dial gages. This will produce mathematical expression for the pressures in the head and rod chambers of the cylinder instead of the pressure tables listed in the tables in chapter seven.

REFERENCES

1. Aardema, J. A. and Kohler, D. W.: System and method for controlling an independent metering valve. United States patent, (5,947,140), 1999.

2. Aardema, J. A.: Hydraulic circuit having dual electro-hydraulic control valves., United States Patent, (5,568,759), 1996.

3. Alciatore, D. G., and Histand, M. B. Introduction to Mechatronics and Measurement Systems. New York, NY: McGraw Hill Inc, second edition, 2003.

4. Andersen, B. R. and Ayeres, J. L.: Load sensing directional valves, current technology and future development. In the Fifth Scandinavian International Conference on Fluid Power, 1997.

5. Andersen, B. R. and Ayeres, J. L.: Load sensing directional valves, current technology and future development. In the Third Scandinavian International Conference on Fluid Power, (Linkoping, Sweden), May 1995.

6. Book, R. and Goering, C. E.: Programmable Electrohydraulic valve. In SAE paper, vol. 1, no.2, pp. 28-34, 1998.

7. Book, R.: Programmable electro-hydraulic valve. Ph.D. Dissertation, University of Illinois at Urbana-Champaign, IL, 1998.

8. Book, W. J., Modeling, Design and Control of Flexible Manipulator Arms. PhD dissertation, Massachusetts Institute of Technology, Boston, MA, April 1974.

9. Bu, F., and Yao, B.: Nonlinear adaptive robust control of hydraulic actuators regulated by proportional directional control valves with deadband and nonlinear flow gains. In Proceedings of the American Control Conference, vol. 6, pp. 4129-4133, 2000.

10. Bu, F. and Yao, B.: Adaptive robust precision motion control of single-rod hydraulic actuators with time varying unknown inertia: a case study. In ASME International Mechanical Engineering Congress and Exposition (IMECEC), FPST-Vol. 6, pp. 131-138, 1999.

11. Bu, F., and Yao, B., and G.T.C Chiu: Nonlinear adaptive robust control of electro-hydraulic servo systems with discontinuous projections. In IEEE Conference on Decision and Control, 37th, pp. 2265-2270. 1998.

12. Cetinkunt S. Design and Control of poppet Type Independently Metering Valves., Department of Mechanical and industrial Engineering, University of Illinois at Chicago, (2005).

13. Crosser, Jeffrey. A.: Hydraulic circuit and control system therefore. United States Patent, (5,138,838), 1992.

14. Deboer, C. C. and Yao, B.: Velocity control of hydraulic cylinders with only pressure feedback. In ASME International Mechanical Engineering Congress and Exposition (IMECEC), DSC-2B-3, 2001.

15. Esposito, Anthony: Fluid Power with Applications. Englewood Cliffs, New Jersey, Prentice-Hall, Inc. 1980.

16. Frankfield, T. and Stavrou, P.: Developing trends in hydraulics tied to electronic controls. Control Engineering, vol. 40, no. 5, pp. 62-66, 1993.

17. Franklin, G. F., Powell, J. D., and Emami-Naeini, A. Feedback Control of Dynamic Systems. Upper Saddle River, NJ: Prentice Hall, fourth edition, 2002.

18. Garnjost, K. D.: Energy-conserving regenerative-flow valves for hydraulic servo-motors. United States Patent, (4,840,111), 1989.

19. Hu, H. and Zhang, Q.: Realization of programmable control using a set of individually Controlled electro-hydraulic valves. International Journal of Fluid Power, pp. 29-34, 2002.

20. HUSCO International (2007). EHPV Technical Information.

21. Jansson, A. and Palmberg, J. O.: Separate control of meter-in and meter-out orifices in mobile hydraulic systems. SAE Technical Paper Series, no. 901583, 1990.

22. Kramer, K. D. and Fletcher, E. H.: Electrohydraulic valve system. United States Patent, (Re. 33,846), 1990.

23. Kuo, B. C. Automatic Control Systems. New York, NY: John Wiley and Sons, 1995.

24. Lieberfarb, Z.: Bi-directional flow control valve. United States Patent, (6,167,906 B1).

25. Liu, S. and Yao, B.: Energy saving control of single-rod hydraulic cylinders with programmable valves and improved working model selection. National Fluid Power Association, vol. 102, no. 2.4, pp. 81–91, 2002.

26. Liu, S. and Yao, B.: Energy saving control of hydraulic systems with novel programmable valves. In Proceedings of the 4th World Congress on Intelligent Control and Automation, vol. 4, pp. 3219-3223, 2002

27. Liu, S. and Yao, B.: Coordinate control of energy-saving programmable valves. In IEEE Transaction on Control Systems Technology, vol. 16, Issue 1, pp. 34-45, 2008.

28. McCloyd, D. and Martin, H. R. The Control of Fluid Power. New York, NY: John Wiley and Sons, 1973.

29. Merritt, H. E. Hydraulic Control Systems. New York, NY: John Wiley & Sons, Inc, 1967.

30. Nice, N. S. Control Systems Engineering. Danvers, MA: John Wiley and Sons, 2004.

31. Norvelle, F. D. Electrohydraulic Control Systems. Upper Saddle River, NJ: Prentice Hall Inc, 2000.

32. O'Hara, D. E.: The smart valve. Industrial Applications of Fluid Mechanics, vol. 100, pp. 95-99, 1990.

33. Opdenbosch, P. Sadegh, N., Book,W., and Enes, A.: Digital hydraulic actuator control using an electrohydraulic poppet valve (EHPV). In IEEE International Conference on Robotics and Automation, pp. 153-158, 2011.

34. Opdenbosch, P., Sadegh, N., Book, W., and Enes, A.: Auto-Calibration based control for independent metering of hydraulic actuators. In IEEE International Conference on Robotics and Automation, 2011.

35. Opdenbosch, P. and Sadegh, N.: Learning control applied to electro-hydraulic poppet valves. In Proceeding of American Control Conference, pp.1225-1232, 2008.

36. Opdenbosch, P.: Auto-calibration and control applied to electro-hydraulic valves. Ph.D. Dissertation, Georgia Institute of Technology, GA, 2007.

37. Opdenbosch, P. and Sadegh, N.: Control of electro-hydraulic poppet valves via online learning and estimation. In Proceedings of IMECE, pp.57-62, November 2004.

38. Opdenbosch, P. and Sadegh, N.: Modeling and control of an electro-hydraulic poppet valve. In Proceedings of IMECE, pp. 103-110, November 2004.

39. Pfaff, J.: Communication protocol for a distributed electro-hydraulic system having multiple controllers. United States Patent, (7,194,855 B2).

40. Pfaff, J. and Tabor, K.: Method of sharing flow of fluid among multiple hydraulic functions in a velocity based control system. United States Patent, (6,779,340), August 2004.

41. Pfaff, J. and Tabor, K.: Velocity based electronic control system for operating hydraulic equipment. United States Patent, (6,732,512), May 2004.

42. Pippenger, J. J. Hydraulic Valves and Controls: Selection and Application. New York, NY: New York and Basel, 1984.

43. Plummer, A. R. and Vaughn, N. D.: Robust adaptive control for hydraulic servo-systems. Transactions of the ASME, Journal of Dynamic Systems, Measurements and Control, vol. 118, no. 2, pp. 237-243, 1996.

44. Reiners, E. A., and Ufheil S. T.: Independent metering valve assembly for multiple hydraulic load functions. United States Patent (6,918,248 B2).

45. Shenouda, Amir.: Quasi-Static Hydraulic Control Systems and Energy Savings Potential Using Independent Metering Four-Valve Assembly Configuration. Ph.D. Dissertation, Woodruff School of Mechanical Engineering at Georgia Institute of Technology, GA, 2006.

46. Singh, K., and Aginhotri, G. System Design through Matlab, Control Toolbox and Simulink. London, Great Britain: Springer-Verlag London Limited, 2001.

47. Tabor, K.: Velocity based method for controlling a hydraulic system. United States Patent, (6,718,759), April 2004.

48. Tabor, K.: Velocity based method for controlling an electro-hydraulic proportional control valve. United States Patent, (6,775,974), August 2004.

49. Tabor, K.: A novel method of controlling a hydraulic actuator with four valve independent metering using load feedback. In SAE Commercial Vehicle Engineering Conference, November 2005.

50. Tabor, K.: Optimal velocity control and cavitation prevention of a hydraulic actuator using four valve independent metering. In SAE Commercial Vehicle Engineering Conference, November 2005.

51. Wilke, R. A. and Yang, X.: Pilot solenoid control valve and hydraulic control system using same. United States Patent, (5,878,647), March 1999.

52. Wilke, R. A., Hamkins, E. P., Layne, M. C., Pedersen, L., and Russell, L. A.: Pressure compensated control system. United States Patent, (5,579,642), December 1996.

53. Yang, X.: Pilot solenoid control valve with pressure responsive diaphragm. United States Patent, (6,149,124), November 2000.

54. Yang, X., Pfaff, J. L., and Paik, M. J.: Pilot operated control valve having a poppet with integral pressure compensating mechanism. United States Patent, (6,745,992), June 2004.

55. Yang, X., Stephenson, D. B., and Paik, M. J.: Bidirectional pilot operated control valve. United States Patent, (6,328,275), 2001.

56. Yao, B.: High performance adaptive robust control of nonlinear systems: a general framework and new schemes. In Proceedings of the 36th IEEE Conference on Decision and Control, vol. 3, pp. 2489-2494, 1997.

57. Yao, B., and Tomizuka, M.: Adaptive coordinated control of multiple manipulators handling a constrained object. In Proceedings of IEEE International Conference on Robotics and Automation, vol. 1, pp. 624-629, 1993.

58. Yoshino, K.: Hydraulic control system with regeneration. United States Patent, (6,694,860 B2).

VITA

PERSONAL INFORMATION

Full Name: Sameh Nabil Alkam

E-mail Address: salkam2@uic.edu, snawad@birzeit.edu

ACADEMIC BACKGROUND

Doctor of Philosophy: University of Illinois at Chicago, 2014

Master of Science: University of Illinois at Chicago, 2006

Bachelor of Science: San Jose State University, California, 2003

ACADEMICA/ TEACHING EXPERIENCE

Teaching Assistant: University of Illinois at Chicago , 2006-2008

Full Time Faculty Member: Birzeit University, Palestine, 2008-2011

Teaching Assistant: University of Illinois at Chicago, 2011-2013

Full Time Faculty Member: Birzeit University , Palestine, 2013-2014

WORK EXPERIENCE

Birzeit University: Mechatronics program design and supervision

Honors:

San Jose State University: Golden Key National Honor Society Member

LANGUAGES

Arabic, English, Spanish